醫學博士 學位論文

Involvement of cardiac nitric oxide synthase in saturated fatty acid regulation of myocyte metabolism and contraction in healthy and hypertensive rat hearts

정상과 고혈압 백서에서 포화지방산의존적 심근대사 및 수축조절에서 산화질소 합성효소의 작용기전

2017年 8月

서울大學校 大學院

醫科學科 醫科學專攻

金 春 丽

Abstract

The heart has a high energy demand and must persistently generate ATP at a high rate to sustain contractile function and ionic homeostasis. Fatty acids (FAs) are the predominant metabolic substrates for myocardial ATP. So far, the effects of FAs on myocyte contraction in normal and hypertensive hearts are unclear. I examined the effects of FA-regulation of contraction and mitochondrial activity in left ventricular (LV) myocytes from healthy and angiotensin II (Ang II)-induced hypertensive (HTN) rat hearts.

My results showed that palmitic acid (PA, 100 μM) increased the amplitudes of sarcomere shortening and intracellular ATP in sham but not in HTN despite that oxygen consumption rate (OCR) was increased by PA in both groups. Carnitine palmitoyl transferase I inhibitor, etomoxir (ETO), reduced OCR and ATP with PA in sham and HTN but prevented PA-potentiation of sarcomere shortening only in sham. Mechanistically, PA increased intracellular Ca^{2+} transient ($[Ca^{2+}]_i$) without changing Ca^{2+} influx *via* L-type Ca^{2+} channel (LTCC) and reduced myofilament Ca^{2+} sensitivity in sham. In HTN, PA reduced $I_{Ca\text{-}L}$ without affecting $[Ca^{2+}]_i$ or myofilament Ca^{2+} sensitivity.

Cardiac neuronal nitric oxide synthase (nNOS) is an important molecule that regulates intracellular Ca^{2+} handling and contractility of healthy and diseased hearts. Accordingly, the effects of nNOS on FA-regulation of LV myocyte contraction in sham and HTN were investigated. PA increased nNOS-derived NO only in HTN. Subsequently,

inhibition of nNOS with S-methyl-l-thiocitrulline (SMTC) prevented PA-induced OCR and restored PA-potentiation of myocyte contraction in HTN but exerted no effect in sham. Furthermore, nNOS inhibition increased $[Ca^{2+}]_i$, $I_{Ca\text{-}L}$ and reduced myofilament Ca^{2+} sensitivity prior to PA supplementation; as such, normalized PA-increment of $[Ca^{2+}]_i$ in sham. In contrast, nNOS inhibition increased $I_{Ca\text{-}L}$, reduced $[Ca^{2+}]_i$ and increased myofilament Ca^{2+} sensitivity prior to PA supplementation. However, PA increased $[Ca^{2+}]_i$ and reduced myofilament Ca^{2+} sensitivity following nNOS inhibition in HTN. PA reduced intracellular pH similarly in sham and in HTN. Myocardial FA uptake *in vivo* with PET/CT (^{18}F-fluoro-6-thia-heptadecanoidc acid, ^{18}F-FTHA) was comparable between two groups but nNOS inhibition increased it only in HTN. These results suggest that nNOS modulation of intracellular Ca^{2+} handling overrides fatty acid-potentiation of cardiac inotropy in hypertensive rats.

On the other hand, since the activity of endothelial nitric oxide synthase (eNOS) is essential in FA-dependent β-oxidation in cardiac muscle, the effect of eNOS on PA-regulation of myocyte contraction was analyzed. Our results showed that Nω-nitro-L-arginine methyl ester hydrochloride (L-NAME) or eNOS gene deletion prevented PA-regulation of the myocyte contraction or OCR, indicating the pivotal role of eNOS in mediating the effects of PA in cardiac myocytes. *S*-palmitoylation is an important post-translational modification that affects the translocation and the activity of target proteins in a variety of cell types including cardiomyocytes. Since eNOS is known to be palmitoylated, the effect of eNOS palmitoylation by PA and its involvement in PA-regulation of myocyte contraction was examined in sham and HTN.

As expected, PA increased the palmitoylation of eNOS in LV myocytes and de-palmitoylation with 2 bromopalmitate (2BP, 100 μM) abolished the increment. Furthermore, although PA did not increase eNOS-Ser^{1177}, 2BP reduced eNOS-Ser^{1177} with and without PA. Intriguingly, 2BP did not affect PA-induced increases in contraction and OCR in sham. In HTN, PA did not affect eNOS palmitoylation, eNOS-Ser^{1177} or myocyte contraction. However, 2BP diminished basal eNOS palmitoylation and eNOS-Ser^{1177} in the presence and absence of PA but did not change myocyte contraction.

Collectively, PA increases myocyte contraction through stimulating mitochondrial activity and $[Ca^{2+}]_i$, secondary to myofilament Ca^{2+} desensitization in healthy hearts. PA-dependent cardiac inotropy was limited in HTN by nNOS, whose activity was increased by PA in HTN, due to its modulatory effect on $[Ca^{2+}]_i$ handling. In addition, our results confirm that eNOS is important in PA-regulation of mitochondrial activity and myocyte contraction. However, palmitoylation of eNOS in LV myocytes, which is up-regulated by PA in sham, plays a negligible role in PA-regulation of myocyte contraction and mitochondrial activity in sham and in HTN.

Most of the results were published in Pflugers Archive European Journal of Physiology (Jin CL et al., Pflugers, 2017 Apr 25 and Jin CL et al., Pflugers, 2017 May 22)

Keyword: cardiac myocyte, Ca^{2+} transients, contraction, fatty acid, myofilament Ca^{2+} sensitivity, nNOS, eNOS mitochondrial oxygen consumption, *S*-palmitoylation

Student number: 2013-30816

Contents

List of Table and figures

List of abbreviations

ANT = adenine nucleotide transferase

ATP = adenosine-5'-triphosphate

Ca^{2+} = calcium

CPT-1 = carnitine palmitoyltransferase 1

eNOS = endothelial nitric oxide synthase

FA = fatty acid

FAT = fatty acid transporter

HF = heart failure

HTN = hypertension

iNOS = inducible isoform of nitric oxide synthase

$I_{Ca\text{-}L}$ = Ca^{2+} current through L-type Ca^{2+} channel

LTCC = L-type Ca^{2+} channel

LV = left ventricular

NCX = sodium/calcium exchanger

nNOS = neuronal nitric oxide synthase

NO = nitric oxide

NOS = nitric oxide synthase

RyR = ryanodine receptor

SERCA = Ca^{2+} ATPase in the sarcoplasmic reticulum

SR = sarcoplasmic reticulum

TnC = troponin C

UCP = uncoupling proteins

Chemicals of abbreviations

Ang II = angiotensin II

2BP = 2 Bromo-palmitic acid

ETO = (+)-etomoxir sodium salt hydrate

FCCP = Carbonyl cyanide-*4*-(trifluoromethoxy)phenylhydrazone

^{18}F-FTHA = [^{18}F] fluorothia-6-heptadecanoic acid

L-NAME = Nω-nitro-L-arginine methyl ester hydrochloride

PA = palmitic acid

SMTC = S-methyl-L-thiocitrulline acetate salt

SNP = sodium nitroferricyanide(III) dihydrate

Tiron = 4,5-dihydroxy-1,3-benzenedisulfonic acid disodium salt monohydrate

$Na_2S_2O_4$ = sodium dithionite (sodium hydrosulfite or hyposulfite)

Introduction

The heart has a very high energy demand and must persistently generate ATP at a high rate to sustain contractile function, basal metabolic processes, and ionic homeostasis. Fatty acids (FAs) are the predominant metabolic substrates for myocardial ATP. Approximately 70% to 90% of cardiac ATP is produced by the oxidation of FAs in healthy adult heart [Lopaschuk GD et al., 2010]. Mitochondria are key organelles for free fatty acid (FFA) oxidation and glucose metabolism. So far, the effects of FAs on myocyte contraction in normal and HTN hearts are unclear.

Fatty acid and LV myocyte contraction

Cardiac work depends strongly on ATP generation, and the impairment of this process can rapidly induce contractile dysfunction. In healthy adult heart, majority of ATP production is derived from mitochondrial oxidative phosphorylation. To sustain sufficient ATP generation, the heart acts as an “omnivore” and can use a variety of different carbon substrates as energy sources if available [Lo paschuk GD et al., 2010]. Approximately 70% to 90% of cardiac ATP is produced by the oxidation of FAs. The remaining 10% to 30% comes from the oxidation of glucose and lactate, as well as small amounts of ketone bodies and certain amino acids [Doenst T et al., 2013]. After entering the cardiac myocytes through FA transporters such as FAT/CD36, FAs are esterified to long chain fatty acyl CoA and shuttled into mitochondrial matrix after the formation of long chain acylcarnitine by carnitine palmitoyltransferase 1 (CPT-1), a key enzyme that determines the fate of FA for beta-oxidation[Lopaschuk GD et al., 2010]. One strategic target has been CPT-1, the enzyme that is the gateway for long-chain FA uptake into the mitochondria. The muscle form of the CPT-1 inhibitors, such as etomoxir, perhexiline, and oxfenicine, have been associated with reduced cardiac FAO and elevated glucose oxidation in both animal models and humans. [Kolwicz SC et al., 2013]

Calcium ion fluxes in cardiac excitation-contraction coupling

The details of the associated calcium ion fluxes that link myocyte contraction to the wave of excitation (excitation-contraction (E-C coupling) are now reasonably well clarified. Contraction is initiated by Ca^{2+} entering via voltage-gated LTCC in the t-tubular system and diffusing into a dyadic cleft to stimulate Ca^{2+} -induced Ca^{2+} -release from the sarcoplasmic reticulum (SR) via ryanodine-sensitive channels (RyR2). The consequent larger Ca^{2+} release interacts with troponin C (TnC) in the regulatory thin-filament complex, initiating conformational changes in troponin I, and shifting tropomyosin's position on the actin monomer to unblock actin myosin-binding sites [Eisner, DA et al., 2000; Palmiter KA et al.,1997]. Hydrolysis of ATP bound to myosin results in a strongly bound actin-myosin cross-bridge and force generation. Relaxation involves removal of Ca^{2+} from TnC, and its subsequent extrusion from the cell via the Na^{+}/ Ca^{2+} exchanger (NCX), or intracellular uptake into the SR through Ca^{2+} -ATPase pump, and mitochondria. The process requires ATP. Note the much higher extracellular Ca^{2+} (10^{-3} M) than intracellular Ca^{2+} values, with much higher Ca^{2+} values in the SR because of its storage function. Mitochondria can act as a buffer against excessive changes in the free cytosolic calcium concentration. (From Opie LH: Heart Physiology, From Cell to Circulation. Philadelphia et al., 2004)

Myofilament Ca^{2+} sensitivity and E-C coupling

Myofilament is the functional unit of contraction and relaxation, myofilament Ca^{2+} sensitivity is imperative in the implementation of myofibril performance, it should be taken into consideration in E-C coupling for mechanistic analysis (Bers, DM et al., 2002). Consequently, the decline in cytosolic Ca^{2+} instigates conformational changes of thin filaments back to the original state, resulting in the dissociation of actin-myosin and myocyte relaxation [Eisner DA et al, 2000; Palmiter KA et al., 1997]. As such, abnormal Ca^{2+} handling by LTCC, RyR and SERCA2a, etc. has been considered the primary

mechanisms for impaired contractility and relaxation in diseased heart [Missiaen L et al., 2000]. In reality, free cytosolic Ca^{2+} that functions as the messenger in E-C coupling accounts for around 1% of total intracellular Ca^{2+} and the majority of Ca^{2+} is bound to intracellular Ca^{2+} buffers [Trafford AW et al., 1999; Berlin JR et al, 1994]. This is due to the fact that various Ca^{2+} buffers are abundant in cardiac myocytes, e.g., membrane phospholipids, ATP, phosphocreatine, calmodulin, parvalbumin, myofibril TnC, myosin, SERCA2a, and calsequestrin in the SR. Among them, SERCA2a and TnC are the predominant Ca^{2+} buffers [Trafford AW et al., 1999; Berlin JR et al., 1994; Robertson SP et al., 1981]. Furthermore, Ca^{2+} binding to its buffers is a dynamic process during twitch (e.g., 30-50% of Ca^{2+} binds to TnC and dissociate from it during Ca^{2+} transients) and the change in Ca^{2+} binding causes additional "release" of free Ca^{2+} to the cytosol, results in the alterations of intracellular Ca^{2+} concentration. Many factors can be the sources of post-transcriptional modifications of myofilament proteins, which influence myofilament Ca^{2+} buffering and myofilament Ca^{2+} sensitivity [Schober T *et al.,* 2012; Briston SJ *et al.,* 2012; Patel BG *et al.*,2013].

Myofilament Ca^{2+} sensitization is defined as the same peak value of $[Ca^{2+}]_i$ with a much greater force development. Proof that there is no increase in the calcium transient as the sarcomere length increases is provided by direct measurements. The favored explanation for the steep length-tension relation of cardiac muscles is length-dependent activation, whereby an increase in calcium sensitivity is the major factor explaining the steep increase of force development as the initial sarcomere length increases. In cardiac muscle, even at 80% of the maximal length, only 10% or less of the maximal force is developed. Rodriguez EK et al. have tested this prediction by relating sarcomere length changes to volume changes of the intact heart [Rodriguez EK et al., 1992]. On the other hand, reduced myofilament Ca^{2+} sensitization is the same force development with higher intracellular Ca^{2+} level, such as in various disease conditions, including hypertension [Jin CZ et al., 2013].

All of E-C coupling components are highly regulated by post-translational modifications coupled to phosphorylation, nitrosylation, oxidation, sumoylation, glycosylation, and probably other “ylations”

were not yet defined. More and more research is revealing the protein targets of such modifications particularly as they appear central to the evolution of contractile failure in many forms of heart disease. It has become necessary to analyze interactions between myofilament and Ca^{2+} handling proteins for thorough investigation of myocyte E-C coupling and cardiac function.

Cardiac mitochondrial activity, oxygen consumption rate and ATP production

Carbohydrates and FAs are essential in cardiac metabolism through glucose oxidation or β-oxidation, respectively. In this process electrons from NADH(H) or $FADH_2$ are transferred to O_2 by electron carriers organized in four respiratory complexes that can be tightly assembled in supramolecular structures termed as super-complexes or respirations [Acin-Perez R et al., 2008]. In particular, electrons are funneled from complex I and II of the respiratory chain to complex IV where more than 90% of the intracellular oxygen is reduced to water. The energy released from the flux of electrons from reducing to oxidizing components of the respiratory chain is converted into proton pumping from the mitochondrial matrix into the intermembrane space, generating a proton motive force (Δp) which is composed of membrane potential (Δψm) and pH gradient (ΔpHm) components. The utilization of this proton motive force allows ATP synthesis, protein import for mitochondrial biogenesis and maintenance of ion homeostasis. A decrease in the amount of functional respirations has been suggested to underlie the defective respiration in mitochondria isolated from failing hearts [Rosca MG et al., 2010].

Compared to glucose, fatty acids are an inefficient energy substrate because cardiac efficiency is a measurement of the amount of oxygen required for a given amount of cardiac work. The full oxidation of 1 glucose molecule requires 6 O_2 and produces 31 ATP. Palmitate oxidation requires 23 O_2 but only produces 105 ATP. However, the actual decrease in cardiac efficiency due to elevated fatty acid oxidation rates is actually much higher than expected due to calculated ATP/O_2 ratios (up to 30% instead of 10%), suggesting that other mechanisms are also involved in fatty acids reducing cardiac

efficiency [Lopaschuk GD et al., 2010]. One of these mechanisms includes FA inhibition of glucose oxidation, a more efficient metabolic pathway (see Randle Cycle section). FAs also inhibit adenine nucleotide transferase (ANT) thereby inhibiting the transport of ATP from the mitochondrial matrix to the outside the mitochondria [Lopaschuk GD et al., 2010]. A third mechanism involves FA activation of sarcolemmal calcium channels. More ATP has to be used to keep the cytosolic calcium levels at normal levels instead of being used for work [Huang JM et al., 1992]. Further, futile cycles may also contribute to FA induced cardiac inefficiency. These futile cycles include uncoupling proteins (UCP) and the cycling of fatty acids between triacylglycerol and acyl CoA moieties [Lopaschuk GD et al., 2010]. Oxygen consumption is a useful dynamic index assessing mitochondrial activity and ATP measurement is an assessment of the outcome of cardiac metabolism in the heart.

Nitric oxide and cardiac metabolism

Nitric oxide (NO) plays important regulatory roles in FA metabolism in the mammalian myocardium from normal heart [Recchia FA et al., 1999]. NO modulates oxygen consumption by inhibiting the complexes I, II and IV of the mitochondrial electron transport chain [Drapier JC et al., 1988]. Some studies indicate that NO facilitates glucose utilization or stimulates total substrate oxidation, by activating a cGMP-dependent protein kinase [Young ME et al., 1998]. Furthermore, reduced bioavailability of NO has been implicated in impaired FA metabolism and cardiac performance in failing heart [Recchia FA et al., 1998; Recchia FA et al., 1999].

Cardiac nitric oxide synthase

Constitutive NOS is well known to be involved in the regulation of myocardial function. Under physiological conditions, NOS-derived nitric oxide regulates almost all aspects of cellular function, including increasing myocardial distensibility, reducing stiffness, lowering diastolic pressure, facilitating relaxation, FA uptake (Shah AM et al., 2000). NO is generated by NOS, which catalyzes

the conversion of L-arginine to L-citrulline in a reaction that requires O_2 and cofactors (Palmer RM et al., 1988). Currently, three distinct isoforms of NOS have been identified and cloned: two are constitutively expressed in cells (neuronal NOS or nNOS or NOS1, endothelial NOS or eNOS or NOS3) and their activities are generally regulated posttranslationally by calmodulin binding as a result of changes in intracellular Ca^{2+} concentration ($[Ca^{2+}]_i$) and phosphorylation.

nNOS is firstly purified from rat cerebellum (Bredt DS et al., 1990) and is the major source of NO in the nervous system. Using nNOS gene knockout mice model, nNOS in the SR is shown to atte nuate cardiac contraction by inhibiting LTCC activities (Sears CE et al., 2003; Sun J et al., 2006). On the other hand, nNOS facilitates basal cardiac relaxation predominantly by increasing phospholamba n Ser^{16} phosphorylation, improving SERCA activity and Ca^{2+} reuptake into SR (Zhang YH et al., 20 08). In addition, nNOS exerts its effects, at least in part, by modulating the activities of NOX and xan thine oxidoreductase [Kinugawa S et al., 2005; Zhang YH et al., 2009], thereby controlling the redox homeostasis in the myocardium. [Zhang YH et al., 2014]. Recently, nNOS have been demonstrated to regulate the mitochondria function and the myocardial contractility in both healthy and ischemic h earts [Zhang YH, Casadei B, 2012]. Research from our own group and that of others has shown that NO modulates myocardial inotropy, facilitates lusitropy and is important in the maintenance of cardi ac function under pathological stimuli [Niu X et al., 2012; Zhang YH et al., 2014; Zhang YH, Casade i B, 2012]. Recent consensus is that nNOS is the predominant isoform of NOS that regulates intracell ular Ca^{2+} handling, myofilament Ca^{2+} sensitivity and contractility in cardiac myocytes from healthy a nd hypertensive rats [Niu X et al., 2012; Zhang YH et al., 2014; Zhang YH, Casadei B, 2012]. Recen tly, we have shown that nNOS protein expression and activity are upregulated in LV myocytes from hypertensive rat hearts whereas eNOS protein expression is reduced [Jin CZ et al., 2013]. nNOS facil itated myocardial lusitropy by reducing myofilament Ca^{2+} sensitivity; myofilament Ca^{2+} desensitizati on, *in turn*, increased Ca^{2+} handling [Jin CZ et al., 2013; Zhang YH, 2016].

During disease progression, β-oxidation is down-regulated and glycolysis becomes the predominant source of energy (metabolic shift) for the preservation of the pumping function of the heart [Lopaschuk GD et al., 2010]. In the failing myocardium, both glucose- and FA-dependent metabolism are limited, energy deficiency becomes an important precursor for impaired myocardial contraction. Until recently, the effects of FA on cardiac contractility in healthy and hypertensive rat hearts remain undetermined. nNOS was protective in cardiomyocyte contractility, may be mediating FA β-oxidation and mitochondria activity. Furthermore, the roles of nNOS on cardiac contraction in the presence of FA and the underlying mechanisms in healthy and hypertensive rat hearts needs to be explored.

eNOS is firstly described and purified from the bovine vascular endothelium (Pollock JS et al., 1991) and studied extensively in many other tissues afterwards. eNOS is mostly localized at the sarcolemmal membrane where it is bound to caveolin 3 (Feron O et al., 1996). eNOS activity was thought to be principally regulated by intracellular Ca^{2+}; however, more recent evidence has suggested phosphorylation at Serine 1177 (Ser^{1177}) residue and activation of the enzyme by the serine-threonine kinases. NO production by eNOS has been implicated to be essential in FA oxidation in mitochondria. Recently, we have shown that nNOS is up-regulated in LV myocytes from hypertensive hearts, whereas eNOS protein expression was reduced. Recently, nNOS has been demonstrated to regulate Ca^{2+} homeostasis, mitochondria function and myocardial contractility in both healthy and diseased heart (Zhang YH, Casadei B, 2012; Kinugawa et al., 2005, Zhang YH et al., 2014).

There is evidence that NO delivery by eNOS may play a role in the regulation of energy production and fatty acid utilization by muscle. Le Gouill et al. measured oxygen consumption in $eNOS^{-/-}$ and control mice, the mean was significantly lower in $eNOS^{-/-}$ mice than in control mice. Additional evidence showed that in $eNOS^{-/-}$ mice the decreased mitochondrial β-oxidation was related to the lack of eNOS activity, while modulation of NO availability (Le Gouill et al.2007). In this context, I consider that eNOS is predominant in cardiac β-oxidation and metabolism. NO has been implicated in FA

uptake and utilization in the myocardium from normal heart; conversely, reduced bioavailability of NO has been associated with impaired FA metabolism and cardiac performance in failing heart.

Le Gouill et al. measured oxygen consumption in $eNOS^{-/-}$ and control mice, the mean was significantly lower in $eNOS^{-/-}$ mice than in control mice, proves that in $eNOS^{-/-}$ mice the decreased mitochondrial β-oxidation was related to the lack of eNOS activity [Le Gouill E et al., 2007]. However, the modulation of myocardial metabolism by endothelium-derived NO may be one of an important aspect. A decrease in NO production is involved in the pathophysiological modifications that occur in heart failure and diabetes. Disease states is associated with altered cardiac metabolism that contributes to the evolution of the disease process. Since NO is involved in controlling mitochondrial respiration and cardiac metabolism [Trochu JN et al., 2000], in this context, I consider that eNOS is predominant in the fatty acid metabolism in LV myocytes.

S-palmitoylation is an important post-translational modification that affects the translocation and the activity of target proteins in the cells, and the reversible nature of palmitoylation provides a potential mechanism for protein shuttling between intracellular compartments [Linder ME et al., 2007]. eNOS is known to be palmitoylated [Liu J et al., 1996] and it is possible that the activity of eNOS is altered to play a part in fatty acid-dependent β-oxidation in cardiac myocyte and regulate myocardial contractility. Recently, we have shown that eNOS protein expression is reduced in Ang II-induced hypertensive myocardium [Jin CZ et al., 2013]. Reduced NO bioavailability is able to impair cardiac metabolism and reduce the capacity of fatty acid oxidation [Hamilton DJ et al., 2016; Lopaschuk GD et al., 2010]. I hypothesize that PA regulation of myocyte contraction is impaired due to the lack of eNOS palmitoylation in hypertensive heart. Here, I aimed to identify whether eNOS is palmitoylated by PA in LV myocytes and how this post-translational modification affects eNOS activity (eNOS phosphorylation) in healthy and HTN heart.

Taken together, the main aim of the research is to study the effect of saturated FA supplementation on myocyte excitation-contraction coupling and mitochondrial activity in healthy and hypertensive rat

hearts. In addition, the roles of cardiac nNOS and eNOS in FA-dependent regulation of myocyte contraction are analyzed in more detail.

Materials & Methods

Animals

Sprague-Dawley rats (12 wk old, male) were used in this study. In some experiments, rats were subjected to Ang II infusion subcutaneously using osmotic minipumps for 4 wks. Those animals were paired with a sham-operated group. Briefly, rats (of 8 wk old, male) were anesthetized with isoflurane (2.5 %). An osmotic minipump (Alzet model 2004, DURECT Corporation, San Francisco, California, USA.) containing Ang II (200 μl, 6 mM, infusion rate 125 ng/min/kg) was implanted in the midscapular region under sterile condition. Sham-operated animals underwent the same surgical procedure, except for no pump insertion. Blood pressures were measured by Non-Invasive Blood Pressure System, tail-cuff method (CODA, Torrington, CT, USA). Rats were warmed at 37 ºC for 15 min before measurement; each value used in analysis was the mean of ten estimates. Control rats were confined to their cages for an equivalent period of time in the same room of treadmill running.

eNOS knockout mice (21- to 25-wk-old male) were provided by Professor Goo Taeg Oh's Laboratory (Ewha Womans University, Seoul, Korea). All mice including C57BL/6J wild type mice were raised and maintained at the animal facility of Seoul National University College of Medicine.

The study protocol was in accordance with the Guide for the Care and Use of Laboratory Animals published by the US National Institutes of Health (NIH Publication No. 85-23, revised 1996), and also conforms to the Institutional Animal Care and Use Committee (IACUC) in Seoul National University (IACUC approval No.: SNU-101213-1; SNU-110629-5; SNU-160119-4-1).

Blood Pressure and LV myocyte dimensions in sham and hypertensive rats.

Both systolic and diastolic blood pressures (SBP and DBP) were increased from 1 week following Ang II infusion (125ng/min/kg) and continuously increased and heart rate was progressively slower up to the period studied. At 4 weeks, SBP, DBP and heart rate were significantly different between

sham and HTN (Table 1). The diastolic sarcomere length was decreased but the width of LV myocytes was not affected in HTN (Table 1). Membrane capacitance (C_m) of LV myocytes (in whole-cell patch clamp technique) was increased in HTN.

Table 1. Heart rate, Blood pressure, LV myocyte dimensions, Cell Capacitance in sham and hypertensive rats.

Characteristics	Sham			HTN			
	Sham value	(heart, n)	(cell, n)	HTN value	(heart, n)	(cell, n)	*p value*
Heart rate (bpm)	465.971±4.224	39		419.124±3.754**	40		< 0.0001
SBP (mmHg)	125.332±1.701	39		165.650±4.660**	40		< 0.0001
DBP (mmHg)	93.702±1.488	39		124.787±3.754**	40		< 0.0001
Cell width (μm)	27.658±0.494	24	124	28.066±0.838	22	51	0.3322
Cell sarcomere length (μm)	1.783±0.008	21	27	1.751±0.008*	20	24	0.0031
Cell Capacitance (pF)	182.060±6.417	25	70	196.765±5.259*	22	63	0.0413

SBP indicates systolic blood pressure and DBP, diastolic blood pressure.
* $p < 0.05$ compared with sham ;
** $p < 0.0001$ compared with sham ;
Values are expressed as means ± SEM

Table 1. Blood Pressure and LV myocyte dimensions in sham and hypertensive rats.

Both systolic and diastolic blood pressures were increased 1 week after Ang II infusion (125ng/min/kg) and continuously increased up to the period studied (Table 1). In addition, heart rate was significantly lower in hypertensive rats. As shown previously, the width of LV myocytes was not affected in HTN but the diastolic sarcomere length was decreased in HTN (Table 1).

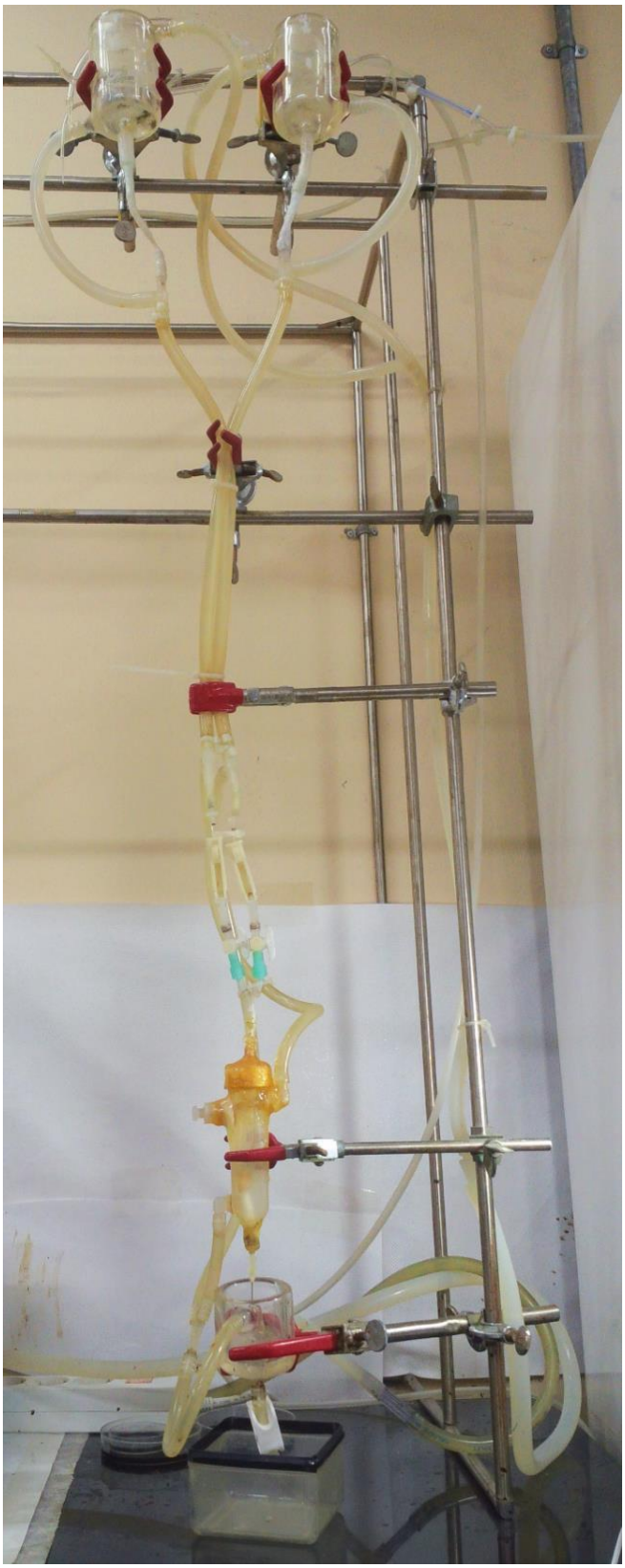

Figure 1 Langendorff perfusion system

Isolation of left ventricular myocytes

LV myocytes were isolated enzymatically by Langendorff perfusion system as recently described [Zhao ZH, Jin CL, Jang JH, Wu Y N, Zhang YH (2016)]. Briefly, the rats were anesthetized with pentobarbital sodium (30 mg/kg, i.p.) and the hearts were extracted and rapidly mounted onto the Langendorff perfusion system (Figure 1). The isolated heart was perfused with nominal Ca^{2+}-free Tyrode solution for 10 minutes (in mM: NaCl 135, KCl 5.4, $MgCl_2$ 3.5, glucose 5, HEPES 5, Na_2HPO_4 0.4, Taurine 20 ; pH titrated to 7.40 using NaOH), followed by a further 8 minutes with the same solution with enzymes added (collagenase type 2, 1 mg/ml, Worthington Biochemical Co.; protease, 0.1 mg/ml, bovine serum albumin (BSA) 1.67 mg/ml; Ca^{2+} 0.05 mM). LV free wall was isolated and placed in a separate flask containing fresh collagenase type 2-containing solution for 8 minutes (oxygenated and maintained at 37◦C). Myocytes were harvested following a further 10-minute digestion period, washed and re-suspended in *storage* solution (in mM: NaCl 120, KCl 5.4, $MgSO_4$ 5, $CaCl_2$ 0.2, Na-pyruvate 5, glucose 5.5, Taurine 20, HEPES 10, D-mannitol 29, pH titrated to 7.40 using NaOH). The myocyte

suspension was stored at room temperature and cells were used within 8 hours of isolation. A portion of LV myocytes were kept in high K^+ and low Cl^- Kraft-Brühe solution for patch clamp experiments (in mM: HEPES 10, KOH 70, L-gutamate 50, KCl 55, Taurine 20, KH_2PO_4 20, EGTA 0.5, $MgCl_2$ 3, Glucose 20, pH titrated to 7.30 using KOH) at 4 ◦C and myocytes were used within 8 hrs.

Measurement of LV myocyte contraction, Ca^{2+} transients & myofilament Ca^{2+} sensitivity

Isolated LV myocytes were superfused with Tyrode solution containing (in mM: NaCl 141.4, KCl 4, NaH_2PO_4 0.33, $MgCl_2$ 1, HEPES 10, Glucose 5.5, $CaCl_2$ 1.8, mannitol 14.5; pH titrated to 7.40 using NaOH) in the recording bath mounted on the stage of a high-resolution inverted microscope (Diaphot 200, Nikon, JP). Changes in sarcomere length and $[Ca^{2+}]_i$ transients were measured in LV myocytes by using a video-sarcomere detection system (IonOptix Corp). For $[Ca^{2+}]_i$ measurement, LV myocytes were pre-incubated with a $[Ca^{2+}]_i$ sensitive fluorescent dye, acetoxymethyl ester of Fura 2-AM (2 μM) in Tyrode solution containing 250 μM Ca^{2+} for 15 minutes in the dark (room temperature). After sedimentation, the supernatant was removed and LV myocytes were washed in Tyrode solution containing 500 μM Ca^{2+} for 10 minutes. The myocytes were kept in fresh Tyrode solution containing 500 μM Ca^{2+} before being used. Fura 2 AM-loaded myocytes were excited at wavelengths of 360nm and 380nm. The emission fluorescence was reflected through a barrier filter (510 ± 15nm) to a photomultiplier tube.The Fura-2 ratios of the F_{360}/F_{380} was analyzed as the relative changes of $[Ca^{2+}]_i$ (Figure 2).

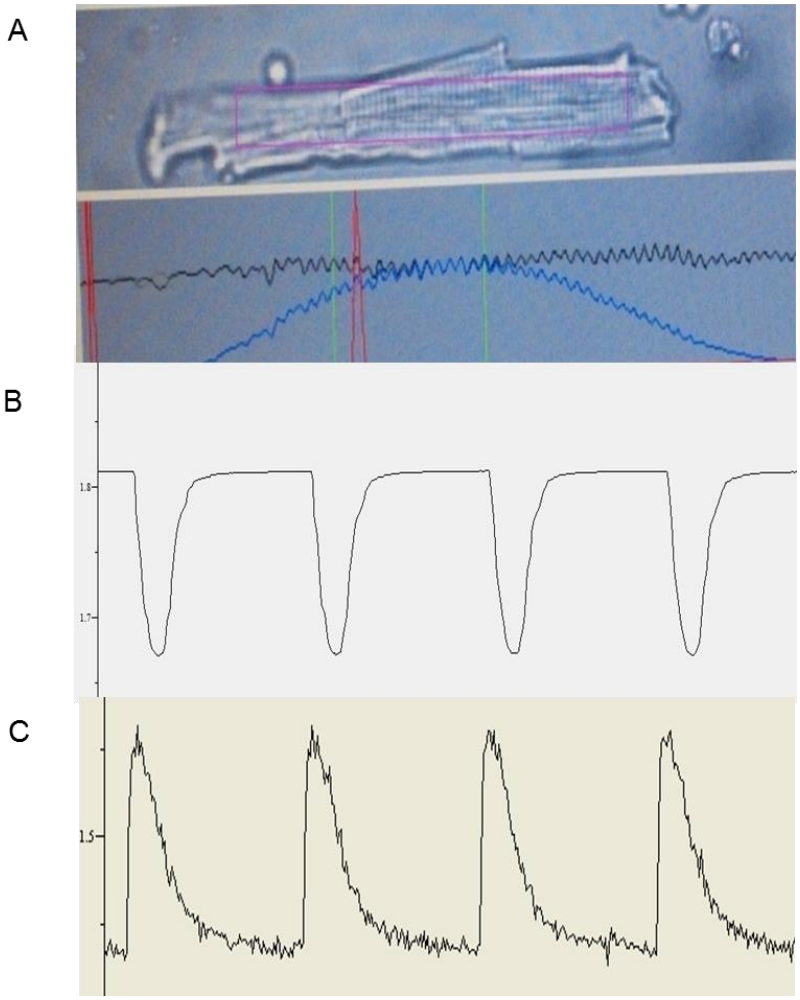

Figure 2. Measurement of sarcomere shortening and the Fura-2 ratio (indicative of the intracellular Ca^{2+} level) in isolated myocyte using IonOptix software.

A. The top image is a Fura-2 AM loaded LV myocyte and the averaged sarcomere length are displayed on the computer. In the lower panel, the black line is the average of each horizontal pixel line within the purple region of interest. The blue line is the same data zeroed at each end. The red line is the fast Fourier transform (FFT) power spectrum, which represents the number of signals the FFT has calculated. One sharp peak means a clean sarcomere recording. **B&C.** Simultaneous recordings representative raw trace of sarcomere length and the Fura-2 ratio in response to field stimulation (2Hz).

In some cells, sarcomere shortening and Fura-2 ratio were recorded simultaneously and phase-plane diagram of Fura-2 ratio *vs.* sarcomere length was used to assess the myofilament Ca^{2+} sensitivity between sham and HTN. The rightward shift of the Fura-2 - sarcomere length trajectory during late relaxation of the twitch contraction indicates reduced myofilament response to Ca^{2+}. The $[Ca^{2+}]_i$ required for half relaxation (EC_{50}) was analyzed to quantify the relative changes in the myofilament Ca^{2+} sensitivity (Figure 2). Measurements from at least 10 steady state contractions were averaged for each intervention. All experiments were carried out at 36 ± 1 ◦C and field-stimulated at 2Hz [Zhao ZH et al., 2016].

Measurement of oxygen consumption rate (OCR) from LV myocytes

OCR was measured using a fluorescence-based oxygen sensor (NeoFox, Ocean Optics) connected to a phase measurement system (Instech). The sensor was calibrated every week according to the manufacturer's instructions. Briefly, isolated LV myocytes (density: 2 x 10^4/ml) were suspended in normal Tyrode's solution and was placed in a sealed chamber (300 μL). Record oxygen level in the chamber over 30 min period (37^{o}C) followed by 5 min recordings with carbonyl cyanide-4-(trifluoromethoxy) phenylhydrazone (FCCP, 20μM) to evaluate maximum OC of the myocytes in the chamber. Changes in the OCR relative to the maximal OC with PA with and without nNOS inhibitor were calculated over 30 min-period in sham and in HTN.

NO production

NO production was detected indirectly by measuring nitrite content in LV myocytes using NO assay kit (Sigma, Griess Reagent System). Briefly, LV myocytes were homogenized in HEPES Buffer solution (in mM: NaCl 141.4, KCl 4, NaH_2PO_4 0.33, $MgCl_2$ 1, HEPES 10, Glucose 5.5, $CaCl_2$ 1.8, mannitol 14.5, mixtures of phosphatase inhibitors and protease inhibitors, pH titrated to 7.40 using NaOH). After assaying the protein content with Bradford protocol, 50 μl of the supernatant of lysates were added to wells and mixed with 50 μl of sulfanilamide solution and incubated for 5-10 min at room temperature in the dark. The same volume of naphthylethylenediamine dihydrochloride (NED, Sigma) solution was added to the wells and incubated for another 5-10 min at room temperature, protecting from light. Absorbance of the mixture was measured with a microplate plate reader (at 540 nm, PowerWave™ XS Microplate Spectrophotometer, BioTek Instruments, USA). Sodium nitrite (Sigma) was used as a standard.

L-type Ca^{2+} current recording

LV myocytes were transferred to the mounting chamber on the stage of an inverted microscope (Nikon) and perfused continuously with Tyrode solution contains (in mM: NaCl 141.4, KCl 4, NaH_2PO_4 0.33, $MgCl_2$ 1, HEPES 10, Glucose 5.5, $CaCl_2$ 1.8, D-mannitol 14.5, pH titrated to 7.40 using NaOH) at 35–37◦C. Patch pipettes with a resistance of 1.5–2.8 MΩ were used and L-type Ca^{2+} current (I_{Ca}) was recorded in the whole-cell configuration using an Axopatch 200A amplifier (Axon Instruments). I_{Ca} was elicited by 200 ms step depolarization from a holding potential of −40 mV to test potentials ranging from −60 to +40 mV. Steady-state I_{Ca} was assessed during a step to 0 mV at a stimulation frequency of 0.1 Hz. Membrane capacitance (C_m) was measured by applying a −10 mV hyperpolarizing ramp pulse immediately followed by a 10 mV depolarizing ramp of the same duration (100 ms) using the method by Golowasch J *et al* [Golowasch J, Thomas G, Nadim F. (2009)]. The range of membrane capacitance was also monitored directly from the window of Clampex 10.4. Recorded I_{Ca} were normalized to C_m and expressed as I_{Ca} density (in pA/pF). Intracellular pipette solution contains (in mM: CsOH 110, TEA-Cl 20, NaCl 10, HEPES 10, $MgCl_2$ 1, MgATP 5, EGTA 10, Aspartate 110, pH titrated to 7.20 using CsOH, Osmolarity 308 mOsm). Ca^{2+} influx *via* LTCC was compared by calculating the integral of I_{Ca}. The average of I_{Ca} integrals at 0 mV with PA was compared between sham and HTN. Data were analyzed in Clampfit 10.

PET/CT image acquisition and analysis of FA oxidation *in vivo*

^{18}F-fluoro-6-thia-heptadecanoidc acid (^{18}F-FTHA) was synthesized from benzyl-14-(R,S)-tosyloxy-6-thiaheptadecanoate.Three sham and Ang II-induced HTN rats (12 weeks) were involved in the PET imaging study using radiotracer ^{18}F-FTHA in a dedicated small animal PET/CT scanner (eXplore Vista CT, GE Healthcare). Following water and food fasting for 6 hours before PET/CT scanning, rats were anesthetized with 2% isoflurane and 2 L/min oxygen and were placed on the scanning bed with prone position and centered the heart in the field of view (FOV). ^{18}F-FTHA (5.0 ± 1.8 MBq) was administered *via* tail vein as a 0.5 ml bolus. In the small-animal PET/CT system, static

PET image acquisition began 40 minutes after the tracer injection for 5 minutes. A CT scan was acquired for image co-registration after the PET acquisition. On separate days, PET/CT acquisitions with the same protocol were performed 10 minutes after admission of NOS inhibitors *i.v.* SMTC (1mg/kg) or L-NAME (5mg/kg). Two-dimensional ordered-subset expectation maximum (OSEM) algorithm was applied to PET image reconstruction. The reconstructed PET images were analyzed by a software package, AMIDE (ver.1.0.4, Stanford University, Palo Alto, CA). After drawing a spherical volume-of-interest (VOI) covering the entire heart, LV myocardium (0.55 cm^3-sized) of highest uptake was segmented in the VOI, in which mean uptake value of ^{18}F-FTHA was measured. The liver was chosen as a reference organ to calculate myocardium-to-liver ratio (MLR), for which mean uptake value of the liver was measured from a spherical VOI (0.57 cm^3-sized). [Hernandez AM et al., 2013; Ohira H et al., 2015]

Measurement of intracellular pH (pH_i)

Temporal intracellular H^+ was measured using a membrane permeant acetoxymethyl ester form of the fluorescent H^+-sensitive indicator, SNARF-1 AM (10 μM, 5–10 min, Molecular Probes, Eugene, OR). All experiments were performed at 37 ℃. In some experiments, pH buffer capacity was increased with $NaHCO_3$ (12.98 mM) + CO_2 (2.9 %) instead of HEPES in the perfusion solution to examine the effect of pH on myocyte responses to PA.

ATP production

Intracellular ATP level was determined using luminescence measurement of LV myocytes (ATP Bioluminescent Assay Kit, Sigma-Aldrich, Saint Louis, MO, USA). Briefly, LV myocytes were incubated in HEPES buffer solution (in mM: NaCl 141.4, KCl 4, NaH_2PO_4 0.33, $MgCl_2$ 1, HEPES 10, Glucose 5.5, $CaCl_2$ 1.8, mannitol 14.5, pH 7.4 NaOH). Cells ($1x10^5$ /ml) were added to 200 μL of mammalian cell lysis solution (Tris-acetate buffer and 10 % Trichloroacetic acid was lysis buffer) and

vortex the cell suspension tube for 10 minutes. Supernatant (100 μL) was added to 96 well white microplate and ATP assay mix solution was added to the wells in dark adapt stand at room temperature for 3 minutes. Take an aliquot of the ATP standard solution and prepare a dilution series in Tris-acetate buffer from a concentration of 2×10^{-4}M down to blank.

S-palmitoylation of eNOS

For blocking the free thiol, LV myocytes were diluted with blocking buffer (100 mM HEPES, 1 mM EDTA, 2.5 % SDS, 1 % MMTS, pH 7.5) and incubated at 40ºC for 4 hrs. Following acetone precipitation, the pellet was rinsed five times with 70 % cold acetone. Following acetone precipitation, the pellet was rinsed five times with 70 % cold acetone and added in binding buffer (100 mM HEPES, 1.0 mM EDTA, 1% SDS, pH 7.5). When employed, an equal volume of freshly prepared 2M NH_2OH (pH adjusted to 7.0 with 2M NaCl) was added followed by prewashed thiopropyl-Sepharose (Sigma-Aldrich, Seoul, Korea). Binding reactions were carried out on a rotator at room temperature for 2.5 hrs. Each of supernatant was saved as the "total input." Resins were washed at least 7 times with binding buffer. For immunoblot analysis, elution was performed using 2X Laemmli sample buffer supplemented with 100 mM DTT and heated to 95°C for 5 min. The obtained sample was separated *via* SDS-PAGE and immunoblotting with eNOS. *S*-palmitoylation of eNOS was compared in LV myocytes before and after palmitic acid treatment [Forrester MT, Hess DT, Thompson JW, Casey PJ (2011)].

Immunoblotting

LV myocytes were lysed in lysis buffer contained 50 mM Tris-HCl (pH 7.4), 100 mM NaCl, 1% Triton X-100, 5 mM EDTA with protease/phosphatase inhibitor cocktail (Roche Diagnostics, Mannhaim, Germany). Cell lysates were then centrifuged at 14,000g for 30 min at 4 °C, and the supernatant were acquired. The protein concentration was determined by the Bradford assay. The

protein sampled were mixed with Laemmli sample buffer, resolved by 6 % and 10 % SDS-PAGE, and transferred to poly-vinylidene difluoride membranes in 25 mM Tris, 192 mM glycine, and 20 % methanol. Membranes were blocked in 1X TBS containing 1 % Tween-20 and 5 % bovine serum albumin (blocking solution) for 1 hr at room temperature with gentle rocking, and incubated overnight at 4 °C with anti-eNOS (BD Transduction Laboratories), eNOS-Ser^{1177} (BD Transduction Laboratories, San Francisco, California, USA), GAPDH (Santa Cruz, Dallas, Texas, USA) primary antibodies followed by relevant secondary antibodies after washing. Blots were developed by ECL plus Western blotting detection reagents (Amersham Bioscience, Piscataway, NJ, USA). Membranes were stripped using Pierce restore western blot stripping buffer (Thermo Scientific, Waltham, MA, USA) for 30 min, and the relative densities were calculated after normalizing the intensity of each sample band to that of GAPDH.

Chemicals

Angiotensin II (Ang II, 6 mM) was injected to the osmotic mini-pumps. S-methyl-L-thiocitrulline acetate salt (SMTC, 100 nM, Sigma) and Nω-nitro-L-arginine methyl ester hydrochloride (L-NAME, 1 mM, Sigma) were used to target nNOS and NOS activity. Sodium nitroferricyanide (III) dehydrate (SNP, 10 μM, Sigma) was an exogenous NO donor. Tiron (1 mM, Sigma) scavenges superoxide. Palmitic aicd (PA, 100 μM, Sigma) was used to stimulate fatty aicd oxidation. ETO (100 μM, sigma or 10 μM, Cayman) was used to inhibit the acitivy of CPT-1. 2-bromopalmitic acid (2BP, 100 μM, Sigma) was an inhibitor of *S*-palmitoylation. Carbonyl cyanide-*4*-(trifluoromethoxy) phenylhydrazone (FCCP, 20 μM, Sigma) was an uncoupling agent induced maximal oxygen consumption rate. Sodium hydrosulfite or hyposulfite ($Na_2S_2O_4$, Sigma) was used in calibration for OCR by minimizing O_2 level in the solution. ^{18}F-FTHA was used to observe FA upteke metabolism *in vivo*.

Statistics

Data are reported as mean ± SEM. N indicates the number of cells used. For all comparisons, cells were obtained from a minimum of three hearts per treatment group per protocol. Data were analyzed using student's paired and unpaired *t* test. A value of $p<0.05$ was considered to be statistically significant.

Results

Part I Effects of fatty acid supplementation on LV myocyte contraction in sham and HTN rats

First, the parameters of angiotensin II-induced HTN rats are as follow: both systolic and diastolic blood pressures were increased 1 week after Ang II infusion (125ng/min/kg) and continuously increased up to the period studied (Table. 1).

At 4 weeks, systolic and diastolic blood pressure were increased in HTN than sham, (systolic blood pressure: mmHg, $p<0.001$, sham 125.332 *vs.* HTN 165.65 sham n=39 and HTN n=40; diastolic blood pressure: mmHg, $p<0.001$, shams 93.702 *vs.* HTN 124.787). Heart rate was significantly lower in HTN (heart rate : beats/min, $p<0.001$, with sham 419.124±3.754 *vs.* HTN 465.971±4.224). Dimensions of LV myocytes were measured to assess whether myocardial hypertrophy was induced by systemic hypertension in these rats. As shown in table 1, dimensions of LV myocytes were measured (LV myocyte width, μm, $p=0.3322$, sham 27.658 *vs.* HTN 28.066, sham n=124 and HTN n=51). Diastolic sarcomere length was decreased in HTN (LV myocyte sarcomere length, μm, $p=0.0031$, sham 1.783±0.008 *vs.* HTN 1.751±0.008, sham n=27 and HTN n=24). Membrane capacitance (C_m) of LV myocytes (in whole-cell patch clamp technique) was increased in HTN (C_m, pF, $p=0.0413$, sham 182.060±6.417 *vs.* HTN 198.765, sham n=70 and HTN n=63).

The sarcomere shortening and intracellular Ca^{2+} transient were different in LV myocytes from sham and HTN.

The basal LV myocytes shortening was not different between two groups (contraction: $p=0.1$, sham *vs.* HTN, n=14 and 13, Figure 3A&B). Systolic $[Ca^{2+}]_i$ amplitude was significantly increased in HTN compared to that in sham (systolic $[Ca^{2+}]_i$: $p=0.02$, sham vs. HTN, n=13 and n=12, Figure 3C&D). Simultaneous recordings of sarcomere length and $[Ca^{2+}]_i$ and the phase-plane plot of the two

parameters were compared between sham and HTN to analyze the myofilament Ca^{2+} sensitivity**.** The EC_{50} (Fura-2 ratio at 50% relaxation) is the qualitative comparison of myofilament Ca^{2+} sensitivity between sham and HTN. The trajectory loop shifted to the right and EC_{50} was higher in HTN, suggesting myofilament Ca^{2+} desensitization (EC_{50}: $p = 0.034$, sham vs. HTN, n=13 and n=12, Figure 3E&F).

PA increased LV myocyte contraction in sham but not in hypertension

The effects of FA on contraction in isolated LV myocytes were examined in sham and in HTN. As shown in Figure 4A-C, PA (100 μM) significantly increased sarcomere shortening in LV myocytes from sham ($p<0.0001$, control *vs.* PA, n=13). In contrast, the positive inotropic effect of PA was absent in HTN ($p=0.1$, control *vs.* PA, n=12). To examine the involvement of β-oxidation in the effect of PA on myocyte contraction, an inhibitor of carnitine palmitoyltransferase 1 (CPT-1), ETO, was used in both models. Pre-treatment of LV myocytes with ETO (10 μM, 30 min-1hr) abolished PA-enhancement of myocyte contraction in sham ($p=0.37$, control *vs.* PA with ETO, n=5, Figure 4D&E) without an effect at basal level. Furthermore, ETO did not affect myocyte contraction in HTN with or without PA ($p=0.1$, control *vs.* PA with ETO, n=5, Figure 4E&F).

Sustained pressure-overload in hypertension is able to increase reactive oxygen species (ROS) and induce oxidative stress in the myocardium [Briones AM et al., 2010]. In addition, FAs have been implicated in the myocardial oxidative stress and modulate myocyte contractility in murine heart [Fauconnier J et al., 2007]. To investigate whether increased ROS in HTN may have prevented PA-regulation of myocyte contraction, the effect of PA on LV myocyte was re-evaluated after incubation with a potent ROS scavenger, tiron (1 mM). Tiron pre-incubation did not affect myocyte contraction with PA in sham (sarcomere shortening, $p<0.0001$, tiron *vs.* tiron+PA, n=8, Figure 5A&C) or in HTN ($p=0.24$, tiron *vs.* tiron+PA, n=7, Figure 5B&C), excluding the role of ROS in preventing PA-induced

myocyte contraction in HTN.

PA regulation of mitochondrial activity in sham and in HTN

I performed experiments to observe whether PA affects mitochondrial activity (oxygen consumption rate, OCR) in LV myocytes from sham and HTN rats. As shown in Figure 6A&B, PA increased basal OCR in both groups (p=0.004 and p=0.004, n=10 and n=9, respectively). Pre-treatment of LV myocytes with ETO (10 μM, 30 min-1hr) prevented PA induced increases of OCR in sham (p=0.045, ETO *vs.* ETO+PA, n=6 and n=9) and in HTN (p=0.01, ETO vs. ETO+PA, n=5 and n=11). Similarly, *in vitro* analysis of ATP level in LV myocytes showed that PA increased intracellular ATP level and ETO prevented the effect in sham (p=0.024, control vs. PA, n=4; p=0.0162, PA *vs.* ETO+PA, n=4, Figure 6C). In HTN, PA did not increase intracellular ATP level, however, ETO significantly reduced intracellular ATP level in the presence of PA in HTN (p=0.209, control *vs.* PA, n=4; p=0.048, PA vs. ETO+PA, n=4, Figure 6D).

PA increased LV myocyte $[Ca^{2+}]_i$ in sham but not in HTN

I detected the responses of $[Ca^{2+}]_i$ with PA in sham and HTN. As shown in Figure 7A&B, PA significantly increased systolic $[Ca^{2+}]_i$ in sham ($[Ca^{2+}]_i$: p=0.002, n=11), but the effect was absent in HTN ($[Ca^{2+}]_i$: p=0.13, n=13, Figure 7C&D).

Next, I examined PA regulation of $I_{Ca\text{-}L}$ in sham and HTN. $I_{Ca\text{-}L}$ was stimulated by a step depolarization protocol at 0 mV for 200 ms (holding potential, -40 mV). As shown in Figure 8, PA reduced peak $I_{Ca\text{-}L}$ at 0 mV in both groups. In addition, PA did not change $I_{Ca\text{-}L}$ integral in sham (Figure 9 A&C) but reduced it in HTN (Figure 9B&D). This is due to the facts that both slow and fast inactivation time of $I_{Ca\text{-}L}$ were prolonged by PA in sham but only slow inactivation time of $I_{Ca\text{-}L}$ was slowed in HTN (Figure 9E&F). I tested whether PA regulates NCX activity in both groups. PA increased inward I_{NCX} at -80 mV in sham (Figure 10A&C). In HTN, PA did not change forward mode

of I_{NCX} at -80 mV and but increased reverse mode of I_{NCX} at +50 mV (Figure 10B&D).

PA modulated myofilament Ca^{2+} sensitivity in sham and in HTN

Myofilament Ca^{2+} sensitivity is a vital regulator of myocyte contraction and relaxation. Importantly, alterations in the myofilament Ca^{2+} sensitivity are involved in Ca^{2+} binding to TnC and Ca^{2+} buffering capacity in the myofilament, consequently affects intracellular Ca^{2+} homeostasis [Briston SJ et al., 2014; Huke S et al., 2010; Khan SA et al., 2003]. Therefore, I detected that phase-plane plot of the Fura-2 ratio *vs.* sarcomere length of the LV myocyte by PA from sham and HTN (Figure 11A&B)**.** EC_{50} (Fura-2 ratio at 50% relaxation) is the qualitative comparison of myofilament Ca^{2+} sensitivity between sham and HTN groups by PA. The trajectory loop is shifted to the right by PA and EC_{50} tends to be lower in sham (Figure 11C). In HTN, myofilament Ca^{2+} sensitivity was maintained unaffected before and after PA supplementation (Figure 11C).

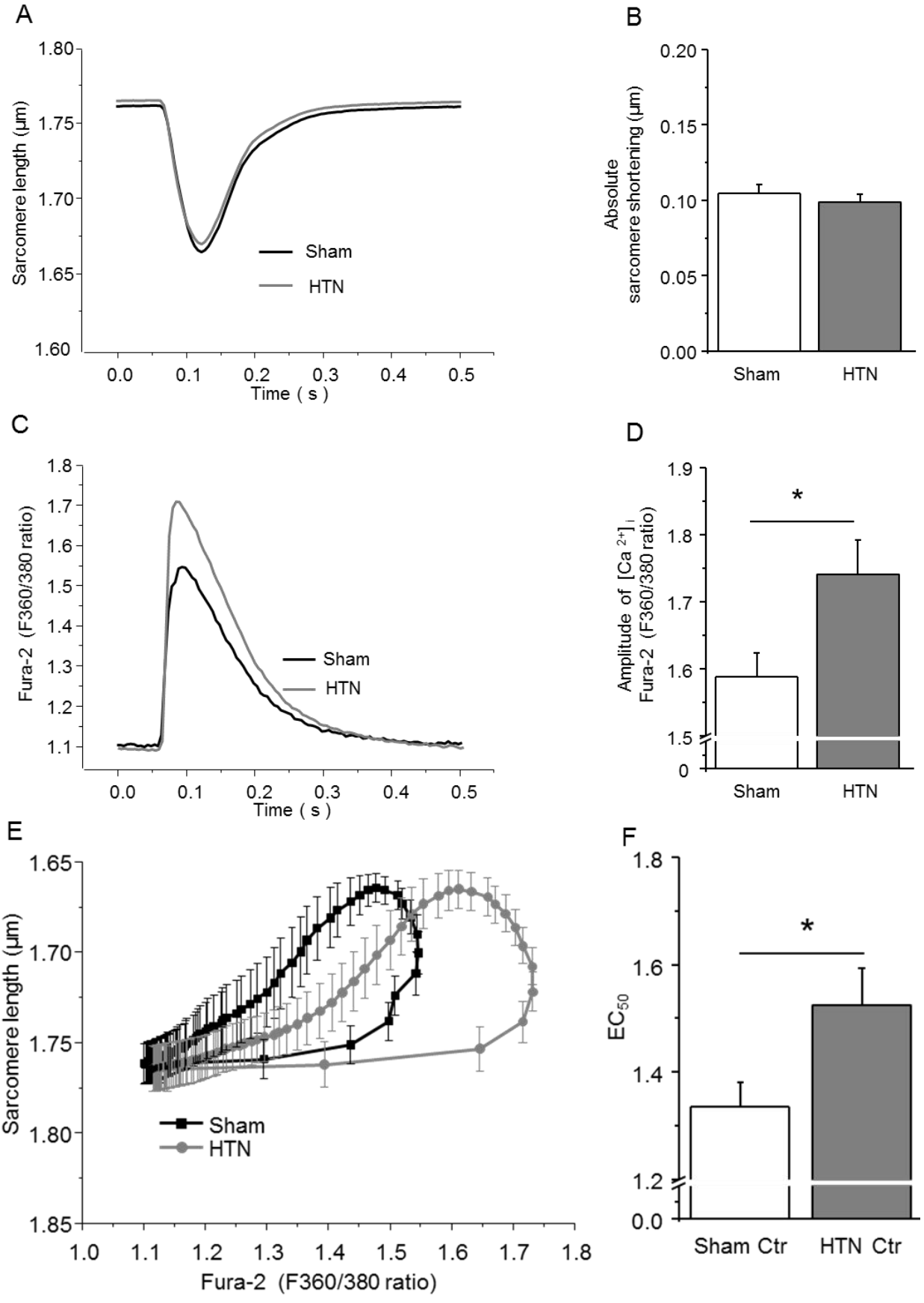
A
Sarcomere length (μm)
Time (s)
Sham
HTN
B
Absolute sarcomere shortening (μm)
Sham
HTN
C
Fura-2 (F360/380 ratio)
Time (s)
Sham
HTN
D
Amplitude of [Ca 2+]i Fura-2 (F360/380 ratio)
*
Sham
HTN
E
Sarcomere length (μm)
Fura-2 (F360/380 ratio)
Sham
HTN
F
EC50
*
Sham Ctr
HTN Ctr

Figure 3. Measurement of sarcomere shortening, intracellular Ca^{2+} transient and myofilament Ca^{2+} sensitivity in LV myocyte from sham and HTN

A & B. Raw representative traces and the averages of sarcomere shortening in sham and HTN. Not effect in control from both groups. **C & D.** Raw representative traces and the averages of increased intracellular Ca^{2+} ($[Ca^{2+}]_i$ transients) in sham and in HTN. $[Ca^{2+}]_i$ transient was significantly increased in HTN. **E.** Phase-plane plot of Fura-2 ratio *vs.* sarcomere length of the LV myocyte from sham and HTN**. F.** EC_{50} tends to be higher in HTN, suggesting myofilament Ca^{2+} desensitization (EC_{50}: $p = 0.034$, sham vs. HTN, n=14 and n=13).

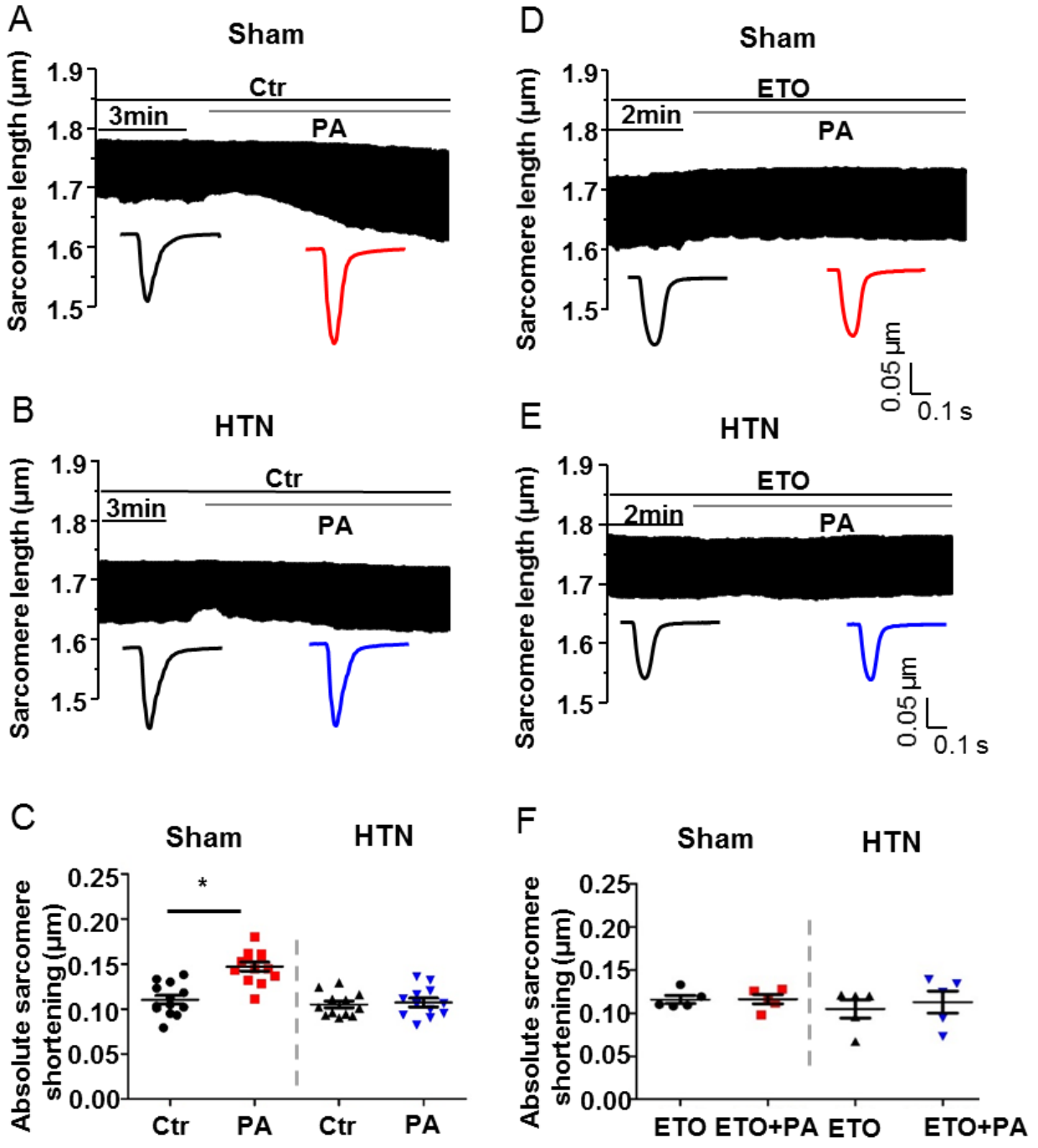

Figure 4. Effects of PA and inhibition of carnitine palmitoyltransferase 1 (CPT-1) on myocyte contraction in sham and HTN

A-C. Raw representative traces and the averages of sarcomere shortening in both groups. PA (100 μM) increased sarcomere shortening in sham but not in HTN. **D-F.** Raw representative traces and the averages of sarcomere shortening following pre-treatment of LV myocytes with ETO (10 μM, 30 min-1hr). ETO abolished PA-enhancement of myocyte contraction in sham with little effect in HTN.

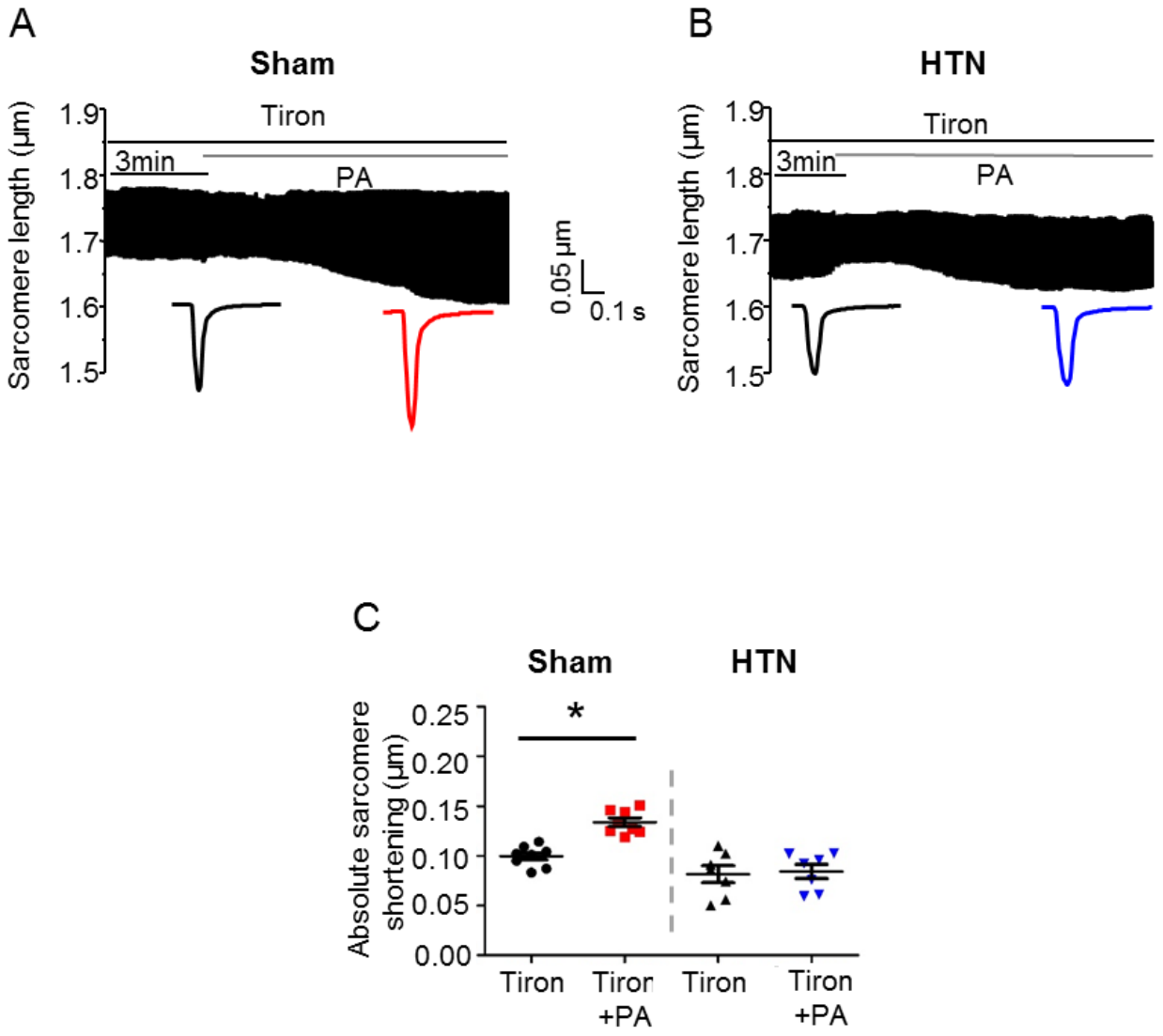

Figure 5. Effects of ROS scavenger, tiron, on PA-regulation of myocyte contraction in sham and in HTN

A-C. Representative raw traces and mean values of sarcomere shortening by PA with tiron (1 mM, 30min-1hr). Sarcomere shortening was remained increased by PA in sham and was unaffected by PA in HTN, despite tiron pre-treatment.

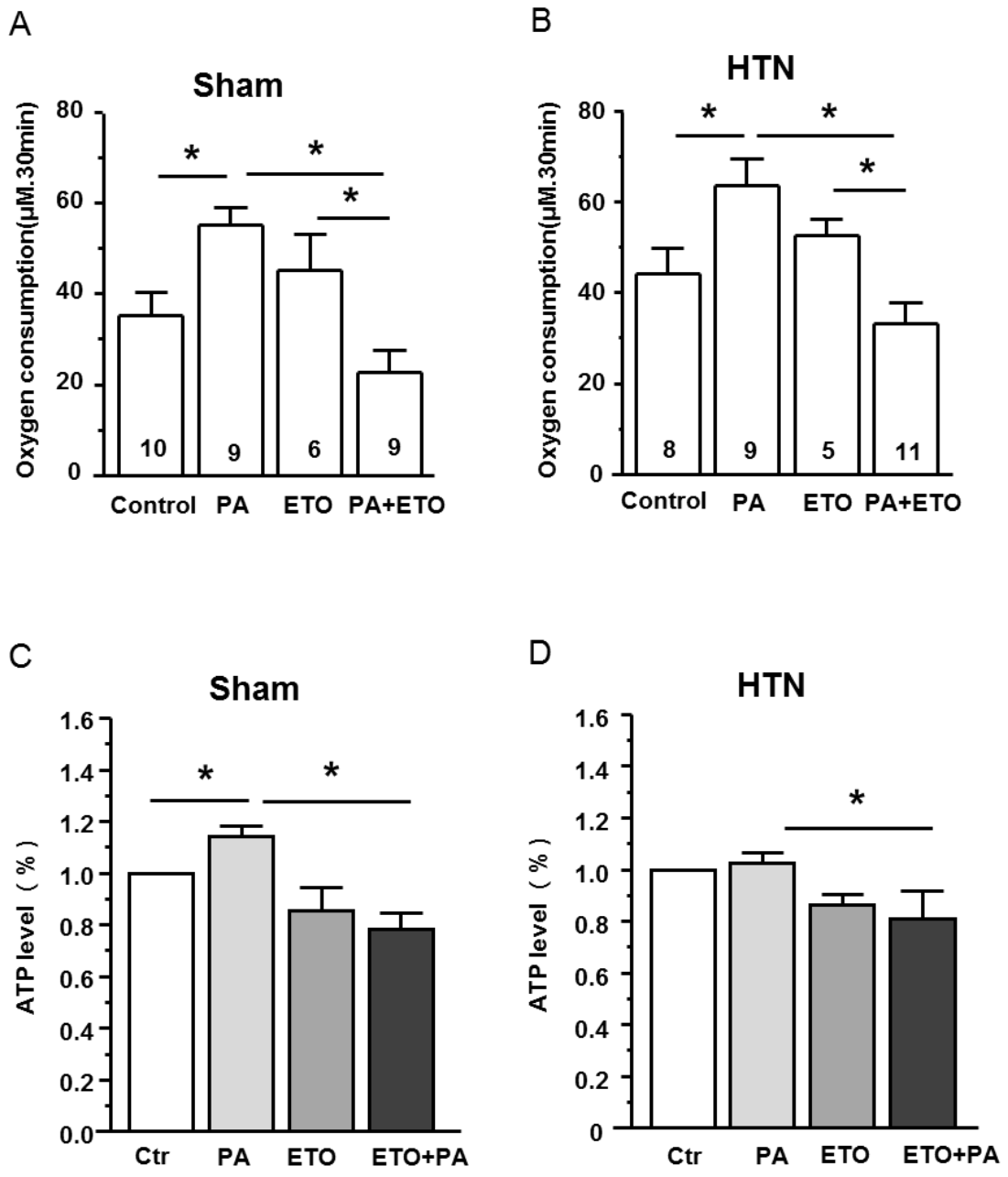

Figure 6. PA regulation of mitochondrial oxygen consumption rate (OCR) and intracellular ATP.

A&B. PA increased OCR in LV myocytes from both sham and HTN rats. Pre-treatment of LV myocytes with CTP-1 inhibitor ETO (10 μM, 30 min-1hr) prevented PA induced OCR in both groups. **C&D**. PA significantly increased intracellular ATP level in sham, which is abolished by ETO (10 μM, 30 min-1hr). In HTN, PA did not affect intracellular ATP but ETO significantly reduced it in the presence of PA.

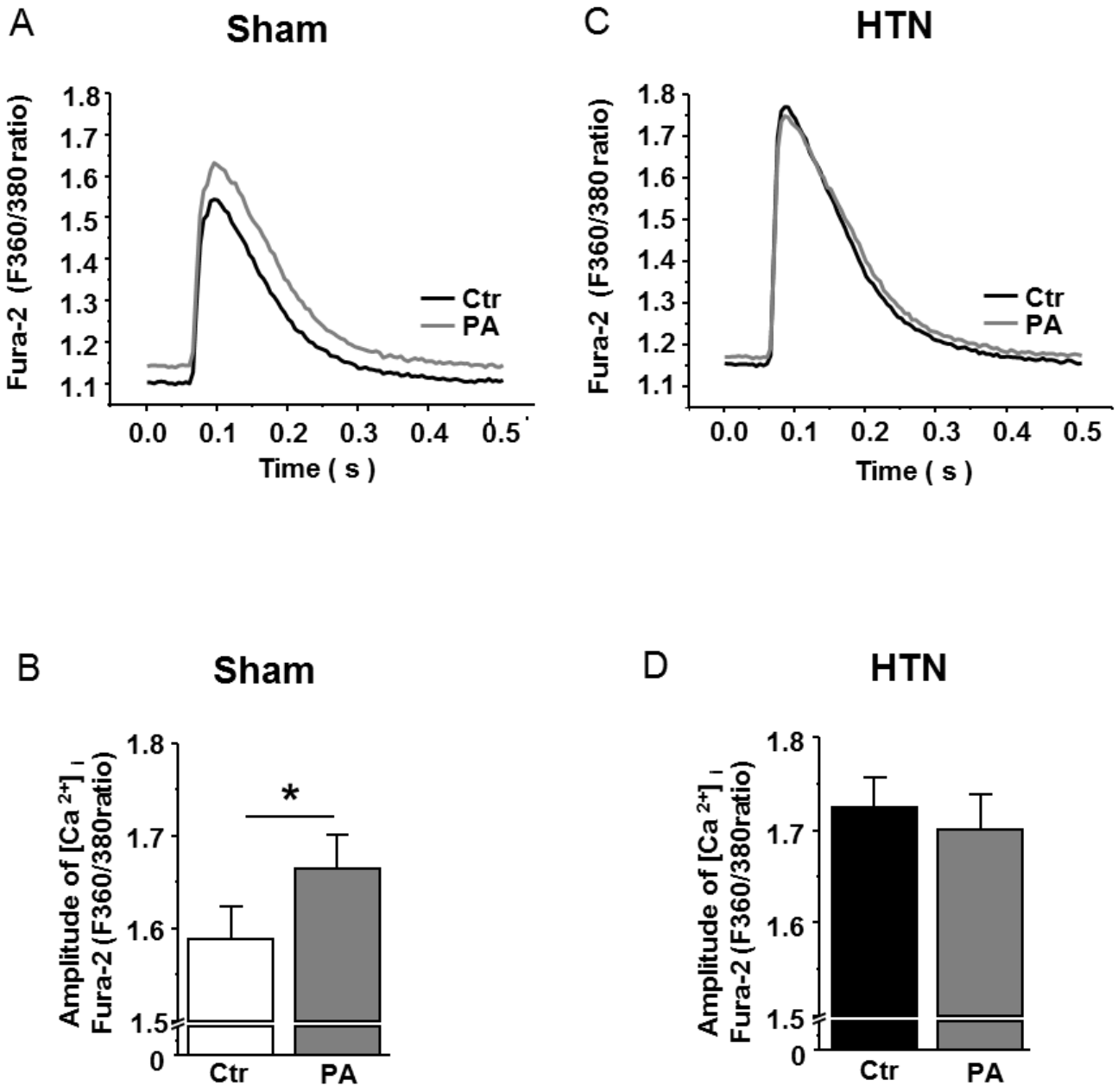

Figure 7. Effects of PA on myocyte $[Ca^{2+}]_i$ transients in sham and HTN

A&B. PA significantly increased systolic $[Ca^{2+}]_i$ in sham. **C&D.** The effect of PA was absent in HTN.

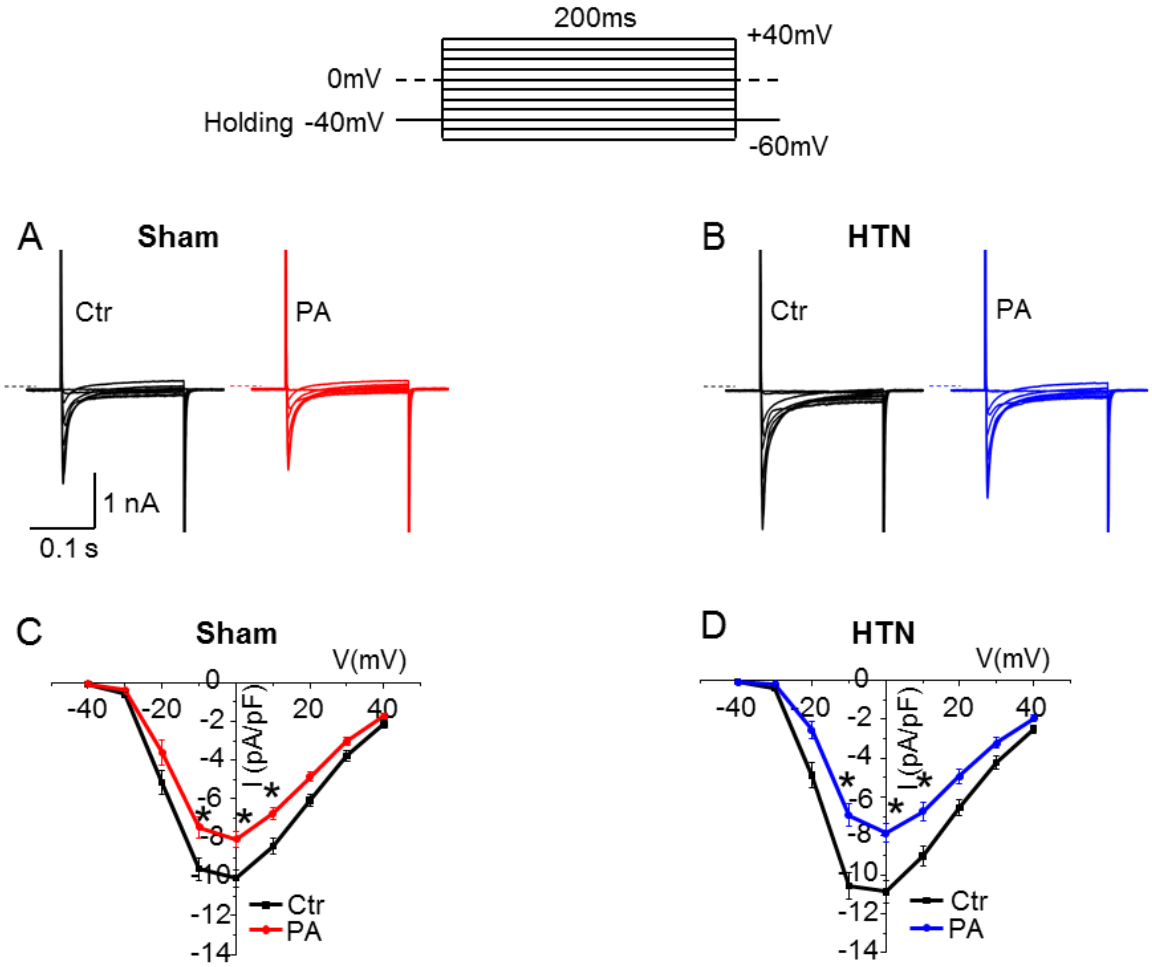

Figure 8. PA regulation of the peak $I_{Ca\text{-}L}$ in sham and HTN.

LTCC was stimulated by a step depolarization protocol from -60 to +40 mV for 200 ms (holding potential, -40 mV). **A&B.** Representative $I_{Ca\text{-}L}$ recordings in sham and HTN. **C&D.** I-V curve with and without PA. PA significantly reduced peak $I_{Ca\text{-}L}$ at 0 mV in both groups.

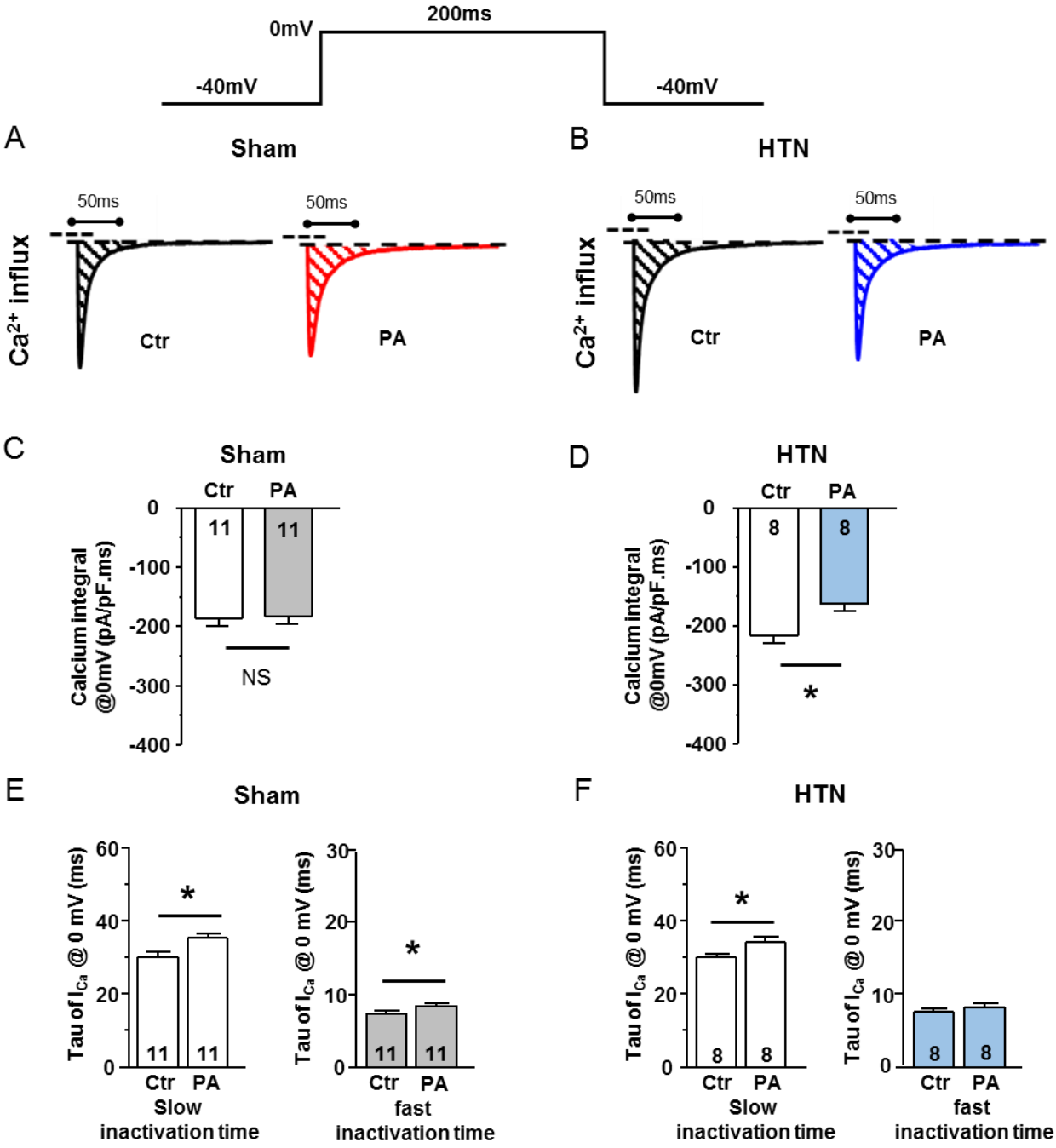

Figure 9. PA regulation of the Ca^{2+} influx through LTCC in sham and HTN.

LTCC was stimulated by a step depolarization protocol at 0 mV for 200 ms (holding potential, -40 mV). **A&B.** Representative peak $I_{Ca\text{-}L}$ at 0 mV in sham and HTN. **C.** PA slightly but significantly reduced peak $I_{Ca\text{-}L}$ at 0 mV but did not change $I_{Ca\text{-}L}$ integral. **D.** PA reduced peak $I_{Ca\text{-}L}$ and $I_{Ca\text{-}L}$ integral at 0 mV in HTN. **E&F.** Slow and fast inactivation time of $I_{Ca\text{-}L}$ was increased by PA in sham. In HTN, only slow inactivation time of $I_{Ca\text{-}L}$ was increased.

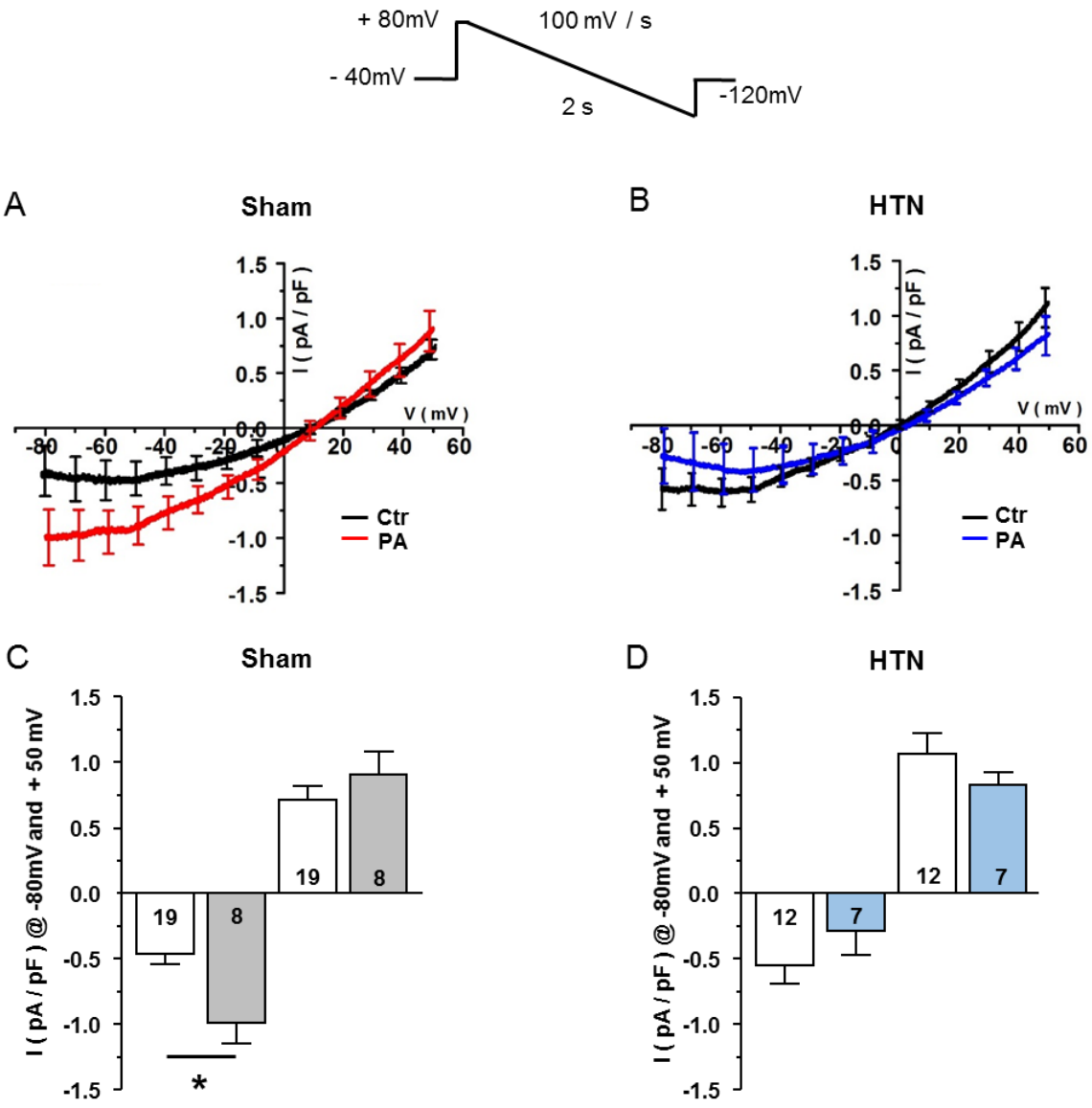

Figure 10. PA regulation of NCX activity in LV myocytes from sham and HTN.

NCX was stimulated by a ramp pulse protocol from +80mV to -120mV for 2000 ms (holding potential, -40 mV). **A&B.** I-V of I_{NCX} in sham and HTN. **C.** PA increased forward mode of I_{NCX} at -80 mV in sham only. **D.** PA did not affect forward or reverse mode of I_{NCX} in HTN.

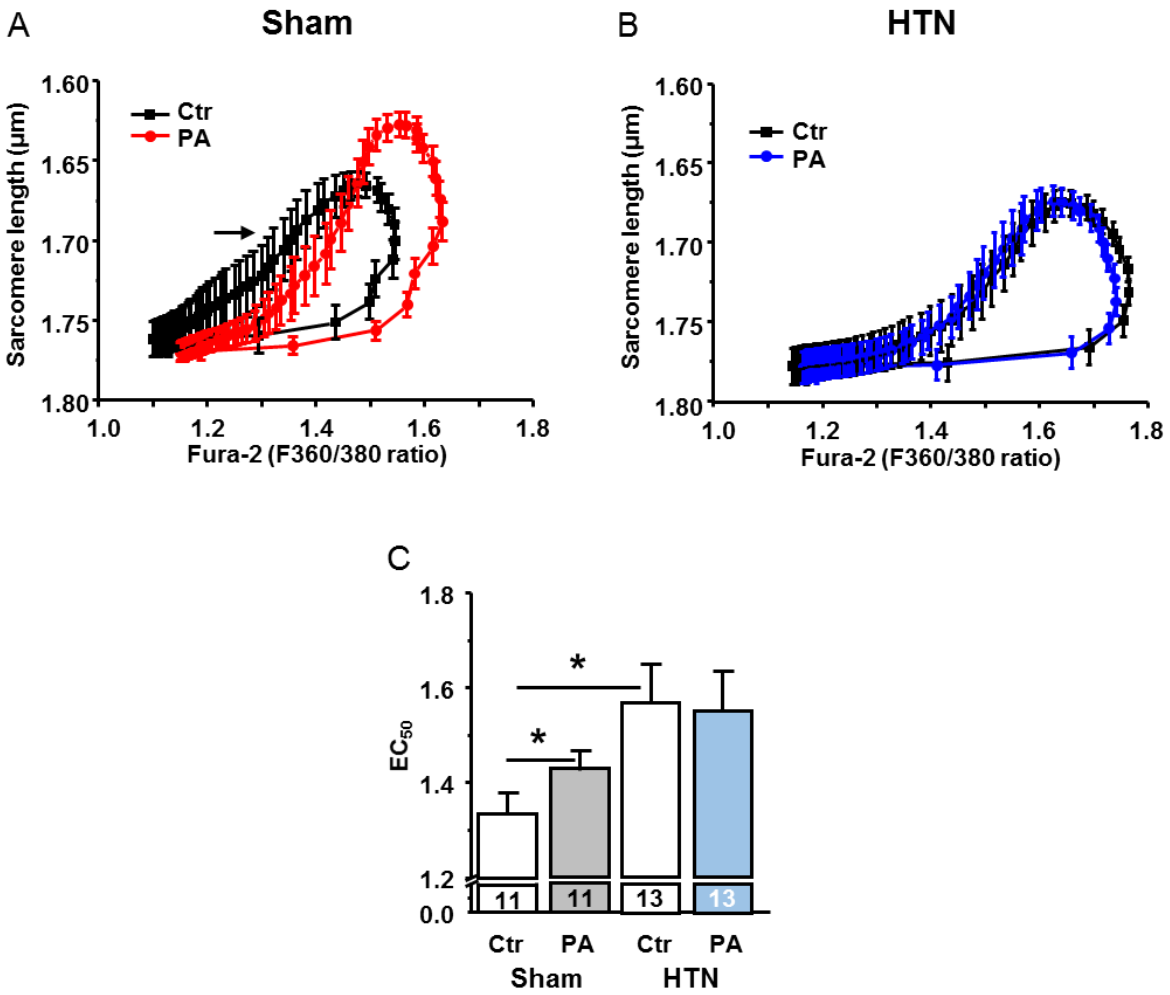

Figure 11. PA regulation of myofilament Ca^{2+} sensitivity in sham and HTN.

A&B. Phase-plane plot of the Fura-2 ratio *vs.* sarcomere length of the LV myocyte by PA from sham and HTN**. C.** The trajectory loop is shifted to the right by PA and EC_{50} tends to be lower in sham. In HTN, myofilament Ca^{2+} sensitivity maintain to by PA,

Part II Neuronal nitric oxide synthase mediates impaired fatty acid-dependent contraction in LV myocytes from hypertensive rat

PA increased nNOS-derived NO in HTN, which in turn, prevents PA-stimulation of myocyte contraction

I aimed to identify PA-regulation of nNOS activity in LV myocytes from sham and HTN rats. As shown in Figure 12A, NO production (relative to control) was slightly but significantly reduced by PA in sham (p=0.03, control *vs.* PA, n=6). nNOS inhibition with SMTC did not affect PA-modulation of NO production (p=0.09, PA *vs.* PA+SMTC, n=6, Figure 12A). In contrast, NO production was increased by PA in HTN (p=0.01, control *vs.* PA, n=5, Figure 12B). SMTC (100 nM, 30 min-1hr) and L-NAME (1 mM, 30 min-1hr) blocked NO increment by PA (p=0.02, PA *vs.* PA with SMTC in HTN; p=0.02, PA *vs.* PA+L-NAME in HTN, Figure 12B), suggesting the role of nNOS.

Figure 12C showed that inhibition of nNOS with SMTC did not affect PA-induced OCR increase in sham (p>0.05, SMTC and SMTC+PA, n=8 and n=10). In HTN, SMTC abolished PA-induced increase in OCR (p<0.05, SMTC and SMTC+PA, n=7 and n=6, Figure 12D). These results suggest that PA-dependent mitochondrial activity is increased in both sham and HTN but this effect is attenuated with nNOS inhibition only in HTN.

Intriguingly, sarcomere shortening of LV myocyte was increased by PA following nNOS inhibition in HTN (SMTC, 100 nM, 30min-1hr; p=0.0005, SMTC *vs.* PA+SMTC, n=10, Figure 12F&G). In contrast, nNOS inhibition exerted no effect on PA-dependent myocyte contraction in sham (p<0.0001, SMTC *vs.* PA+SMTC, n=15, Figure 12E&G). There is no difference in sarcomere shortening with PA between two groups following nNOS inhibition (p=0.1, in sham and HTN with SMTC+PA, Figure 12G). These results suggest that nNOS is important in restricting PA-enhancement of myocyte contraction in HTN.

FA-metabolism and the response to NOS inhibition *in vivo* with PET/CT scanning in LV myocardium

I have examined FA-metabolism and the response to nNOS and NOS inhibition by quantifying ^{18}F-FTHA uptake *in vivo* with PET/CT scanning in LV myocardium from sham and HTN rats. PET/CT images were obtained by using ^{18}F-FTHA in the LV at basal, in the presence of nNOS inhibitor, SMTC (1mg/kg) and L-NAME (5mg/kg). Using the protocol shown in Figure 13A, myocardial ^{18}F-FTHA uptake was not different between two groups at basal (p=0.2382, sham control *vs.* HTN control, n=3 each group, Figure 13B&C). Inhibition of nNOS with SMTC did not affect ^{18}F-FTHA uptake in sham (p=0.187, control *vs.* SMTC) but increased it in HTN (p=0.0284, control *vs.* SMTC). Subsequent infusion of L-NAME increased ^{18}F-FTHA uptake in sham (p=0.0095, control *vs.* L-NAME, n=3, Figure 13B&C) and in HTN (p=0.0397, control *vs.* L-NAME, n=3, Figure 13B&C). These results indicate that basal FA uptake is not different between sham and HTN; nNOS modulates myocardial FA uptake in HTN.

nNOS modulation of Ca^{2+} handling prevents the inotropic effect of PA in HTN

I evaluated PA-regulation of the key parameters of E-C coupling and the responses of these parameters to nNOS inhibition in sham and HTN. First, inhibition of nNOS with SMTC increased peak $I_{Ca\text{-}L}$ with and without PA in sham (p=0.06, control *vs.* SMTC and p=0.01, control *vs.* SMTC+PA, n=11&7, Figure 14A&B) and slowed inactivation kinetics further, compared to those without SMTC application (Figure 14E&F), Accordingly, integral of $I_{\text{-}LTCC}$ was increased after nNOS inhibition with and without PA in sham (p=0.001 and p=0.003, n=11&7, respectively, Figure 15 A&B).

In HTN, inhibition of nNOS with SMTC significantly increased peak $I_{Ca\text{-}L}$ at 0 mV (Figure 14C&D) and slowed tau of $I_{\text{-}LTCC}$ further (Figure 14G&H). Consequently, integral of $I_{\text{-}LTCC}$ was significantly increased following nNOS inhibition with PA in HTN (p=0.001, PA *vs.* SMTC+PA, n=8, at 0 mV,

Figure 15C&D).

Next, I detected the changes in $[Ca^{2+}]_i$ following PA supplementation with and without nNOS inhibition in sham and HTN. As shown in Figure 16, PA significantly increased systolic and diastolic $[Ca^{2+}]_i$ in sham (systolic $[Ca^{2+}]_i$: p=0.002, n=11; diastolic $[Ca^{2+}]_i$: p=0.03, n=11), but the effects were absent in HTN (systolic $[Ca^{2+}]_i$: p=0.13, n=13; diastolic $[Ca^{2+}]_i$: p=0.31, n=13). Inhibition of nNOS with SMTC significantly increased the amplitude of basal $[Ca^{2+}]_i$ in sham (p=0.04, Figure 16A,C,D) and PA no longer increased $[Ca^{2+}]_i$ amplitude in the presence of SMTC in sham (p=0.3, n=11, Figure 16A,C,D).

In contrast, SMTC pre-treatment significantly reduced the amplitude of basal $[Ca^{2+}]_i$ in HTN (p=0.043, n=13&9, Figure 16B&E). In addition, PA significantly increased $[Ca^{2+}]_i$ in the presence of SMTC (p=0.009, SMTC *vs.* SMTC+PA, n=9, Figure 16B&E). These results indicate that PA increased $[Ca^{2+}]_i$ in sham. nNOS inhibition restores PA-regulation of intracellular $[Ca^{2+}]_i$ in HTN.

Myofilament Ca^{2+} sensitivity with PA before and after nNOS inhibition in sham and HTN

Accordingly, I investigated the changes in the myofilament Ca^{2+} sensitivity by analyzing the relationship between sarcomere shortening and $[Ca^{2+}]_i$ with PA before and after nNOS inhibition in sham and HTN.

As shown in Figure 17A&C, PA shifted the relaxation phase of the sarcomere shortening and $[Ca^{2+}]_i$ relationship to the right and increased EC_{50} in sham (p=0.01, n=11, Figure 17E). Inhibition of nNOS with SMTC reduced myofilament Ca^{2+} sensitivity under basal conditions (EC_{50}, p=0.04, n=11&11, Figure 17B,D,E) and abolished the relationship between sarcomere shortening and $[Ca^{2+}]_i$ with PA (EC_{50}, p=0.2, n=11, Figure 17E).

In contrast, PA did not affect sarcomere shortening and $[Ca^{2+}]_i$ relationship in HTN (EC_{50}, p=0.7, n=13, Figure 18A,C,E). Inhibition of nNOS sensitized the myofilament response to Ca^{2+} in HTN without PA (EC_{50}, p=0.04, n=13&9, Figure 18B,D,E) but PA significantly reduced myofilament Ca^{2+} sensitivity in the presence of SMTC (100 nM, 30 min-1hr) (EC_{50}, p=0.01, n=9, Figure 18E). These results indicate that PA modulates myofilament Ca^{2+} sensitivity in sham and in HTN. nNOS maintains myofilament Ca^{2+} sensitivity in sham but reduces it in HTN, which *in turn*, masks the effects of PA on $[Ca^{2+}]_i$ and myocyte contractility in HTN.

Furthermore, intracellular pH (pH_i) was shown to be gradually decreased with PA (6–8 min) in both groups. Averaged results showed that PA significantly reduced pH_i (p<0.05, p<0.05 n=7, respectively, Figure 19; Figure 20). Increasing pH buffer capacity in PA using $NaHCO_3$ + CO_2 (5 %) weaken the changes in pH_i by PA in sham and in HTN (p>0.05, p>0.05, n=7, respectively, Figure 19; Figure 20).

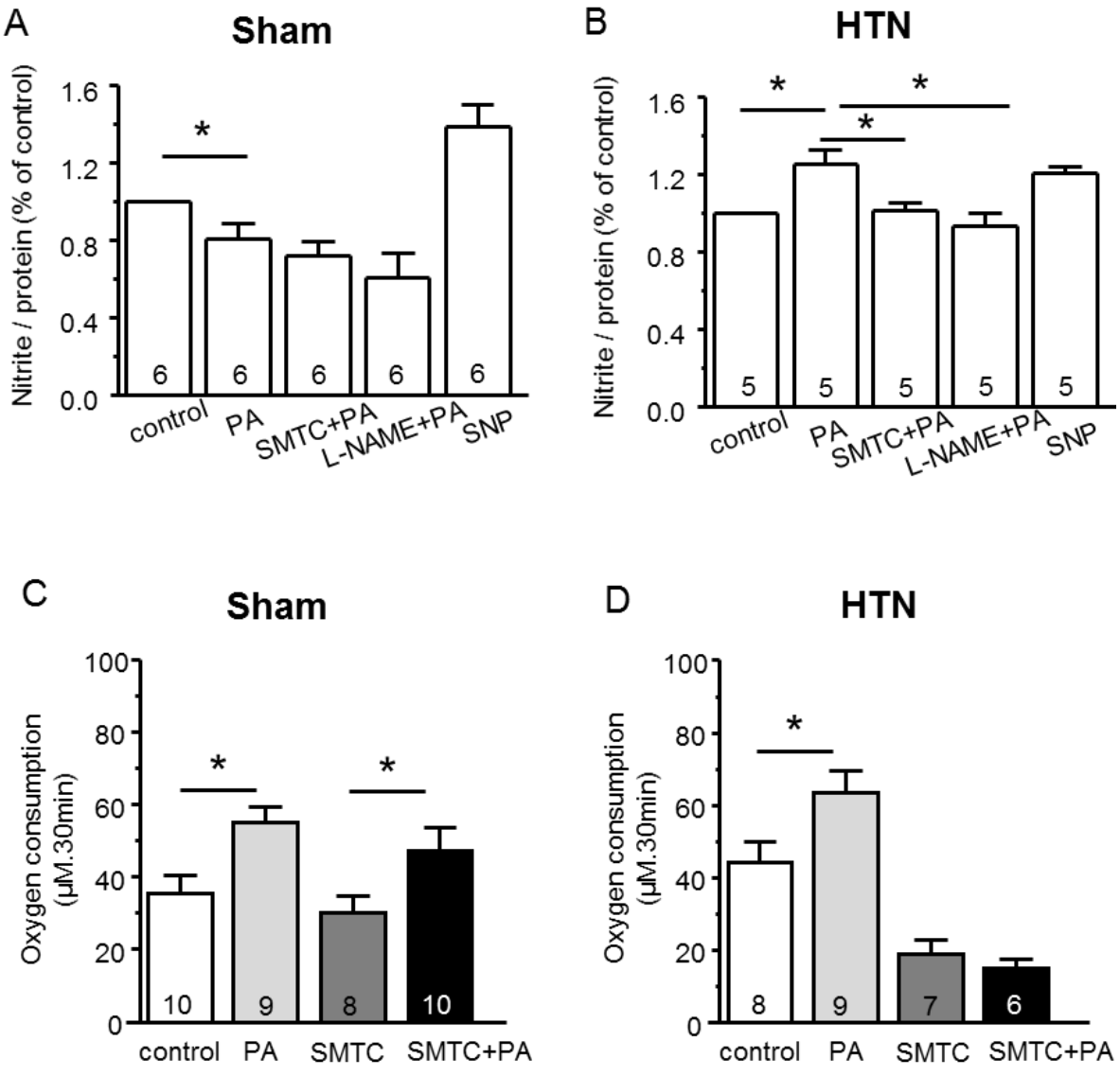

Figure 12. Effects of PA on nNOS production of NO and nNOS regulation of oxygen consumption rate (OCR) and myocyte contraction in sham and HTN.

A&B. NO production (nitrite level relative to control) was significantly increased by PA in HTN, which was prevented by SMTC (100 nM, 30 min-1hr) and L-NAME (1 mM, 30 min-1hr). PA failed to increase NO production in sham. Neither SMTC nor L-NAME affected NO production in the presence of PA. **C&D.** PA increased OCR in LV myocytes from sham and HTN rats. Pre-incubation with SMTC did not affect PA-induced OCR increase in sham. However, SMTC abolished PA-induced increase in OCR in HTN.

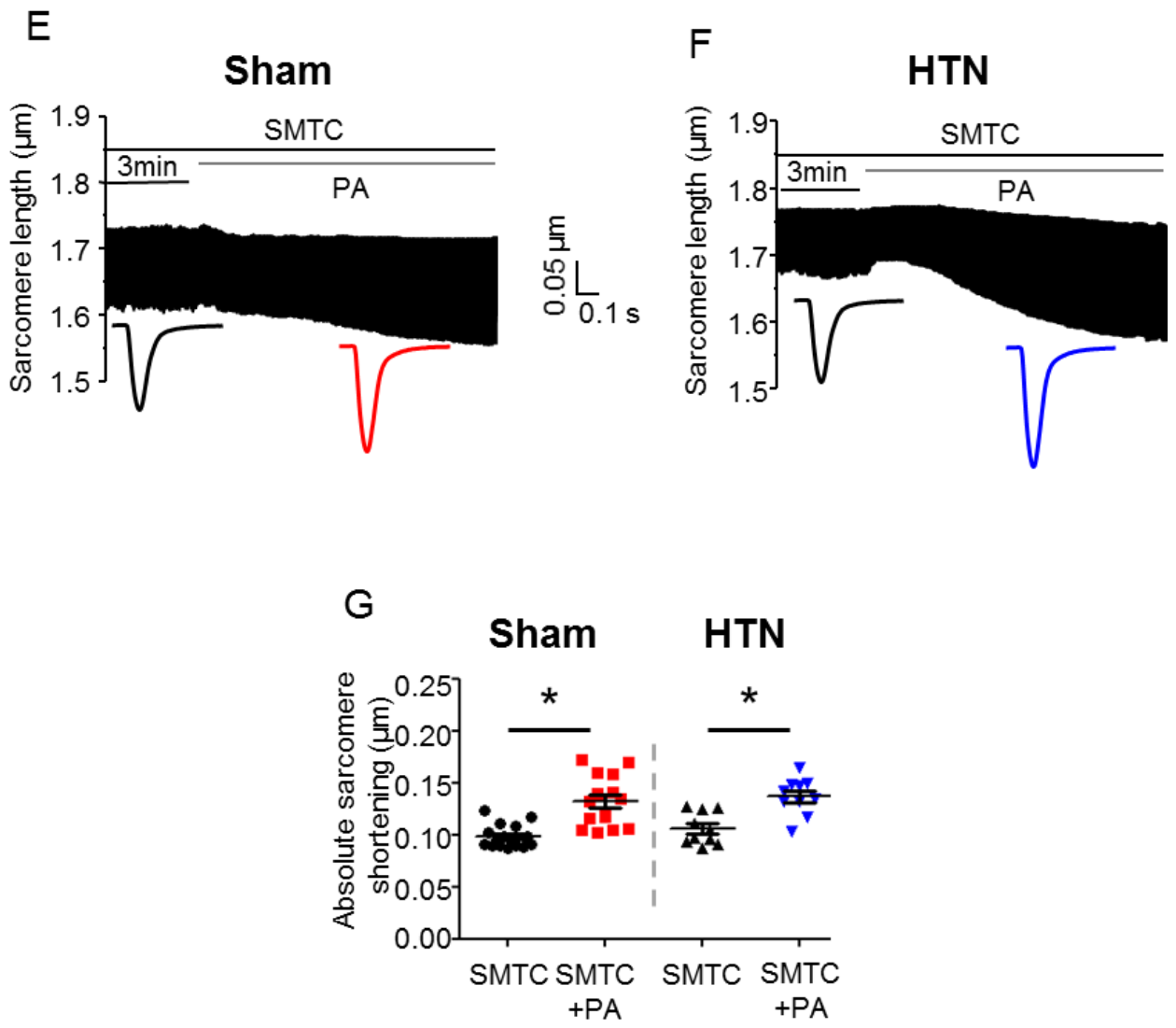

Figure 12. Effects of PA on nNOS production of NO and nNOS regulation of oxygen consumption rate (OCR) and myocyte contraction in sham and HTN.

E-G. Raw representative traces and the averages of sarcomere shortening with PA following pre-treatment of LV myocytes with nNOS inhibitor, SMTC (100 nM, 30-1hr), Myocyte contraction was maintained to be increased by PA with SMTC in sham. However, PA increased sarcomere shortening following SMTC pre-treatment in HTN.

A

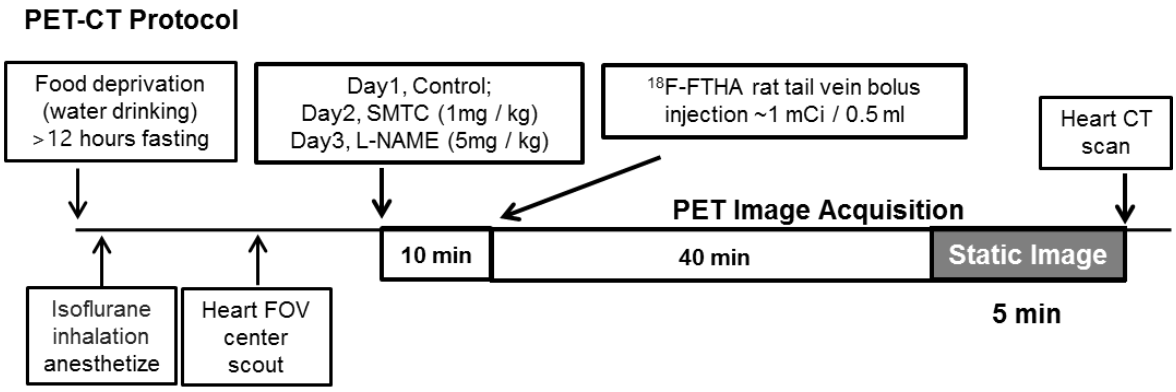
PET-CT Protocol
Food deprivation (water drinking) >12 hours fasting
Day1, Control; Day2, SMTC (1mg / kg) Day3, L-NAME (5mg / kg)
18F-FTHA rat tail vein bolus injection ~1 mCi / 0.5 ml
Heart CT scan
PET Image Acquisition
10 min
40 min
Static Image
5 min
Isoflurane inhalation anesthetize
Heart FOV center scout

B

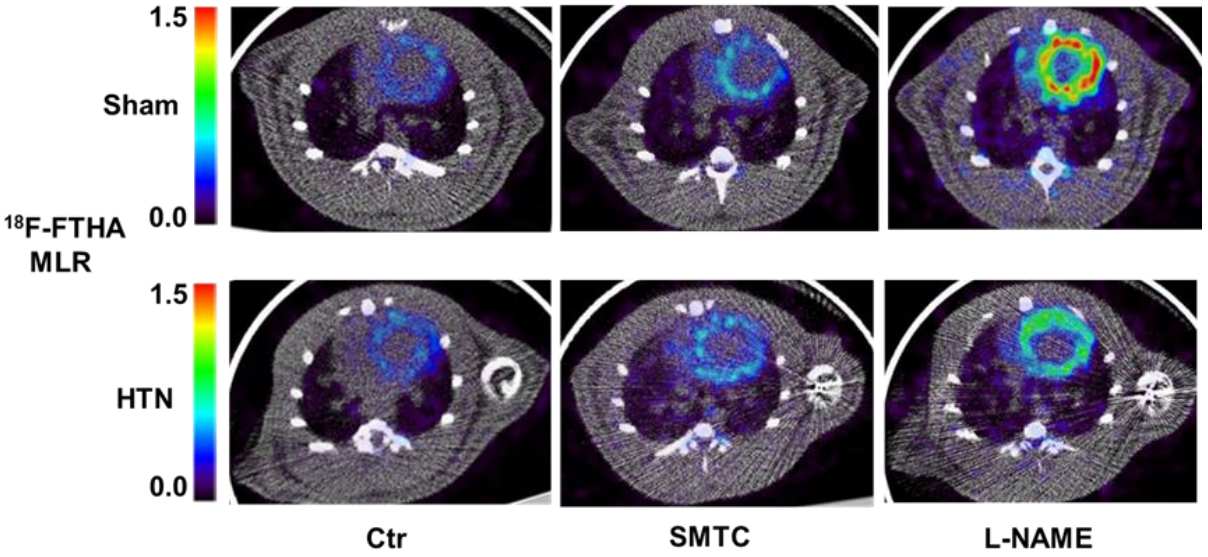
1.5
Sham
0.0
18F-FTHA MLR
1.5
HTN
0.0
Ctr
SMTC
L-NAME

C

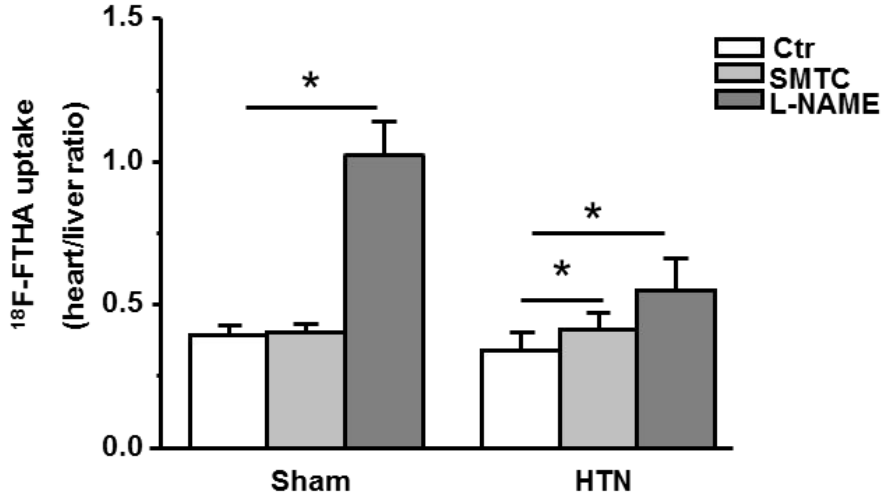
1.5
1.0
0.5
0.0
18F-FTHA uptake (heart/liver ratio)
Ctr
SMTC
L-NAME
*
*
*
Sham
HTN

Figure 13. Examination of FA uptake with PET/CT and the measurement of mitochondrial activity by oxygen consumption rate in sham and HTN rats

A. PET/CT images were obtained by using ^{18}F-FTHA in the LV at basal, in the presence of nNOS inhibitor, SMTC (1mg/kg) and L-NAME (5mg/kg). **B.** Averaged mean values of ^{18}F-FTHA uptake in the myocardium between sham and HTN with and without NOS inhibition. nNOS inhibition induced small but significant increase in ^{18}F-FTHA uptake in HTN only. L-NAME significantly increased ^{18}F-FTHA uptake in both groups, with an effect significantly higher in sham compared to that in HTN.

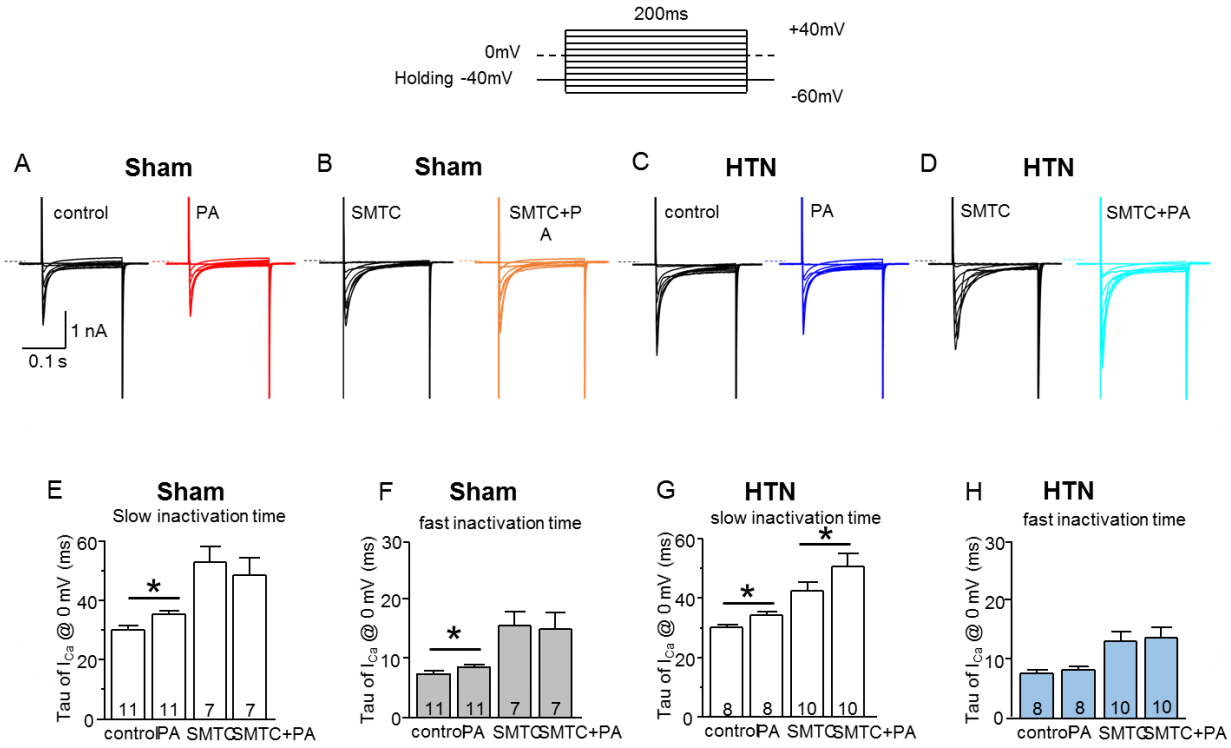

Figure 14. PA regulation of the peak $I_{Ca\text{-}L}$ density and inactivation kinetics with and without nNOS inhibition in sham and HTN.

$I_{Ca\text{-}L}$ was stimulated by a step depolarization protocol from -60 mV to +40 mV (10 mV interval) for 200 ms (holding potential, -40 mV). **A-D** representative $I_{Ca\text{-}L}$ density with and without PA before and after nNOS inhibition (SMTC, 100 nM, 30 min-1hr). PA slightly but significantly reduced peak $I_{Ca\text{-}L}$ density at 0 mV in both groups. nNOS inhibition increased $I_{Ca\text{-}L}$ density at 0 mV and abolished PA-regulation in both groups. **E-H** Inactivation of $I_{Ca\text{-}L}$ was slowed by PA in both groups; nNOS inhibition (SMTC, 100 nM, 30min-1hr) significantly reduce inactivation and abolish PA-dependent responses in sham and in HTN.

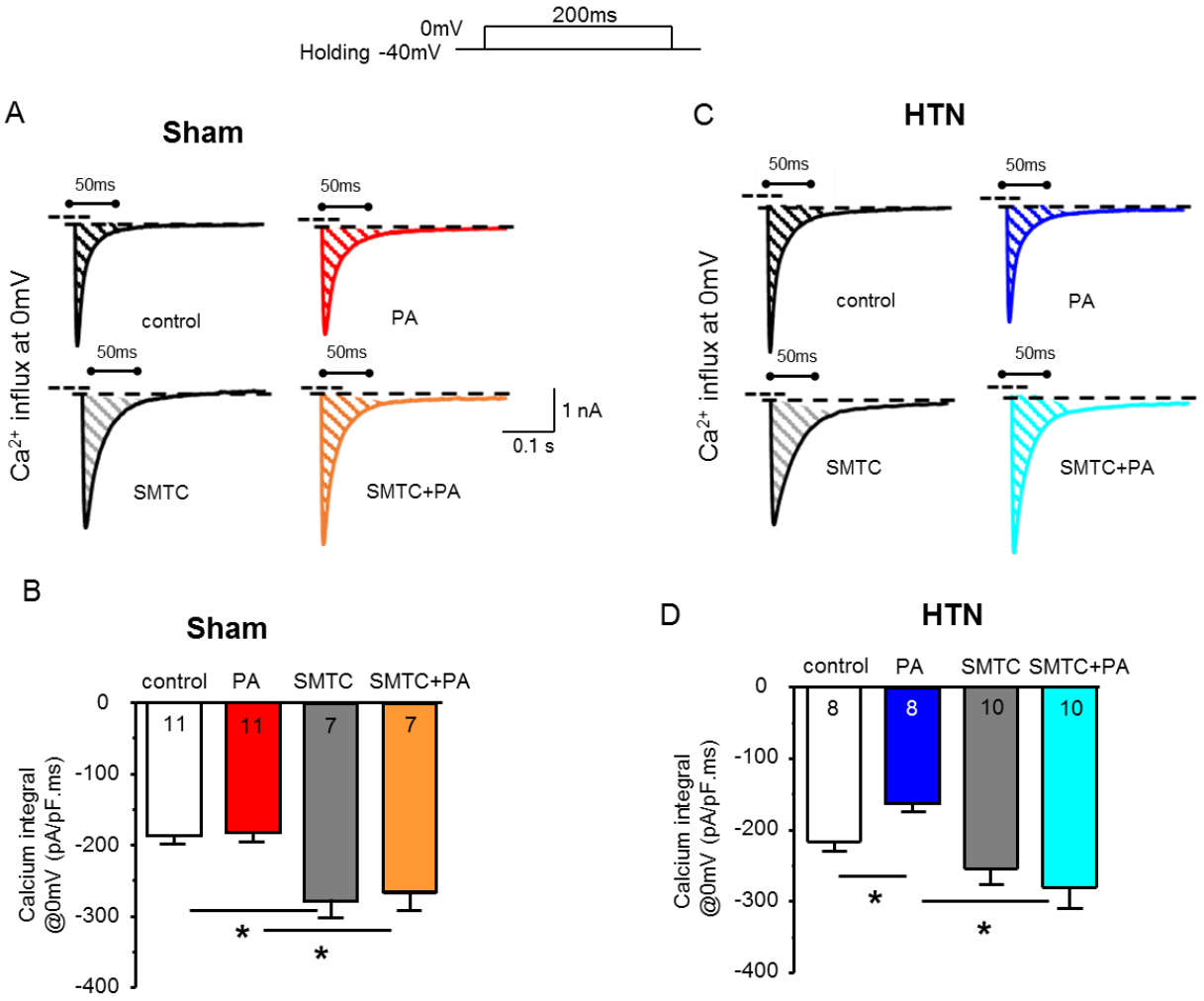

Figure 15. PA regulation of the Ca^{2+} influx through LTCC

LTCC was stimulated by a step depolarization protocol from -60 mV to +40 mV (10 mV interval) for 200 ms (holding potential, -40 mV). **A & C.** Representative $I_{Ca\text{-}L}$ integral at 0 mV in sham and HTN before and after nNOS inhibition with and without PA. **B & D.** Averaged mean values showed that PA did not change $I_{Ca\text{-}L}$ integral in sham but significantly reduced it in HTN. nNOS inhibition increased $I_{Ca\text{-}L}$ integral with and without PA in both groups and abolished the response of PA in two groups.

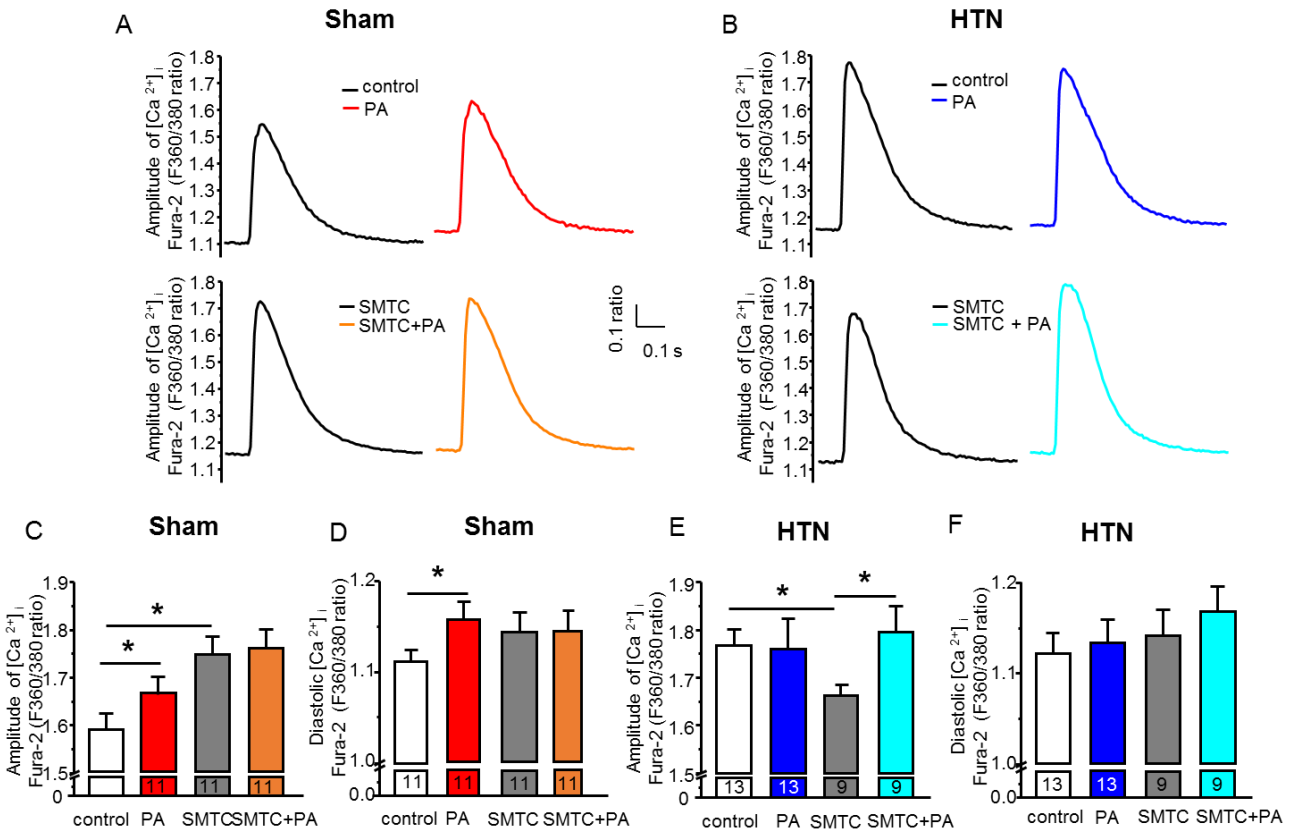

Figure 16. PA regulation of $[Ca^{2+}]_i$ with and without nNOS inhibition (SMTC, 100 nM, 30 min-1hr) in sham and HTN

A, C&D Representative raw traces and averaged values of $[Ca^{2+}]_i$ transient with PA before and after SMTC treatment in sham. PA significantly increased the peak $[Ca^{2+}]_i$ amplitude but failed to affect $[Ca^{2+}]_i$ after SMTC pre-treatment in sham. **B, E&F** Representative raw traces and averaged values for $[Ca^{2+}]_i$ with PA before and after SMTC treatment in HTN. PA failed to affect basal Ca^{2+} transient and SMTC reduced peak $[Ca^{2+}]_i$ in HTN. In the presence of SMTC, PA significantly increased $[Ca^{2+}]_i$ amplitude.

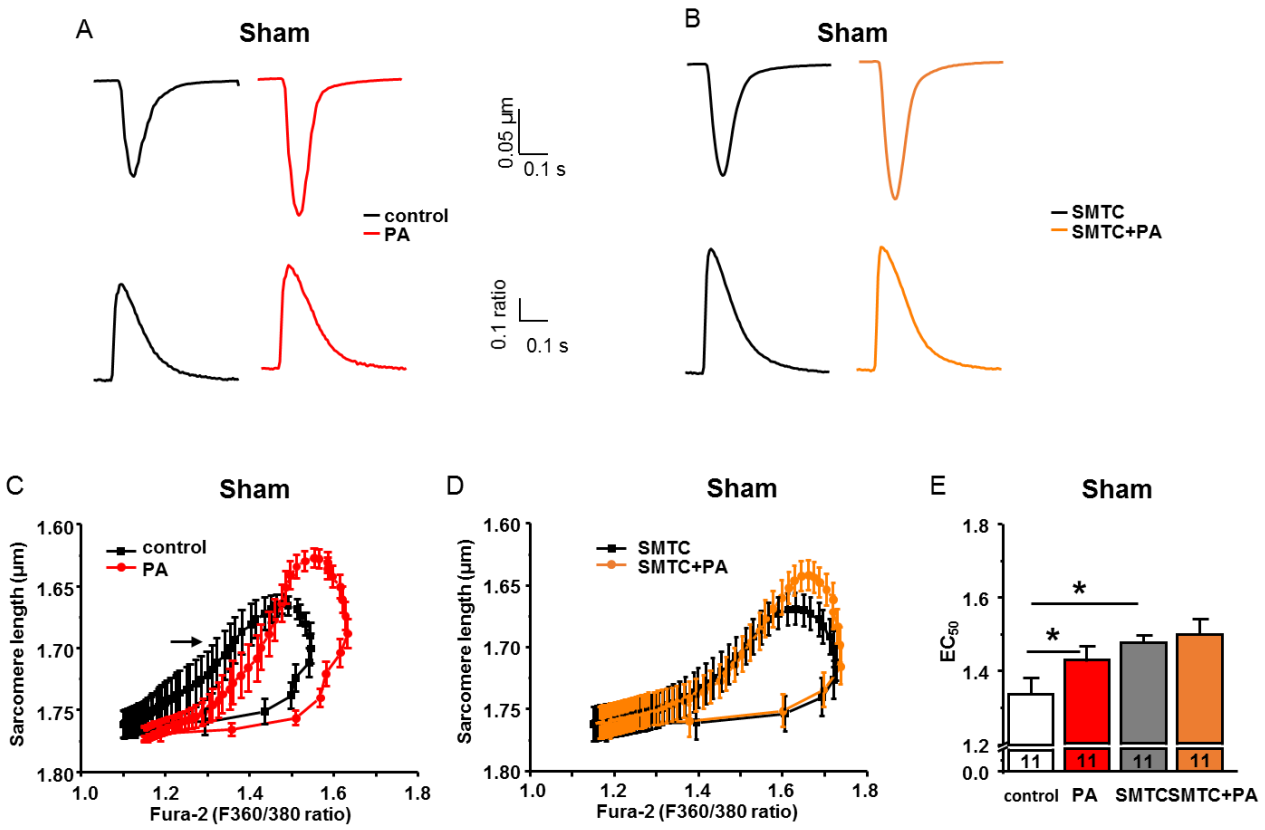

Figure 17. PA regulation of myofilament Ca^{2+} sensitivity before and after nNOS inhibition in sham

A&B. representative raw traces of sarcomere shortening and $[Ca^{2+}]_i$ transient with PA before (A) and after nNOS inhibition (B) in sham. **C&D** Phase-plane diagram of Fura-2 ratio *vs.* sarcomere length with PA in the presence and absence of SMTC in sham. PA shifted the relaxation phase of the relationship to the right. **E** EC_{50} was increased by PA in sham, indicating reduced myofilament Ca^{2+} sensitivity. EC50 was increased in the presence of SMTC, PA no longer affected EC_{50} under these conditions.

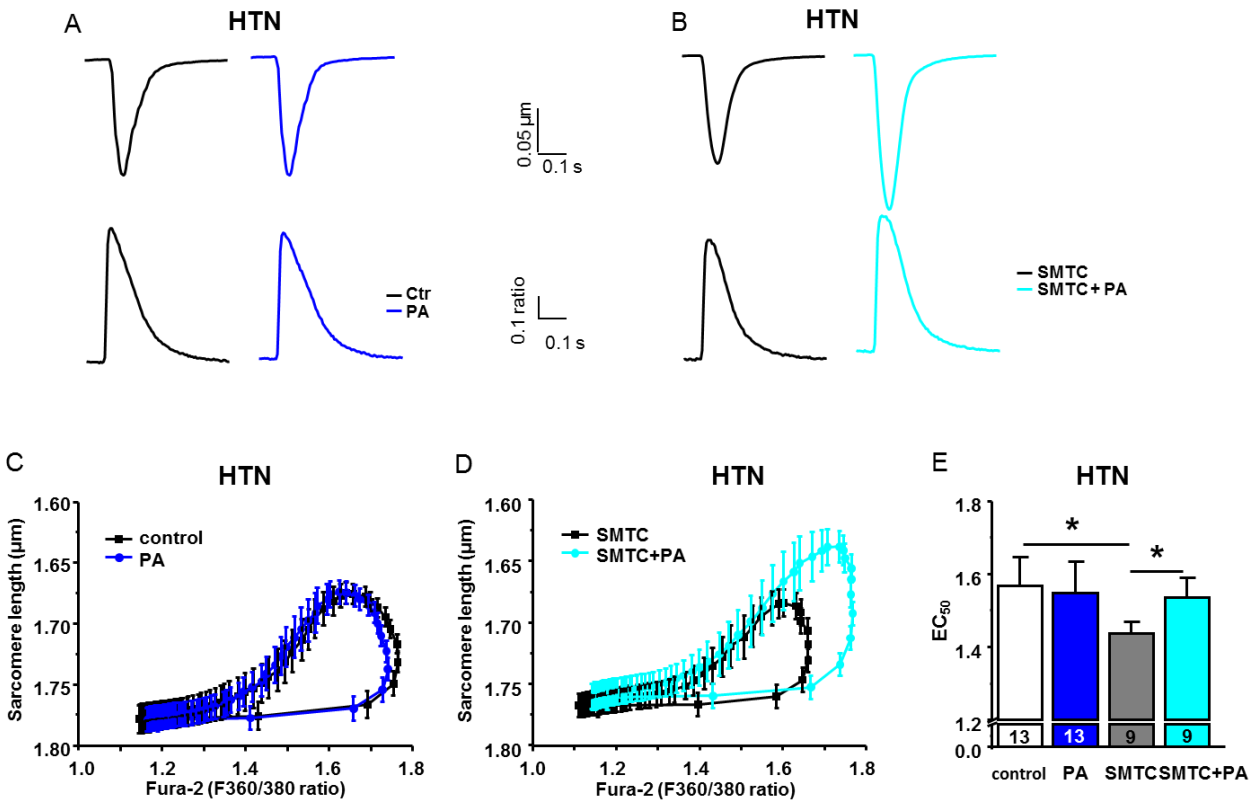

Figure 18. PA regulation of myofilament Ca^{2+} sensitivity before and after nNOS inhibition in HTN

A&B. Representative raw traces of sarcomere shortening and $[Ca^{2+}]_i$ transient with PA before (**A**) and after nNOS inhibition (**B**) in HTN. **C&D** Phase-plane diagram of Fura-2 ratio *vs.* sarcomere length with PA in the presence and absence of SMTC in HTN. PA did not affect the relaxation phase of the relationship, indicating no effect on myofilament Ca^{2+} sensitivity. **E** EC_{50} was reduced in HTN compared to that in sham. SMTC reduced EC_{50} and restored EC_{50} increment by PA in HTN.

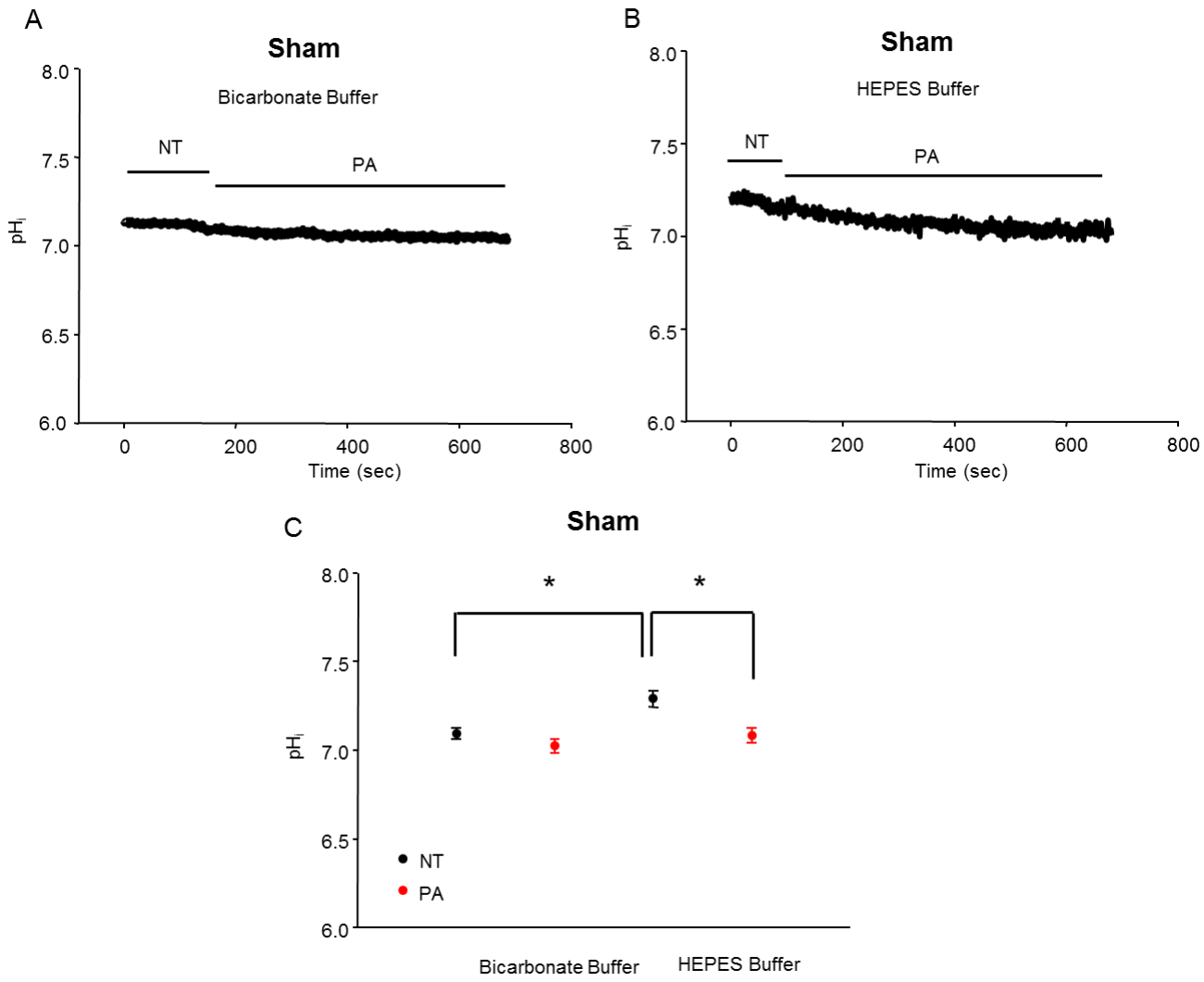

Figure 19. Regulation of intracellular $[pH]_i$ by PA in sham.

$[pH]_i$ (SNARF-1/AM) was significantly reduced by PA in HEPS buffer. Increase $[pH]_i$ buffer capacity using $NaHCO_3$ + CO_2 (5 %) weaken the changes in $[pH]_i$ by PA in sham.

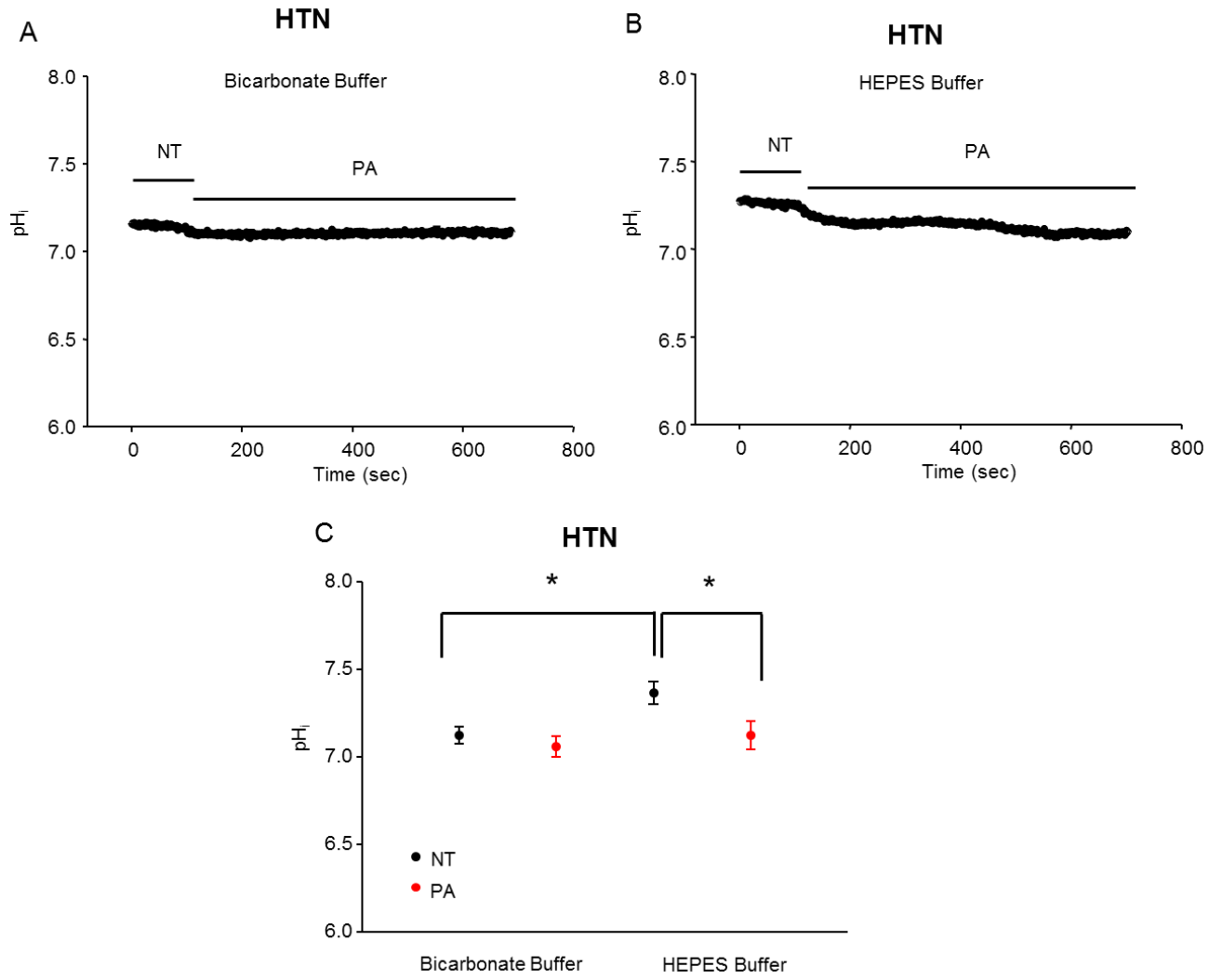

Figure 20. Regulation of intracellular $[pH]_i$ by PA in HTN.

$[pH]_i$ (SNARF-1/AM) was significantly reduced by PA in HEPS buffer. Increase $[pH]_i$ buffer capacity using $NaHCO_3$ + CO_2 (5 %) weaken the changes in $[pH]_i$ by PA in HTN.

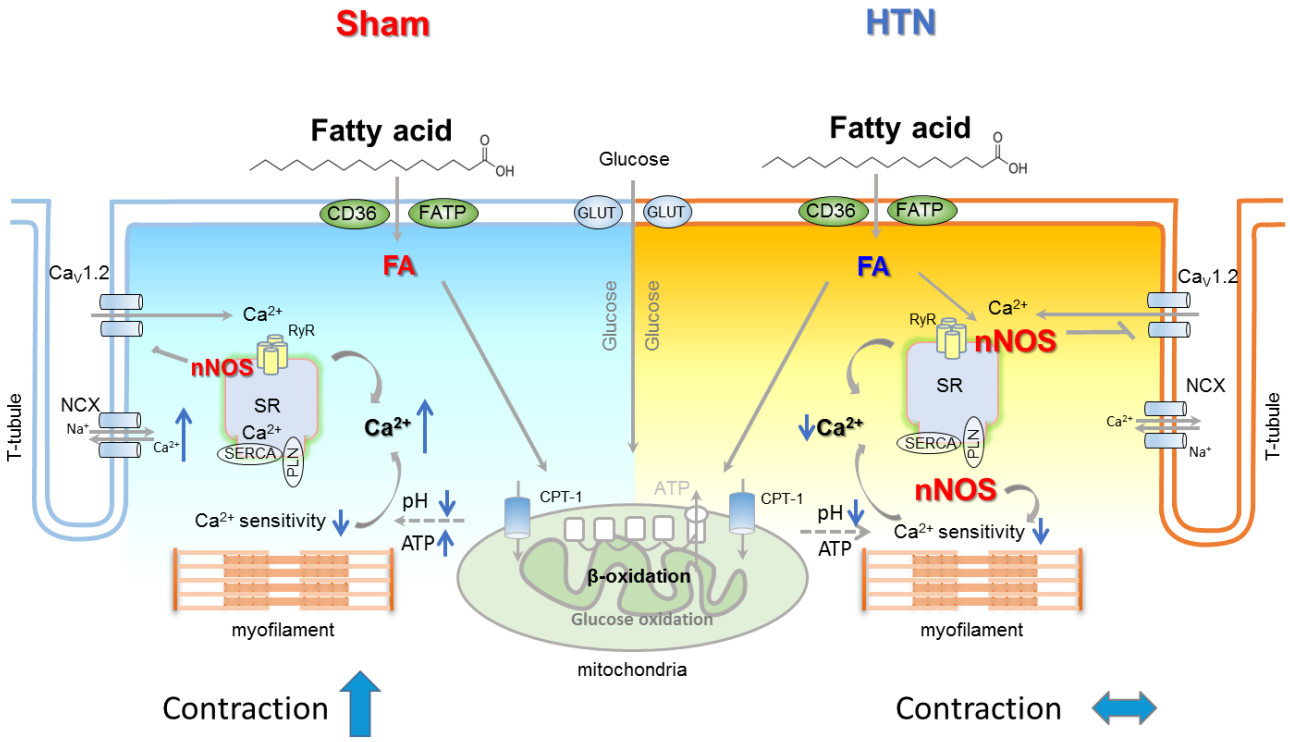

Figure 21. Schematic diagram of mechanism mediating FA-regulation of myocyte contraction and the regulation by nNOS in healthy and hypertensive rat hearts.

PA increases myocyte contraction by enhancing $[Ca^{2+}]_i$ transient secondary to myofilament Ca^{2+} desensitization in sham. In HTN, PA stimulates nNOS activity, nNOS-derived NO reduces Ca^{2+} influx through I_{LTCC} and intracellular Ca^{2+}, modulates myofilament Ca^{2+} sensitivity, as a result, overrides PA-induced increase of myocyte contraction.

Part III Palmitoylation of endothelial nitric oxide synthase in mediating fatty acid-dependent contraction in sham and hypertensive rat left ventricular myocytes.

eNOS mediates PA-regulation of myocyte contraction

Figure 22A&D showed that PA (100 μM) significantly increased sarcomere shortening in LV myocytes from sham rats (p<0.0001, control *vs.* PA in shams, n=13). However, the positive inotropic effect of PA was absent in the presence of a non-specific inhibitor of NOS, Nω-nitro-L-arginine methyl ester hydrochloride (L-NAME, 1 mM, 30 min-1hr), (p=0.26, control *vs.* PA in pre-treatment of L-NAME in shams, n=8; p<0.001, PA *vs.* L-NAME+PA in sham, n=13 and n=8, Figure 22B&D) and in LV myocytes from $eNOS^{-/-}$ mice (p=0.2927, control *vs.* PA in $eNOS^{-/-}$, Figure 22C&E).

I performed additional experiments to observe whether eNOS affects mitochondrial activity (oxygen consumption rate, OCR) in LV myocytes from sham rats with and without eNOS inhibition and from $eNOS^{-/-}$ mice. As shown in Figure 23A, PA significantly increased OCR in LV myocytes from sham at control but not with L-NAME (p=0.004, control *vs.* PA in shams, n=10 and n=9; p=0.4935*,* L-NAME *vs*. L-NAME+PA, n=8 each; p=0.1951, control *vs.* L-NAME in sham, n=10 and n=8; p=0.008, PA *vs*. L-NAME+PA, n=9 and n=8). This is in contrast to the inhibition of nNOS with SMTC (100nM, 30min~1hr), where PA failed to affect the OCR (p=0.0239, SMTC *vs.* SMTC+PA in shams, n=8 and n=10, Figure 23A). In line with this result, PA failed to increase myocyte shortening following SMTC-pretreatment (data not shown). In addition, PA did not induce an increase in OCR in LV myocytes from $eNOS^{-/-}$ mice, on the contrary, PA reduced OCR in $eNOS^{-/-}$ (p=0.0329, control *vs.* PA in $eNOS^{-/-}$ mice, n=6 and n=7, Figure 23B). These data indicate that eNOS is essential in mediating PA-regulation of myocyte contraction through stimulating mitochondrial activity.

S-palmitoylation of eNOS and its regulation of eNOS-phosphorylation and OCR

Figure 24A showed that PA (100 μM) increased eNOS palmitoylation in LV myocytes from sham rats (p=0.023, control *vs.* PA in sham, n=6, Figure 24A). Pre-treatment of LV myocytes with a palmitate analog that is the most commonly used to inhibit palmitoylation in cells, 2-bromopalmitic acid (2BP, 100 μM, 10-30min), abolished PA-induced eNOS palmitoylation (p=0.005, PA *vs.* PA+2BP in sham, n=6).

Furthermore, I aimed to observe whether the palmitoylation of eNOS affects its activity by regulating eNOS-Ser^{1177}. As shown in Figure 24B, eNOS-Ser^{1177} was not affected by PA in LV myocytes from sham. However, 2BP significantly reduced eNOS-Ser^{1177} with and without PA (p=0.235, control *vs.* PA; p=0.02677, control *vs.* 2BP; p=0.00949, PA *vs.* PA+2BP; p=0.01294, 2BP *vs.* PA+2BP in sham, n=6, Figure 24B). Paradoxically, the NO production (nitrite level relative to control), which was reduced by PA (84% of control, p=0.045, n=6), significantly increased by 2BP in sham (112%, p=0.152, control *vs.* 2BP, n=6; 139%, p=0.028, PA *vs.* PA+2BP, n=6). Furthermore, neither SMTC nor L-NAME prevented the effect of 2BP (147%, p=0.03, SMTC *vs.* SMTC+PA+2BP, n=8; 149%, p=0.02, L-NAME *vs.* L-NAME+PA+2BP, n=8). Therefore, the effect of 2BP on eNOS-Ser^{1177} does not associate with myocyte NO level in sham.

To examine whether eNOS palmitoylation affects the function of PA-dependent responses in LV myocytes, both OCR and myocyte contraction were detected with 2BP pre-treatment. As shown in Figure 24C, pre-treatment LV myocytes with 2BP failed to affect PA-potentiation of OCR in sham (p =0.004, control *vs.* PA; p<0.0001, 2BP *vs.* PA+2BP; p=0.0752, PA *vs.* PA+2BP, Figure 24C). NOS inhibition with L-NAME prevented PA-dependent OCR increase in the presence of 2BP (p<0.0001, PA+2BP *vs.* L-NAME+PA+2BP, Figure 24C).

Furthermore, treatment of LV myocytes with 2BP did not affect myocyte contraction with PA in sham (p<0.0001, control *vs.* PA, p=0.0015, PA *vs.* PA+2BP, n=13, Figure 25A&D). Pre-treatment of 2BP did not prevent PA-dependent myocyte contraction (p=0.005, 2BP *vs.* 2BP+PA, n=8, Figure

25B&E). Similarly, 2BP did not affect myocyte contraction in the presence of L-NAME, *i.e.* PA did not increase myocyte contraction in the presence of L-NAME and 2BP (p=0.406, L-NAME+PA *vs.* L-NAME+PA+2BP, n=8, Figure 25C&F). These results exclude the effect of eNOS palmitoylation on eNOS-mediated and PA-induced myocyte contraction in sham.

Palmitoylation of eNOS in PA-regulation of LV myocytes contraction and OCR from HTN rats

In HTN, PA did not increase eNOS palmitoylation (p=0.58, control *vs.* PA, n=4, Figure 26A). However, 2BP significantly reduced eNOS palmitoylation in the presence and absence of PA (p=0.04, PA *vs.* PA+2BP, Figure 26A), suggesting that basal eNOS is palmitoylated and PA does not affect it further. Similar to that in sham, 2BP significantly reduced eNOS-Ser^{1177} in HTN with and without PA (with PA, p=0.038, PA *vs.* PA+2BP; without PA, p=0.05, control *vs.* 2BP, n=3, Figure 26B). In addition, the NO production was significantly increased by 2BP in the presence of SMTC and L-NAME (140%, p=0.02 SMTC *vs.* SMTC+PA+2BP, n=8; 180%, p=0.01, L-NAME *vs.* L-NAME+PA+2BP, n=8). Unexpectedly, 2BP reduced PA-induced OCR in HTN (p=0.0177, control and PA, n=8 and n=9; p=0.0198, PA *vs.* PA+2BP, n=9 and n=10; p=0.2419, 2BP *vs.* PA+2BP, n=8 and n=10, Figure 26C).

Finally, the effect of PA on myocyte contraction and the involvement of eNOS palmitoylation are examined. As shown in Figure 27, PA-dependent positive inotropic effect was absent in HTN (p=0.3896, control *vs.* PA, n=12, Figure 27A&D). This effect was unaffected by 2BP (p=0.069, 2BP *vs.* PA+2BP in HTN, n=5, Figure 27B&E). NOS inhibition with L-NAME significantly increased myocyte contraction with PA and 2BP did not affect such an effect (Figure 27C & F), indicating the lack of an effect of eNOS and its palmitoylation on myocyte contraction in HTN. These results show clear evidence that eNOS is palmitoylated in LV myocytes from HTN and does not change myocyte contraction with or without PA.

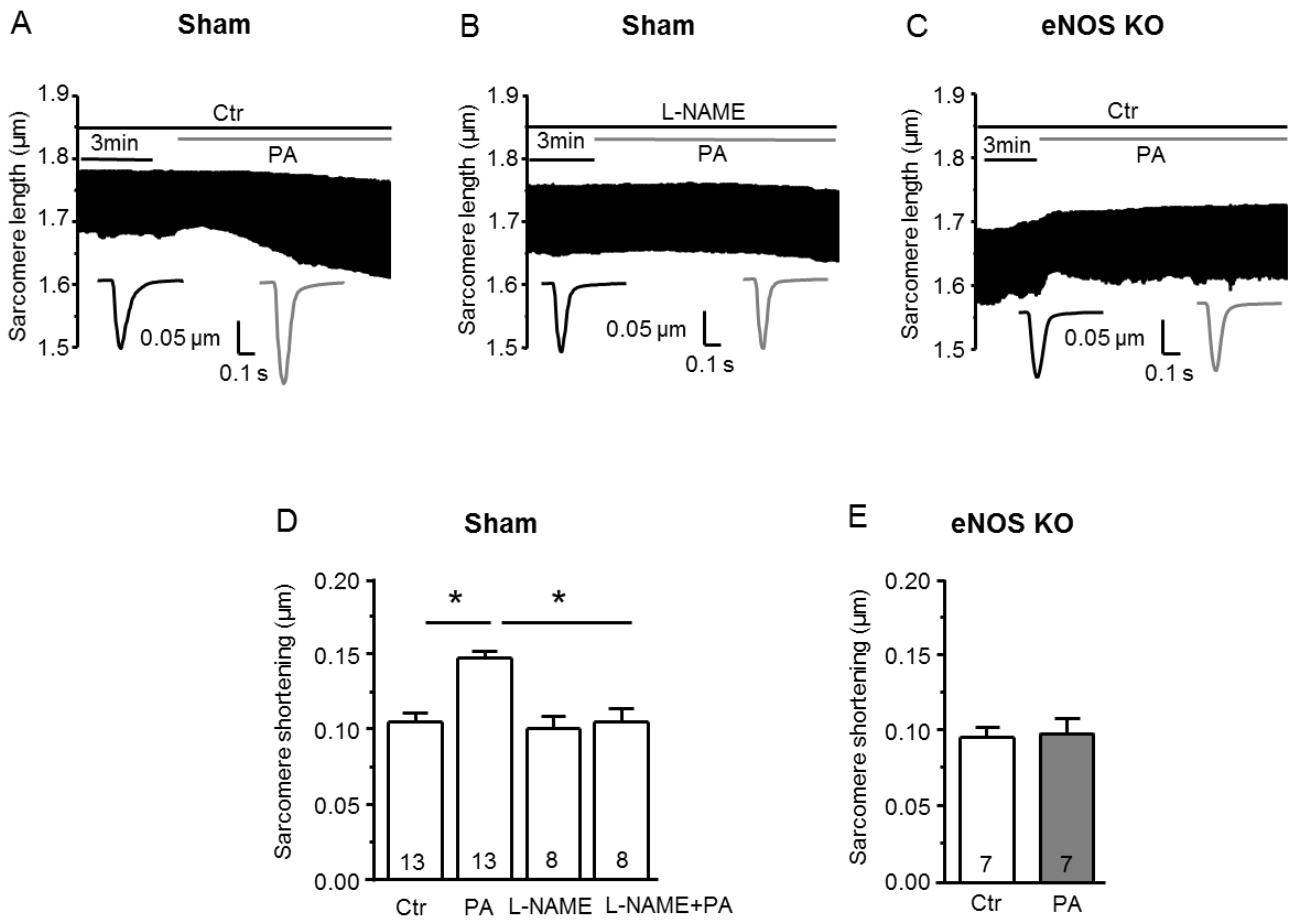

Figure 22. eNOS is essential in mediating PA-regulation of myocyte contraction.

Changes in sarcomere length were measured in LV myocytes by using a video-sarcomere detection system (IonOptix Corp). **A&B, D.** PA (100 μM) significantly increased sarcomere shortening in LV myocytes from sham rats (p<0.0001, n=13). The positive inotropic effect of PA was prevented by L-NAME pre-treatment (1 mM, 30 min-1hr) (p<0.001, PA *vs.* L-NAME+PA in sham, n=8). **C&E.** PA failed to affect myocyte contraction from eNOS$^{-/-}$ mice. (p=0.2927, n=7)

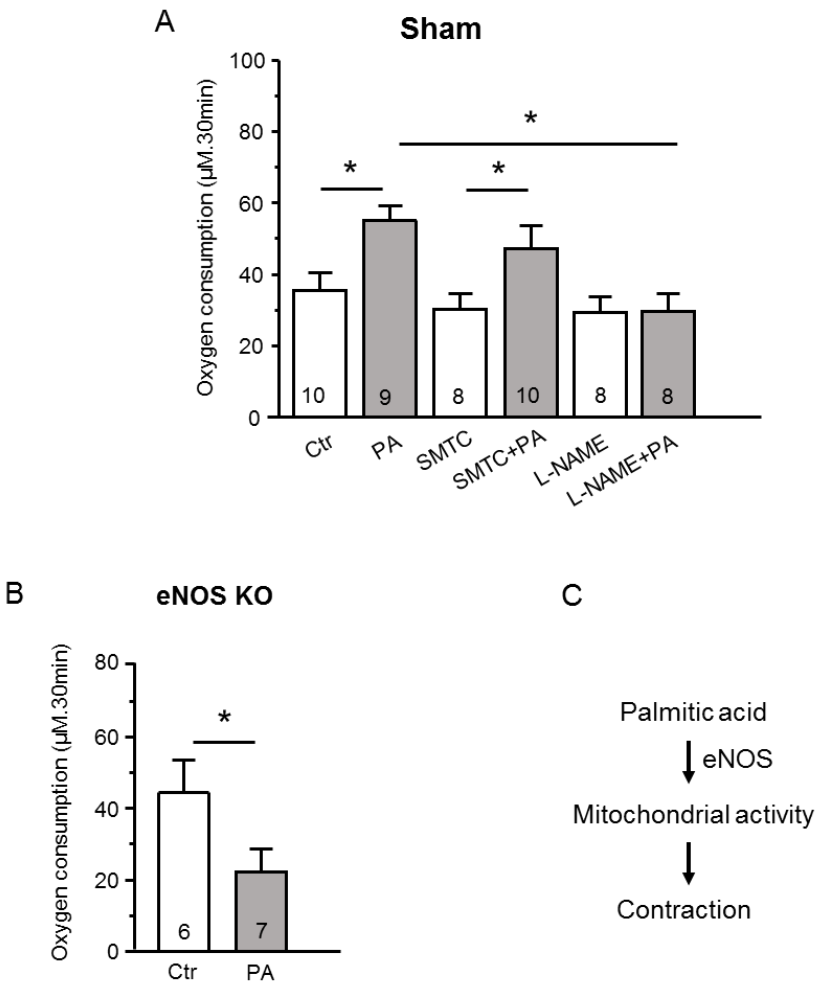

Figure 23. eNOS regulation of mitochondrial activity (oxygen consumption rate, OCR) in LV myocytes from rats and eNOS$^{-/-}$ mice.

OCR was measured using a fluorescence-based oxygen sensor (NeoFox, Ocean Optics) connected to a phase measurement system (Instech). Bars represent average values ± SEM.

A. PA significantly increased OCR in LV myocytes from sham at control. L-NAME (1mM, 30min~1hr) prevented PA-induced OCR increase, but nNOS with SMTC (100nM, 30min~1hr) failed to affect the OCR by PA (OCR, μM.30min, p<0.0001, control *vs.* PA; p=0.008, PA *vs*. L-NAME+PA; p=0.0239, μM.30min, p=0.0329, control *vs.* PA). **C.** Flow chart shows: eNOS mediates PA-regulation of myocyte contraction through stimulating mitochondrial activity (oxygen consumption rate) in cardiac myocytes.

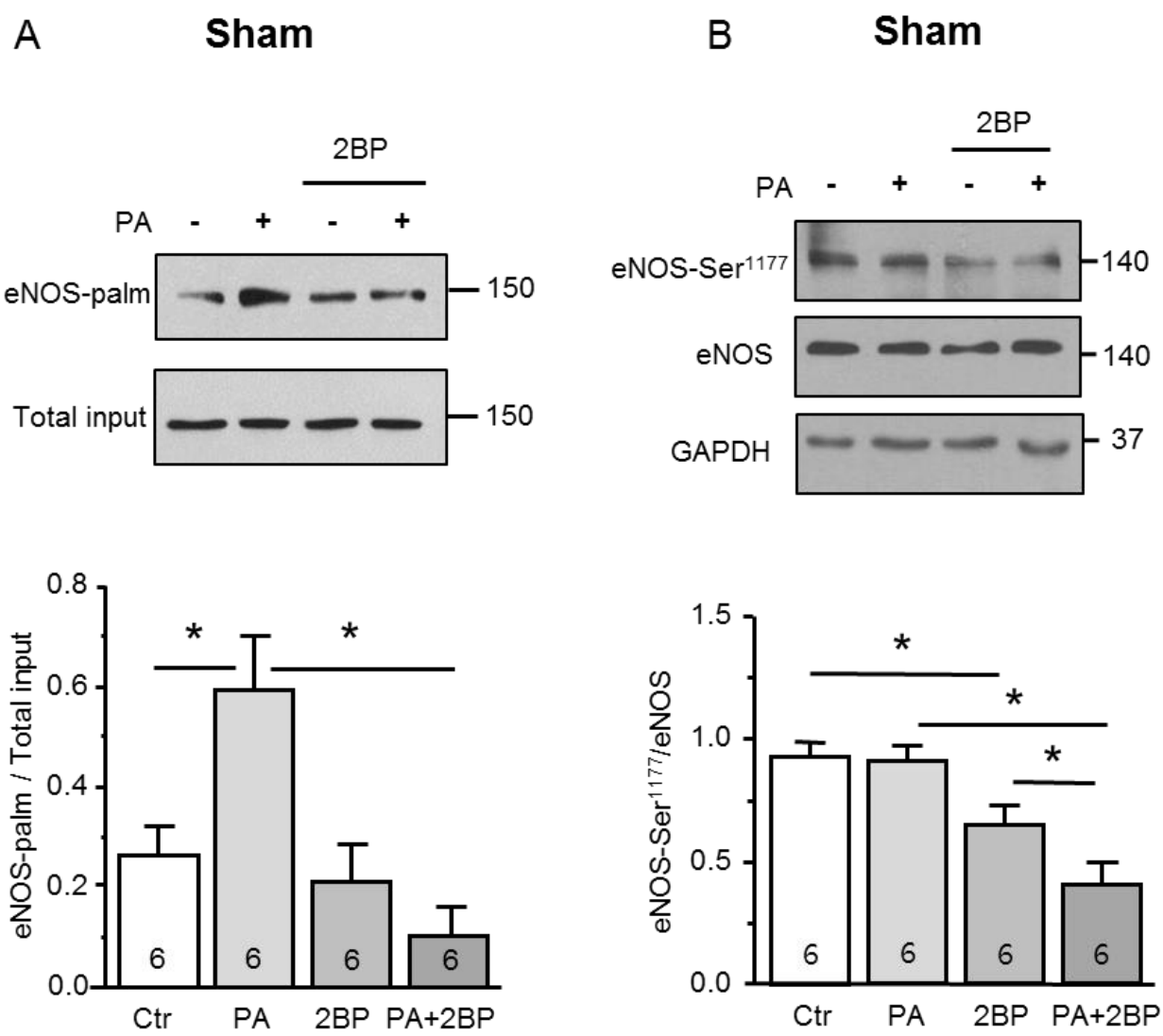
A
Sham
2BP
PA - + - +
eNOS-palm
150
Total input
150
B
Sham
2BP
PA - + - +
eNOS-Ser1177
140
eNOS
140
GAPDH
37
eNOS-palm / Total input
0.8
0.6
0.4
0.2
0.0
6 6 6 6
Ctr PA 2BP PA+2BP
eNOS-Ser1177/eNOS
1.5
1.0
0.5
0.0
6 6 6 6
Ctr PA 2BP PA+2BP

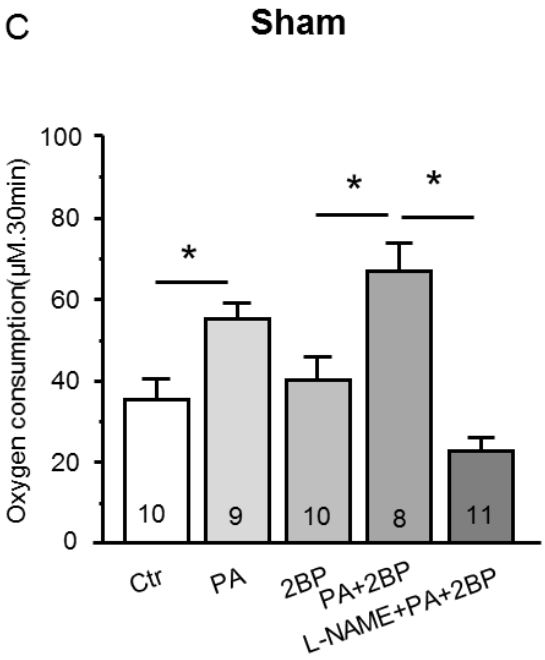
C
Sham
Oxygen consumption(μM.30min)
100
80
60
40
20
0
10 9 10 8 11
Ctr PA 2BP PA+2BP L-NAME+PA+2BP

Figure 24. The palmitoylation and phosphorylation of eNOS by PA and its effects on mitochondrial activity in LV myocytes from sham rats.

A. PA (Palmitic acid, 100 μM) increased eNOS-palmitoylation in LV myocytes from sham rats (p=0.023, control *vs.* PA) and 2BP (100 μM) prevented eNOS-palmitoylation (p=0.005, PA *vs.* PA+2BP in sham, n=6). **B.** eNOS-Ser^{1177} was not increased by PA in LV myocytes from sham (p=0.235, control *vs.* PA). 2BP significantly reduced both basal eNOS-Ser^{1177} and eNOS-Ser^{1177} with PA in sham (p=0.02677, control *vs.* 2BP; p = 0.00949, PA *vs.* PA+2BP; p=0.01294, 2BP *vs.* PA+2BP). **C.** 2BP showed negligible effect on PA-regulation of OCR; NOS inhibition with L-NAME prevented PA-dependent OCR increase.

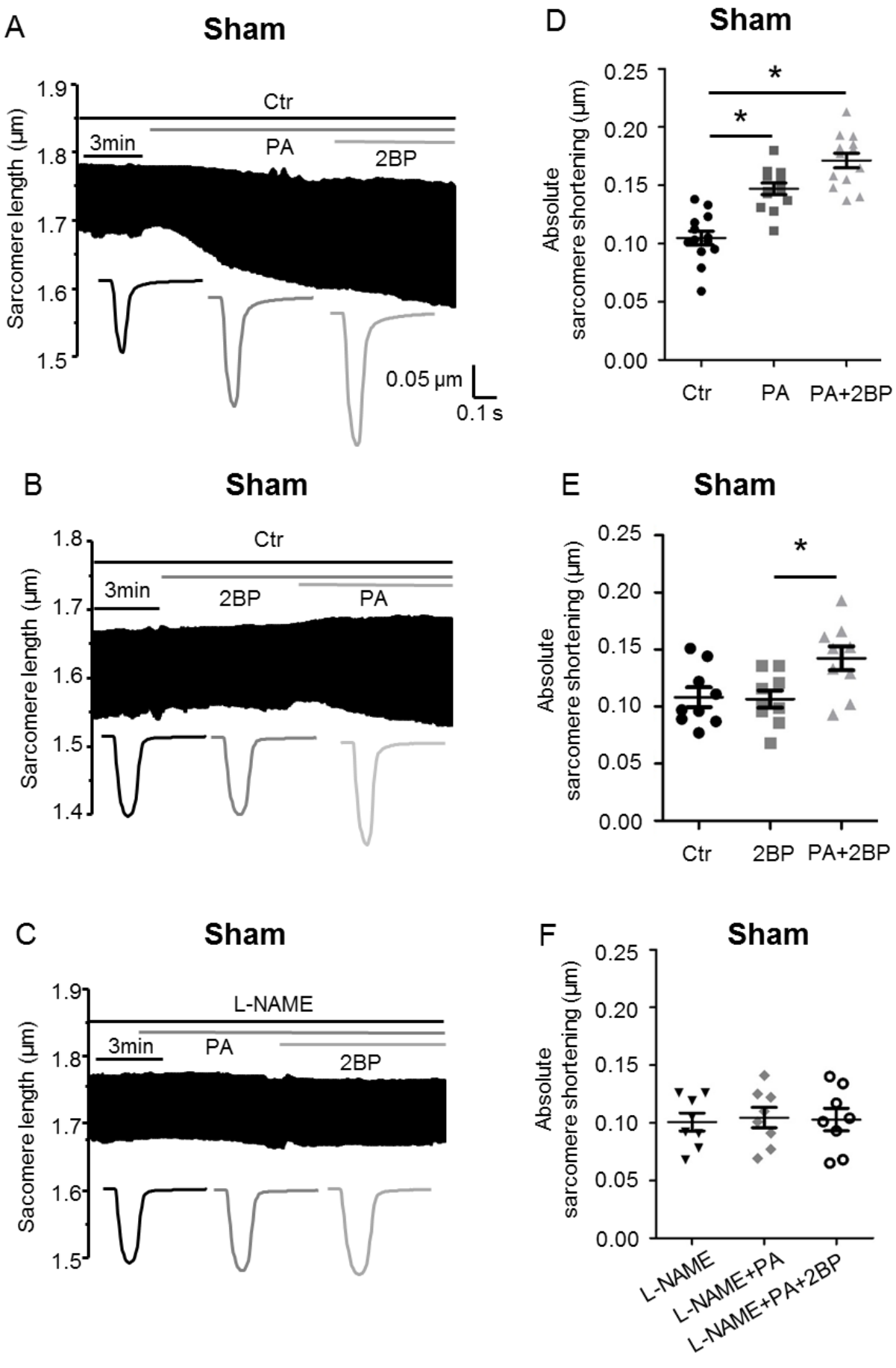
A
Sham
Sarcomere length (µm)
1.9
1.8
1.7
1.6
1.5
Ctr
3min
PA
2BP
0.05 µm
0.1 s
D
Sham
Absolute sarcomere shortening (µm)
0.25
0.20
0.15
0.10
0.05
0.00
*
*
Ctr
PA
PA+2BP
B
Sham
Sarcomere length (µm)
1.8
1.7
1.6
1.5
1.4
Ctr
3min
2BP
PA
E
Sham
Absolute sarcomere shortening (µm)
0.25
0.20
0.15
0.10
0.05
0.00
*
Ctr
2BP
PA+2BP
C
Sham
Sacomere length (µm)
1.9
1.8
1.7
1.6
1.5
L-NAME
3min
PA
2BP
F
Sham
Absolute sarcomere shortening (µm)
0.25
0.20
0.15
0.10
0.05
0.00
L-NAME
L-NAME+PA
L-NAME+PA+2BP

Figure 25. Effect of eNOS-palmitoylation on PA-induced LV myocyte contraction in sham

A, B, D&E. Post or pre-treatment of LV myocytes with 2BP did not reduce PA-induced myocyte contraction (sarcomere shortening, p=0.0015, PA *vs.* PA+2BP, post-treatment 2BP, n=13; p=0.005, 2BP *vs.* 2BP+PA, pre-treatment, n=8). **C&F.** NOS inhibition (L-NAME, 1mM, 30min -1hr) abolished PA-dependent increase of myocyte contraction even in the presence of 2BP in sham (Sarcomere shortening, p=0.406, L-NAME+PA *vs.* L-NAME+PA+2BP, n=8). Bars represent average values ± SEM.

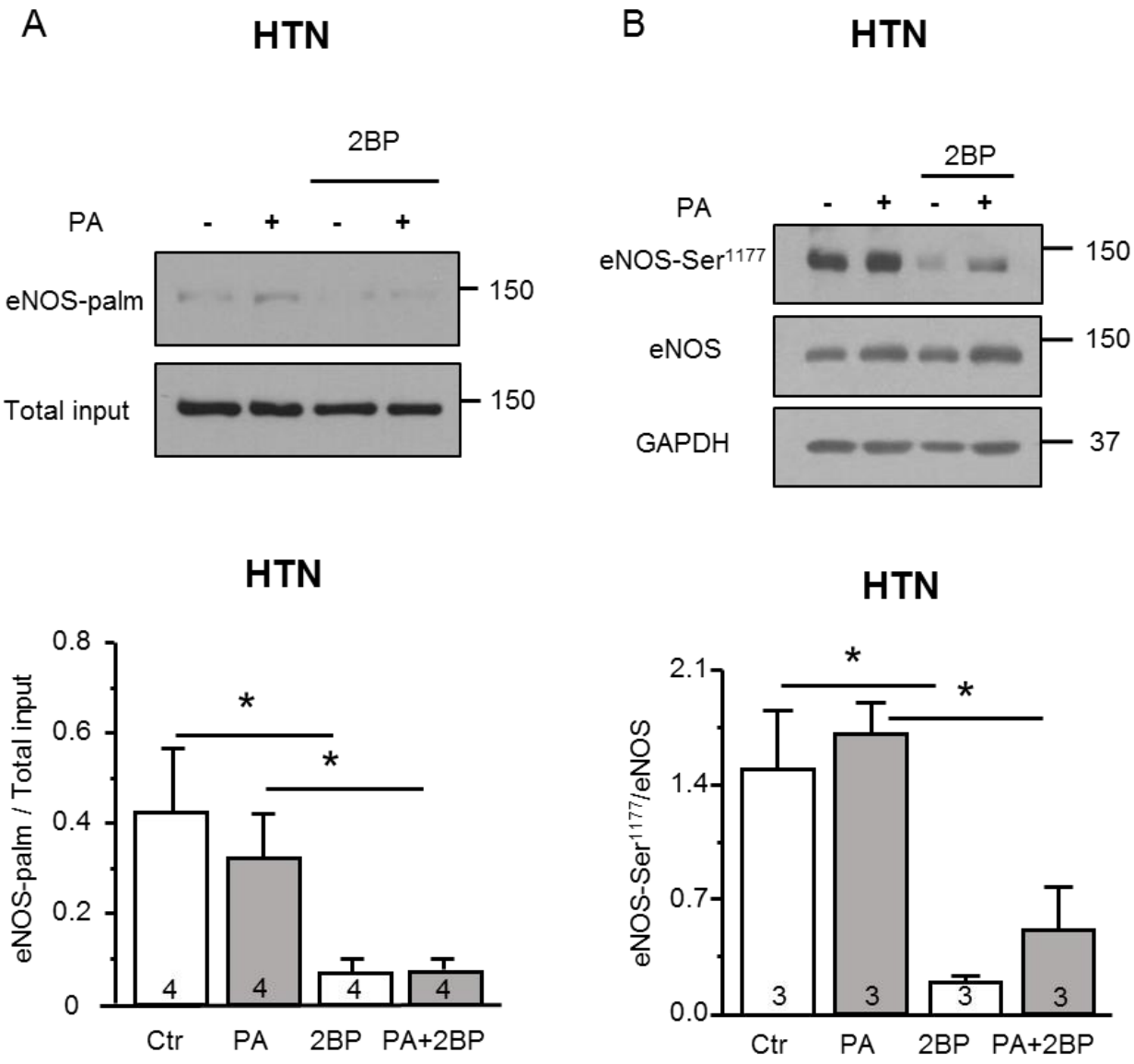
A
HTN
2BP
PA
- + - +
eNOS-palm
150
Total input
150
B
HTN
2BP
PA
- + - +
eNOS-Ser1177
150
eNOS
150
GAPDH
37
HTN
eNOS-palm / Total input
0.8
0.6
0.4
0.2
0
*
*
4 4 4 4
Ctr PA 2BP PA+2BP
HTN
eNOS-Ser1177/eNOS
2.1
1.4
0.7
0.0
*
*
3 3 3 3
Ctr PA 2BP PA+2BP
C
HTN
Oxygen consumption(μM.30min)
100
80
60
40
20
0
*
*
8 9 8 10
Ctr PA 2BP PA+2BP

Figure 26. Palmitoylation of eNOS in LV myocytes from hypertensive rats and the effects on OCR

A. In HTN, PA did not increase eNOS palmitoylation (p=0.58, control *vs.* PA in HTN, n=4). However, 2BP significantly reduced basal eNOS palmitoylation in the presence and absence of PA (p=0.04, PA *vs.* PA+2BP in HTN). **B.** Similar to that in sham, 2BP significantly reduced eNOS-Ser^{1177} in HTN with and without PA (p=0.038, PA *vs.* PA+2BP; p=0.05, control *vs.* 2BP, n=3). **C.** 2BP reduced PA-induced OCR in HTN (p=0.0177, control *vs.* PA, n=8 and n=9; p=0.0198, PA *vs.* PA+2BP, n=9 and n=10; p=0.2419, 2BP *vs.* PA+2BP in HTN, n=8 and n=10).

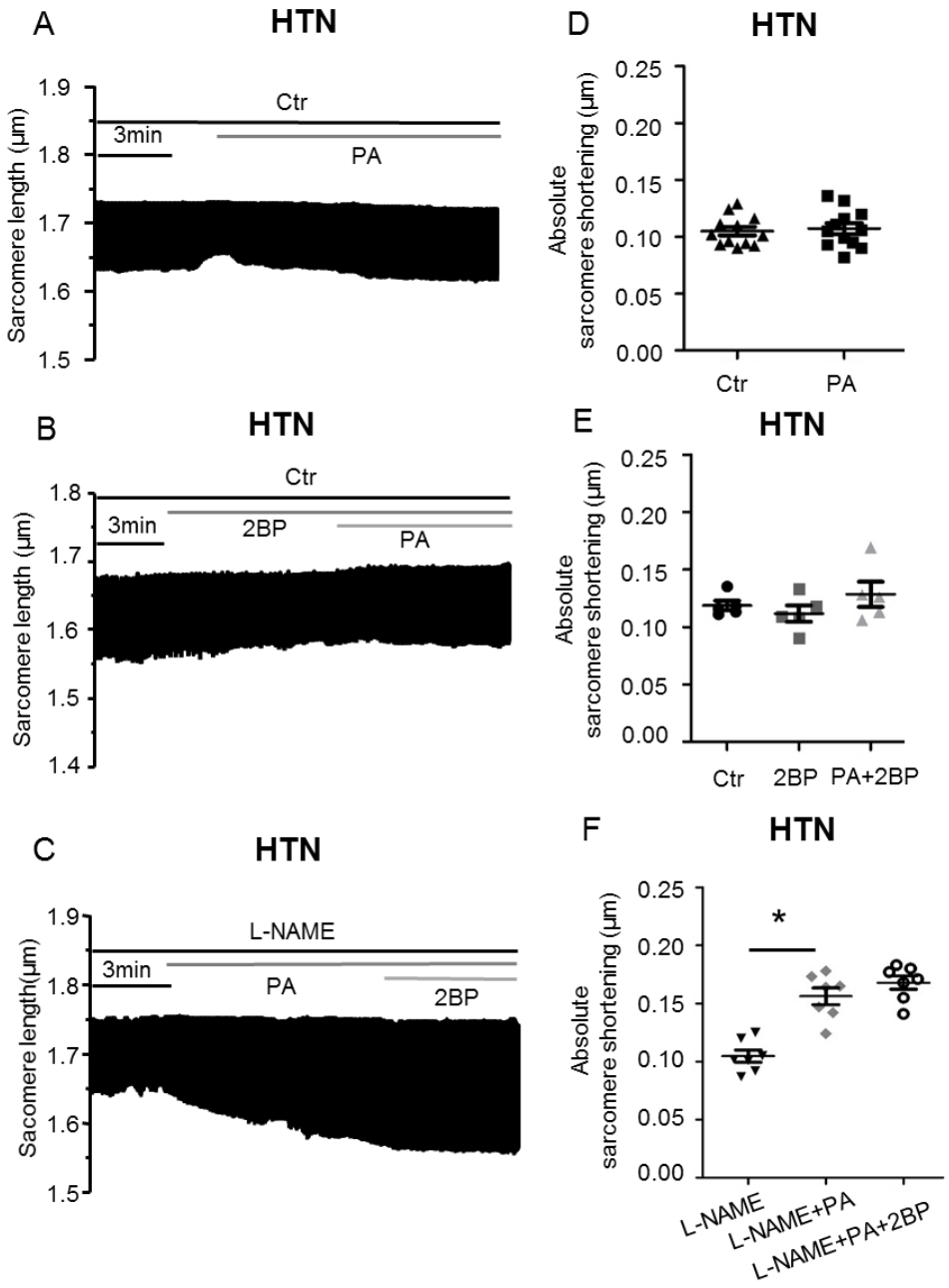

Figure 27. Effect of 2BP on LV myocyte contraction from hypertensive rats.

A&D. PA-dependent positive inotropic effect was absent in HTN (p=0.3896, control *vs.* PA in HTN, n=12). **B&E.** PA-dependent positive inotropic effect was unaffected by 2BP pre-treatment (p=0.069, 2BP *vs.* PA+2BP in HTN, n=5). **C&F.** NOS inhibition with L-NAME significantly increased myocyte contraction with PA (p=0.001, L-NAME *vs.* L-NAME+PA in HTN, n=7), 2BP did not affect such an effect (p=0.2668, L-NAME+PA *vs.* L-NAME+PA+2BP in HTN, n=7).

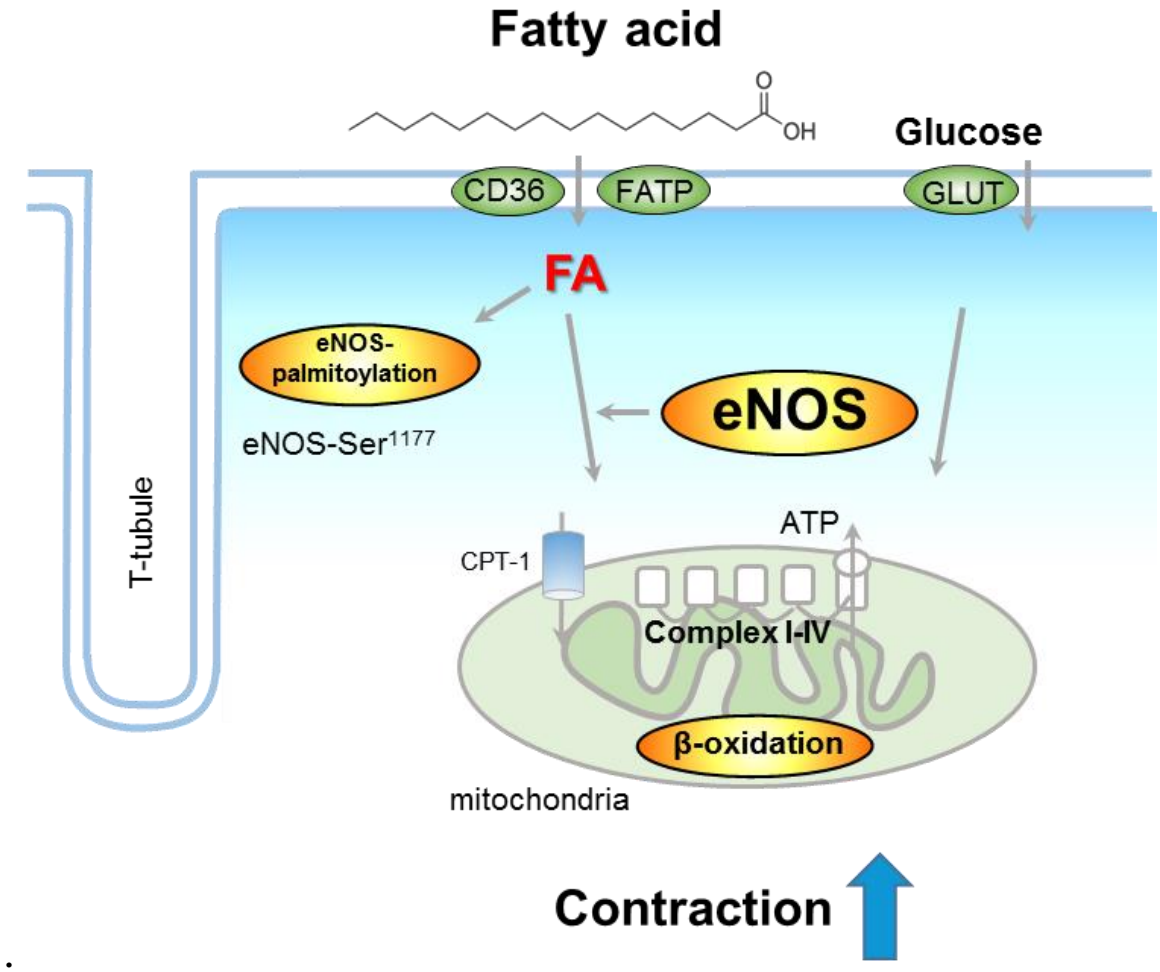

Figure 28. Schematic diagram of eNOS and eNOS palmitoylation in mediating saturated FA-regulation of mitochondrial activity and myocyte contraction

It is shown that eNOS palmitoylation is not the main mechanism to mediate PA-dependent inotropic response in healthy or HTN heart. Nevertheless, the "un-palmitoylated" eNOS is significant in regulating cardiac metabolism and contraction in healthy and hypertensive heart.

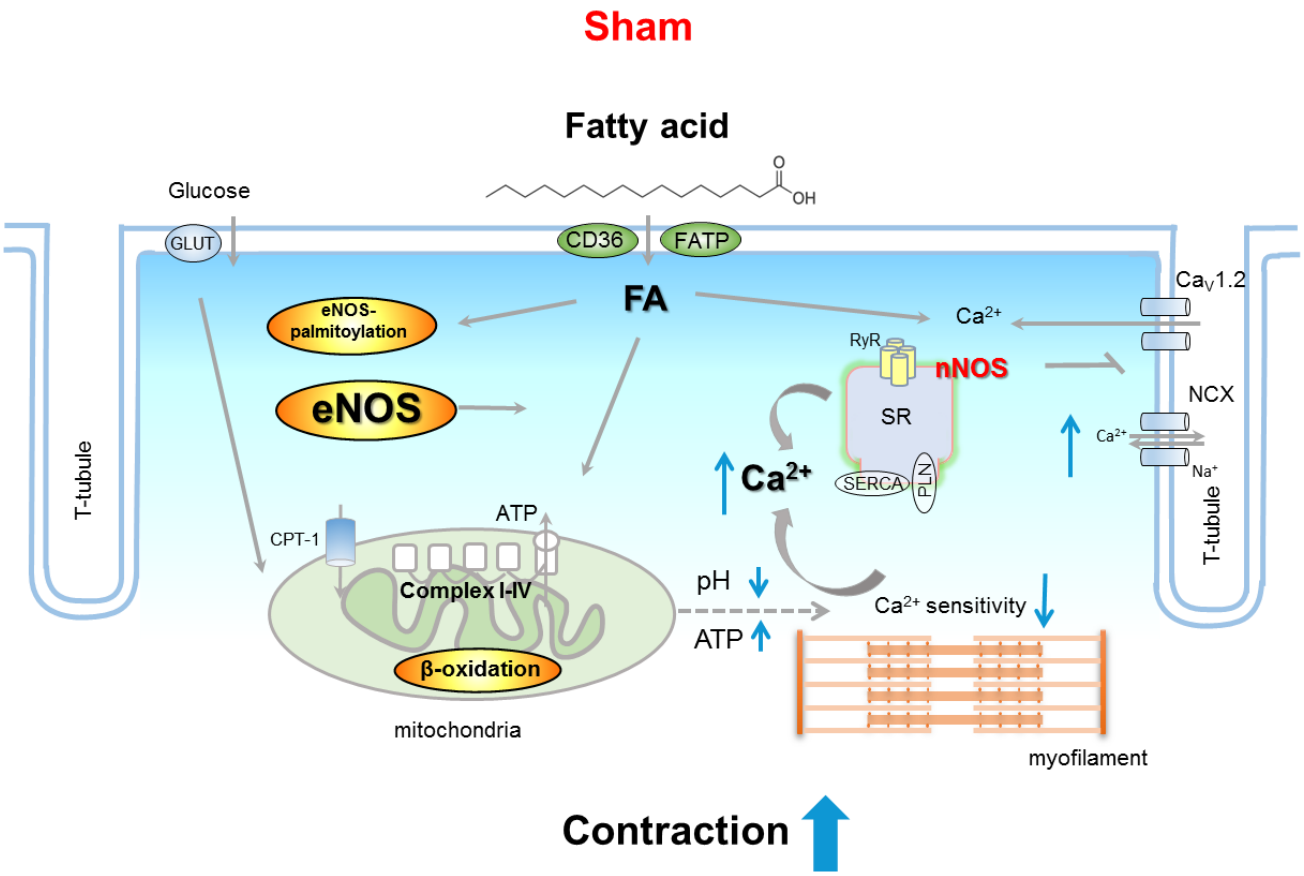

Figure 29. Conclusion in sham

eNOS is essential in mediating PA-regulation of myocyte contraction through stimulating mitochondrial activity and PA increased Ca^{2+} transients. However, eNOS palmitoylation is not the main mechanism to mediate PA-dependent inotropic response in sham.

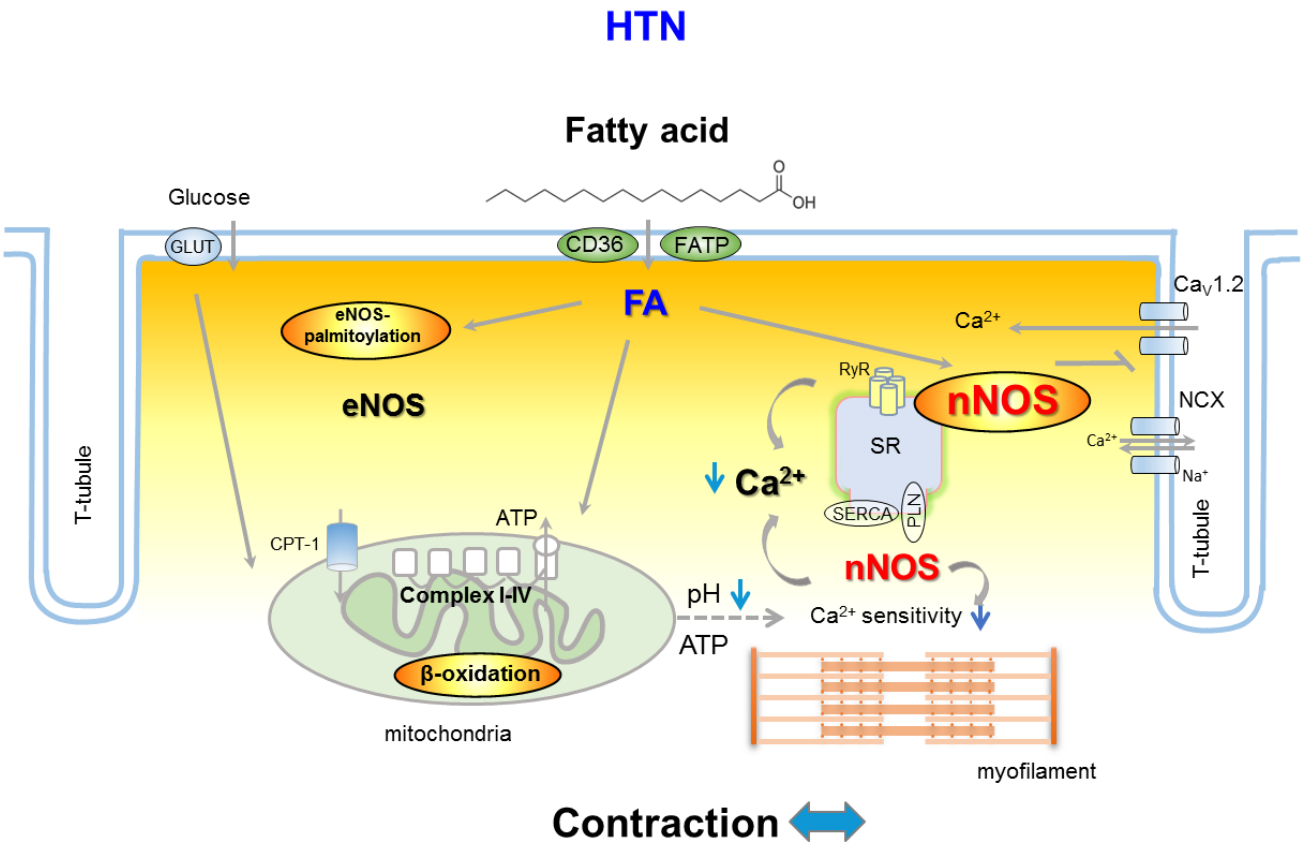

Figure 30. Conclusion in HTN

nNOS-derived NO is up-regulated by FA in HTN, which in turn, modulates key elements of Ca^{2+} handling process and controls myocardial response to FA. This effect overrides eNOS-mediated cardiac metabolism and contraction in hypertensive heart.

Discussion

Part I: Mechanism of FA regulation of LV myocyte contraction in sham and in HTN (E-C coupling)

FAs are the predominant metabolic substrates for cardiac metabolism and supplementation of PA is likely to activate β-oxidation in the mitochondria and produces energy in the myocardium. Here, my results showed, for the first time, that PA significantly increased myocyte contraction in rat LV myocytes.

I showed convincing evidence that PA increased myocyte contraction by affecting $[Ca^{2+}]_i$ handling in sham. I.e. PA increased the amplitude of $[Ca^{2+}]_i$ without changing Ca^{2+} influx through LTCC. Forward mode of I_{NCX} was increased by PA, indicating greater Ca^{2+} extrusion. Myofilament Ca^{2+} sensitivity, however, was reduced, which is seemingly contrary to PA potentiation of myocyte contraction. In fact, myofilament Ca^{2+} desensitization is associated with reduced Ca^{2+} binding affinity to TnC and/or $[Ca^{2+}]_i$ buffering capacity [Huke S, et al., 2010; Recchia FA et al., 1999]. Therefore, it is possible that reduced myofilament Ca^{2+} sensitivity by PA increased the amplitude of $[Ca^{2+}]_i$, which *in turn,* contributed to PA-enhancement of myocyte contraction. Recently, our results have shown that FA-containing metabolic substrates increase myocyte contraction, reduce myofilament Ca^{2+} sensitivity in healthy rat hearts [Zhao ZH et al., 2016]; reduced intracellular pH_i, which is a potent modulator of myofilament Ca^{2+} sensitivity in cardiac and skeletal muscle [Ashley CC et al., 1977; Fabiato A et al., 1978; Li D et al., 2013; Shah AM et al., 2000], may mediate PA-dependent myofilament Ca^{2+} desensitization and the subsequent regulation of $[Ca^{2+}]_i$ by PA. Our results with pH confirmed the reduction in pH with PA in both sham and HTN. In HTN, myofilament Ca^{2+} sensitivity was reduced before the application of PA; consequently, PA exerted little effect on myofilament Ca^{2+} sensitivity, $[Ca^{2+}]_i$ and myocyte contraction, suggesting the importance of myofilament Ca^{2+} desensitization in the

regulation of intracellular Ca^{2+} homeostasis and contractile phenotype of PA.

During disease progression, glucose oxidation or glycolysis becomes the predominant sources of energy whereas both glucose and FA metabolism are downregulated in the failing myocardium [Pelli eux C et al., 2009]. Understanding the mechanisms regulating cardiac contractility through FA-dependent metabolism in healthy and diseased hearts are important in better defining the molecular targets underlying cardiac contraction in these conditions. Here, our results showed that PA increased myocyte contraction and mitochondrial activity (OCR). It is possible that PA exerts these effects through promoting β-oxidation in the mitochondria because our additional studies showed that PA increased ATP production from LV myocytes and both myocyte contraction and ATP level were normalized following the inhibition of carnitine palmitoyl transferase, a key limiting factor of β-oxidation **[**He L et al., 2012**]**. The effect of PA on myocyte contraction was absent in HTN, indicating functional remodeling of cardiac metabolism in regulating contraction under pressure-overload.

CTP-1 inhibitor (ETO) prevented the effect of PA in sham and ETO blocked PA-regulation of mitochondrial activity and myocyte contraction from healthy hearts, supporting the role of beta-oxidation by PA. Increased beta-oxidation with PA may increase cellular ATP level which in turn modulate myofilament sensitivity to Ca^{2+} and affects the phosphorylation status of proteins those are involved in myocardial contractile function [Best PM et al., 1977; Godt RE et al., 1974]. In contrast, PA exerted no effect in HTN.

High concentrations of FAs (at mM range) have been implicated in the myocardial oxidative stress [Fauconnier J et al., 2007]. Intracellular ROS*, in turn,* either increase LV myocyte contraction by stimulating intracellular protein kinases (e.g. PKA) or by direct oxidation of proteins those are involved in myocyte contraction [Zhao ZH et al., 2016] or decrease myocyte contraction secondary to increased ROS in the myocardium from hypertensive models [Welter R et al., 1996]. Pre-incubation of LV myocytes with tiron exerted no effect on myocyte responses to PA in sham or in HTN, excluding

the role of ROS in affecting PA-induced myocyte contraction in either group.

Part II: nNOS modulation of $[Ca^{2+}]_i$ and LV myocyte contraction by FA in sham and in HTN

The present study demonstrates that nNOS-derived NO is enhanced in LV myocytes from hypertensive rats which was further increased by PA and is responsible for PA-dependent increase in mitochondrial activity but prevented myocyte contraction increase. This is in contrast to the positive inotropic effect of PA in healthy heart. Mechanistically, PA increased $[Ca^{2+}]_i$ and reduced myofilament Ca^{2+} sensitivity in sham without affecting Ca^{2+} influx through LTCC in sham. In contrast, PA exerted no effect on $[Ca^{2+}]_i$ or myofilament Ca^{2+} sensitivity and reduced Ca^{2+} influx *via* LTCC in HTN. Further analysis revealed that nNOS-derived NO reduced myofilament Ca^{2+} sensitivity, increased $[Ca^{2+}]_i$ and reduced Ca^{2+} influx *via* LTCC in HTN, limiting myocyte responses to PA. These results demonstrate that PA is an active regulator of myocyte contraction through intracellular Ca^{2+} handling in LV myocytes from both healthy and hypertensive rat hearts. nNOS in HTN modulates Ca^{2+} handling and myocyte contractility despite its involvement in PA-induced mitochondrial activity and myofilament property.

Previously, we have shown that nNOS protein expression and activity were increased in hypertensive rat LV myocytes which is responsible for myofilament Ca^{2+} desensitization but enhanced $[Ca^{2+}]_i$ transient [Jin CZ et al., 2013]. Here, PA increased nNOS-derived NO in HTN and nNOS is responsible for greater reduction in Ca^{2+} influx through LTCC and myofilament Ca^{2+} desensitization and restricts PA-potentiation of myocyte contraction, confirming that nNOS-dependent modulation of $[Ca^{2+}]_i$ handling and myofilament Ca^{2+} sensitivity overrides the greater contraction induced by PA.

In vivo examination of FA metabolism using PET/CT scanner in both sham and HTN showed that basal ^{18}F-FTHA uptake in LV myocyte was not different between two groups. Inhibition of nNOS

with SMTC only marginally increased FA metabolism in HTN without affecting it in sham. In contrast, subsequent treatment with L-NAME to block NOS significantly increased myocardial ^{18}F-FTHA uptake in both groups (significantly higher in sham). Although the reason for the effect of L-NAME is not clear, NO has also been implicated in modulating FA uptake and utilization in the mammalian myocardium from normal heart [Briston SJ et al., 2014; Khan SA, et al., 2003; Kolwicz SC et al., 2013; Ohira H et al., 2015; Pellieux C et al., 2009] Furthermore, nNOS may affect myocardial function *via* regulating mitochondrial proteins since nNOS-derived NO has been shown to inhibit mitochondrial respiration chain, including complex I, III and IV, [Chouchani ET et al., 2013; Takahashi R et al., 2001; Torres J et al., 1995] and reduces mitochondrial oxygen consumption and affects cardiac metabolism. However, inhibition of NOS *in vivo* may affect hemodynamics of the cardiovascular system, resulting in NOS-independent effect on myocardial metabolism. The effect of NO and the NOSs on myocardial FA metabolism and its roles in myocardial contractile function remain to be determined.

Part III: Effect of eNOS palmitoylation on PA regulation of LV myocyte contraction in sham and HTN rats

In the present study I showed convincing evidence that a long chain fatty acid, PA, significantly increased LV myocyte contraction from healthy rat heart. This effect was prevented by pharmacological inhibition of eNOS with L-NAME or with eNOS gene deletion ($eNOS^{-/-}$). Furthermore, PA increased mitochondrial activity (OCR) which was prevented by L-NAME or in $eNOS^{-/-}$. In contrast, inhibition of nNOS with SMTC did not affect PA-induced myocyte contraction or mitochondrial activity. These results suggest that the effects of PA on myocyte contraction and mitochondrial activity are mainly mediated by eNOS but not by nNOS. Immunoblotting experiments showed direct evidence that PA increased the palmitoylation of eNOS which was abolished by a potent blocker of palmitoylation, 2BP. Interestingly, de-palmitoylation of eNOS with 2BP was associated with a reduction of eNOS phosphorylation at Ser^{1177}. However, 2BP, either pre-treatment or post-treatment,

did not affect the inotropic effect of PA or PA regulation of mitochondrial activity, excluding the role of eNOS-palmitoylation as the mediating mechanism. In addition, eNOS was shown to be palmitoylated in LV myocytes from HTN rats. Depalmitoylation of eNOS with 2BP did not affect LV myocyte contraction in the presence and absence of PA, despite its inhibitory effect on eNOS Ser^{1177} in HTN. To our knowledge, this is the first study to exam the influence of eNOS and its palmitoylation in the regulation of LV myocyte contraction following supplementation of a favorable metabolic substrate of the myocardium in healthy and hypertensive hearts.

On the other hand, PA is also the essential substrate for a post-translational modification, *S*-palmitoylation. As such, PA may affect myocyte contraction through changing the activities of the mediator proteins. Intriguingly, my results showed that eNOS plays a critical role in mediating PA-regulation of myocyte contraction. Furthermore, eNOS palmitoylation is significantly increased by PA, which was reversed by pre-treatment of the inhibitor, 2BP. It is well established that the palmitoylation of eNOS is associated with its translocation to plasma membrane (caveolae) and increased its activity in endothelial cells [Liu J et al., 1996]. There are evidences showed the interplays between eNOS palmitoylation and phosphorylation, that is, inhibition of eNOS palmitoylation with another potent inhibitor of palmitoylation, triacsin C, significantly reduced eNOS phosphorylation in cultured endothelial cells [Blakeman N et al., 2014]. Paradoxically, triacsin C increased NO level in these experiments. Similar to the responses in the report, my results showed that eNOS-Ser^{1177} was significantly reduced by 2BP in the presence and absence of PA. Moreover, in line with the results shown in endothelial cells [Blakeman N et al., 2014]. 2BP increased NO production in LV myocytes before and after PA supplementation. However, neither L-NAME nor SMTC affected the increment of NO, excluding the roles of eNOS or nNOS. Although 2BP is a potent and reliable inhibitor of palmitoylation, it has been shown to exert off-target effects [Davda D et al., 2013]. Therefore, 2BP may regulate NO level in myocyte samples through alternative mechanisms – it is speculative to suggest that 2BP increases cellular NO by preventing cysteine residues of NO-binding proteins.

Nevertheless, 2BP did not affect OCR with or without PA supplementation, *i.e.* PA increased OCR in 2BP pre-treated LV myocytes, suggesting that 2BP does not affect the functional regulation of PA on the mitochondria in LV myocytes (despite increased NO level). Accordingly, 2BP was used to exam the effect of de-palmitoylation on PA-regulation of myocyte contractility. Similar to its effect on mitochondrial activity, 2BP did not affect myocyte contraction, either pre-treated or post-treated, demonstrating that de-palmitoylation process, eNOS de-palmitoylation in particular, is not the major mechanism mediating PA-regulation of myocyte contraction.

In HTN, cardiac NOSs are remodeled, exhibiting reduced eNOS protein level and greater nNOS protein expression and activity [Jin CZ et al., 2013]. Furthermore, the residual eNOS was palmitoylated in HTN, judging from the significant reduction of eNOS palmitoylation by 2BP with and without PA. Palmitoylation of eNOS may have maintained the activity of eNOS since eNOS-Ser^{1177} was minimized by 2BP and 2BP reduced PA-dependent OCR increment in HTN. However, the significance of this modification remains uncertain. It is possible that reduced eNOS activity underlie the lack of PA-dependent inotropic response on LV myocytes in HTN, regardless of its palmitoylation since 2BP did not affect myocyte contraction in HTN. Inhibition of cardiac NOSs with L-NAME significantly increased myocyte contraction in HTN, similar results were shown with SMTC, suggesting nNOS modulation of myocyte contraction by PA in HTN. Notably, 2BP did not affect myocyte contraction even in the presence of L-NAME, excluding the involvement of eNOS palmitoylation in myocyte contraction by PA in HTN.

Conclusion & future prospective

In conclusion, my results show that FA-dependent metabolism is an important regulator of myocardial contraction in healthy and hypertensive rats. Furthermore, I provide novel evidence to show that nNOS-derived NO is up-regulated by FA in hypertension, which *in turn*, modulates key

elements of Ca^{2+} handling process and controls myocardial response to FA. The functional relevance and the mechanistic insights into FA-regulation of myocardial contractile function and its regulation by nNOS is important in better understanding the cardiac physiology under pressure-overload. My observations suggest a role of eNOS in mediating PA-regulation of myocyte contraction in healthy rat heart through stimulating mitochondrial activity. Although PA increases eNOS palmitoylation and maintains the phosphorylation of eNOS at Ser^{1177}, I present clear evidence to show that eNOS palmitoylation is not the main mechanism to mediate PA-dependent inotropic response in healthy heart or the lack of this increment in HTN. The significance of eNOS and its post-transcriptional modification in regulating cardiac metabolism and contraction in healthy and diseased heart needs further investigation, which may provide novel insights into therapeutic targets to improve myocardial contractile function.

References

Acin-Perez R, Fernandez-Silva P, Peleato ML, Perez-Martos A, Enriquez JA (2008). Respiratory active mitochondrial super-complexes. Mol Cell 32:529-539.

Ashley CC, Moisescu DG (1977). Effect of changing the composition of the bathing solutions upon the isometric tension-pCa relationship in bundles of crustacean myofibrils. J Physiol 270 (3):627-652.

Berlin JR et al., (1994). Intrinsic cytosolic calcium buffering properties of single rat cardiac myocytes. Biophys J. 67 (4):1775-1787.

Bers DM et al., (2002). Cardiac excitation-contraction coupling. Nature 415 (6868): 198-205.

Best PM, Donaldson SK, Kerrick WG (1977). Tension in mechanically disrupted mammalian cardiac cells: effects of magnesium adenosine triphosphate. J Physiol 265 (1):1-17.

Blakeman N, Weis M (2014). The interplay between eNOS palmitoylation and phosphorylation: the triacsin C effect. FASEB J 28 Supplement 1075.9.

Boehm EA et al., (2001). Increased uncoupling proteins and decreased efficiency in palmitate-perfused hyperthyroid rat heart, Am J Physiol Heart Circ Physiol 280: H977- H983.

Briones AM, Touyz RM (2010). Oxidative stress and hypertension: current concepts. Curr Hypertens Rep 12 (2):135-142.

Briston SJ, Dibb KM, Solaro RJ, Eisner DA, Trafford AW (2014). Balanced changes in Ca buffering by SERCA and troponin contribute to Ca handling during beta-adrenergic stimulation in cardiac myocytes. Cardiovasc Res 104 (2):347-354.

Chouchani ET, Methner C, Nadtochiy SM, Logan A, Pell VR, Ding S, James AM, Cochemé HM, Reinhold J, Lilley KS, Partridge L, Fearnley IM, Robinson AJ, Hartley RC, Smith RA, Krieg T, Brookes PS, Murphy MP (2013). Cardioprotection by S-nitrosation of a cysteine switch on mitochondrial complex I. Nat Med 19 (6):753-759.

Davda D, El Azzouny MA, Tom CT, Hernandez JL, Majmudar JD, Kennedy RT, Martin BR

(2013). Profiling targets of the irreversible palmitoylation inhibitor 2-bromopalmitate. ACS Chem Biol 8:1912-7

Doenst T, Nguyen TD, Abel ED (2013). Cardiac metabolism in heart failure: implications beyond ATP production. Circ Res 113 (6):709-724.

Drapier JC, Hibbs JB et al., (1988). Differentiation of murine macrophages to express nonspecific cytotoxicity for tumor cells results in L-arginine-dependent inhibition of mitochondrial iron-sulfur enzymes in the macrophage effector cells. J Immunol 140(8): 2829-2838.

Eisner DA et al., (2000). Integrative analysis of calcium cycling in cardiac muscle. Circ Res 87 (12): 1087-1094

Fabiato A, Fabiato F (1978). Effects of pH on the myofilaments and the sarcoplasmic reticulum of skinned cells from cardiace and skeletal muscles. J Physiol 276:233-255.

Fauconnier J, Andersson DC, Zhang SJ, Lanner JT, Wibom R, Katz A, Bruton JD, Westerblad H (2007). Effects of palmitate on Ca^{2+} handling in adult control and ob/ob cardiomyocytes: impact of mitochondrial reactive oxygen species. Diabetes 56 (4):1136-1142.

Forrester MT, Hess DT, Thompson JW, Hultman R, Moseley MA, Stamler JS, Casey PJ (201 1). Site-specific analysis of protein S-acylation by resin-assisted capture. J Lipid Res 52:39 3-8.

Godt RE (1974). Calcium-activated tension of skinned muscle fibers of the frog. Dependence on magnesium adenosine triphosphate concentration. J Gen Physiol 63 (6):722-739.

Golowasch J, Thomas G, Taylor AL, Patel A, Pineda A, Khalil C, Nadim F (2009). Membrane capacitance measurements revisited: dependence of capacitance value on measurement method in nonisopotential neurons. J Neurophysiol 102 (4):2161-2175.

Hamilton DJ, Zhang A, Li S, Cao TN, Smith JA, Vedula I, Cordero-Reyes AM, Youker KA, Torre-Amione G, Gupte AA (2016). Combination of angiotensin II and l-NG-nitroarginine methyl ester exacerbates mitochondrial dysfunction and oxidative stress to cause heart failu

re. Am J Physiol Heart Circ Physiol 310:H667-H680.

He L, Kim T, Long Q, Liu J, Wang P, Zhou Y, Ding Y, Prasain J, Wood PA, Yang Q (201 2). Carnitine palmitoyltransferase-1b deficiency aggravates pressure overload-induced cardiac hypertrophy caused by lipotoxicity. Circulation 126(14):1705-1716.

Hernandez AM, Huber JS, Murphy ST, Janabi M, Zeng GL, Brennan KM, O'Neil JP, Seo Y, Gullberg GT (2013). Longitudinal evaluation of left ventricular substrate metabolism, perfusion, and dysfunction in the spontaneously hypertensive rat model of hypertrophy using small-animal PET/CT imaging. J Nucl Med 54 (11):1938-1945.

Huang JM et al., (1992). Long-chain fatty acids activate calcium channels in ventricular myocytes, Proc Natl Acad Sci 89:6452.

Huke S, Knollmann BC (2010). Increased myofilament Ca^{2+}-sensitivity and arrhythmia susceptibility. J Mol Cell Cardiol 48 (5):824-833.

Jang JH, Kang MJ, Ko GP, Kim SJ, Yi EC, Zhang YH (2015). Identification of a novel splice variant of neuronal nitric oxide synthase, nNOSbeta, in myofilament fraction of murine cardiomyocytes. Nitric Oxide 50: 20-27.

Jaswal JS et al., (2011). Targeting fatty acid and carbohydrate oxidation - a novel therapeutic intervention in the ischemic and failing heart. Biochim Biophys Acta Mol Cell Res. 1813:1333−1350.

Jin CZ, Jang JH, Kim HJ, Wang Y, Hwang IC, Sadayappan S, Park BM, Kim SH, Jin ZH, Seo EY, Kim KH, Kim YJ, Kim SJ, Zhang YH 2013. Myofilament Ca^{2+} desensitization mediates positive lusitropic effect of neuronal nitric oxide synthase in left ventricular myoc ytes from murine hypertensive heart. J Mol Cell Cardiol 60:107-115

Khan SA, Skaf MW, Harrison RW, Lee K, Minhas KM, Kumar A, Fradley M, Shoukas AA, Berkowitz DE, Hare JM (2003). Nitric oxide regulation of myocardial contractility and calcium cycling: independent impact of neuronal and endothelial nitric oxide synthases. Circ Res 92 (12):1322-1329.

Kinugawa S, Huang H, Wang Z, Kaminski PM, Wolin MS, Hintze TH (2005). A defect of neuronal nitric

oxide synthase increases xanthine oxidase-derived superoxide anion and attenuates the control of myocardial oxygen consumption by nitric oxide derived from endothelial nitric oxide synthase. Circ Res 96:355-362.

Kolwicz SC, Jr Purohit S, Tian R (2013). Cardiac metabolism and its interactions with contraction, growth, and survival of cardiomyocytes. Circ Res 113(5): 603-616.

Le Gouill E, Jimenez M, Binnert C, Jayet PY, Thalmann S, Nicod P, Scherrer U, Vollenweid er P (2007). Endothelial nitric oxide synthase (eNOS) knockout mice have defective mitoc hondrial beta-oxidation. Diabetes 56:2690-2696.

Li D, Nikiforova N, Lu CJ, Wannop K, McMenamin M, Lee CW, Buckler KJ, Paterson DJ (2013). Targeted neuronal nitric oxide synthase transgene delivery into stellate neurons reverses impaired intracellular calcium transients in prehypertensive rats. Hypertension 61(1):202-207.

Linder ME, Deschenes RJ (2007). Palmitoylation: policing protein stability and traffic. Nat Re v Mol Cell Biol 8:74-84

Liou YM, Kuo SC, Hsieh SR (2008). Differential effects of a green tea-derived polyphenol (-)-epigallocatechin-3-gallate on the acidosis-induced decrease in the Ca^{2+} sensitivity of cardiac and skeletal muscle. Pflugers Arch; 456 (5):787-800.

Liu J, Garcia-Cardena G, Sessa WC (1996). Palmitoylation of endothelial nitric oxide synthase is necessary for optimal stimulated release of nitric oxide: implications for caveolae localiz ation. Biochemistry 35:13277-13281

Lopaschuk GD, Ussher JR, Folmes CD, Jaswal JS, Stanley WC (2010). Myocardial fatty acid metabolism in health and disease. Physiol Rev 90:207-58.

Mancini A, Imperlini E, Nigro E, Montagnese C, Daniele A, Orrù S, Buono P (2015). Biological and Nutritional Properties of Palm Oil and Palmitic Acid: Effects on Health. Molecules 20 (9):17339-17361.

Massion PB, Feron O, Dessy C, Balligand JL (2003). Nitric oxide and cardiac function: ten y

ears after, and continuing. Circ Res 93:388-398.

Missiaen L et al., (2000). Abnormal intracellular Ca^{2+} homeostasis and disease. Cell Calcium. 28 (1):1-21.

Murray AJ, Anderson RE, Watson GC, Radda GK, Clarke K (2004). Uncoupling proteins in human heart, Lancet 364:1786-1788.

Niu X, Watts VL, Cingolani OH, Sivakumaran V, Leyton-Mange JS, Ellis CL, Miller KL, Vandegaer K, Bedja D, Gabrielson KL, Paolocci N, Kass DA, Barouch LA (2012). Cardioprotective effect of beta-3 adrenergic receptor agonism: role of neuronal nitric oxide synthase. J Am Coll Cardiol 59 (22):1979-1987.

Ohira H, deKemp R, Pena E, Davies RA, Stewart DJ, Chandy G, Contreras-Dominguez V, Dennie C, Mc Ardle B, Mc Klein R, Renaud JM, DaSilva JN, Pugliese C, Dunne R, Beanlands R, Mielniczuk LM (2015). Shifts in myocardial fatty acid and glucose metabolism in pulmonary arterial hypertension: a potential mechanism for a maladaptive right ventricular response. Eur Heart J Cardiovasc Imaging 17(12):1424-1431.

Opie LH: Heart Physiology, From Cell to Circulation. Philadelphia, Lippincott Williams & Wilkins, 2004. © D. M. Bers and L. H. Opie, 2004;Bers DM: Cardiac excitation-contraction coupling. Nature 415:198, 2002.

Palmiter KA et al., (1997). Molecular mechanisms regulating the myofilament response to Ca^{2+}: implications of mutations causal for familial hypertrophic cardiomyopathy. Basic Res Cardiol 92 (S1), 63-74

Patel BG, Wilder T, John Solaro RJ (2013). Novel control of cardiac myofilament response to calcium by S-glutathionylation at specific sites of myosin binding protein C. Front Physiol 4:336.

Pellieux C, Montessuit C, Papageorgiou I, Lerch R (2009). Angiotensin II downregulates the f atty acid oxidation pathway in adult rat cardiomyocytes via release of tumour necrosis fact or-alpha. Cardiovasc Res 82:341-50.

Recchia FA, McConnell PI, Loke KE, Xu X, Ochoa M, Hintze TH (1999). Nitric oxide controls cardiac substrate utilization in the conscious dog. Cardiovasc Res; 44 (2):325-332.

Recchia, FA, McConnell PI, Bernstein RD, Vogel TR, Xu X, Hintze TH (1998). Reduced nitric oxide production and altered myocardial metabolism during the decompensation of pacing-induced heart failure in the conscious dog. Circ Res 83(10): 969-979.

Robertson SP et al., (1981). The time-course of Ca2+ exchange with calmodulin, troponin, parvalbumin, and myosin in response to transient increases in Ca^{2+}. Biophys J 34 (3):559-569.

Robinson P, Griffiths PJ, Watkins H, Redwood CS (2007). Dilated and hypertrophic cardiomyopathy mutations in troponin and alpha-tropomyosin have opposing effects on the calcium affinity of cardiac thin filaments. Circ Res 101 (12):1266-1273.

Rodriguez EK, Hunter WC, Royce MJ (1992). A method to reconstruct myocardial sarcomere lengths and orientations at transmural sites in beating canine hearts. Am J Physiol 263: H293.

Rosca MG, Hoppel CL (2010). Mitochondria in heart failure. Cardiovasc Res 88:40-50.

Schober T et al., (2012). Myofilament Ca^{2+} sensitization increases cytosolic Ca^{2+} binding affinity, alters intracellular Ca^{2+} homeostasis, and causes pause-dependent Ca^{2+}-triggered arrhythmia. Circ Res 112(2): 170-9.

Sears CE, Bryant SM, Ashley EA, Lygate CA, Rakovic S, Wallis HL, Neubauer S, Terrar DA, Casadei B (2003). Cardiac neuronal nitric oxide synthase isoform regulates myocardial contraction and calcium handling. Circ Res 92 (5):e52-59.

Seifert EL et al., (2008). Essential role for uncoupling protein-3 in mitochondrial adaptation to fasting but not in fatty acid oxidation or fatty acid anion export, J Biol Chem 283: 25124-25131.

Shah AM, MacCarthy PA (2000). Paracrine and autocrine effects of nitric oxide on myocardial function. Pharmacol Ther 86 (1):49-86.

Takahashi R, Shimazaki Y, Endoh M (2001). Decrease in Ca^{2+}-sensitizing effect of UD-CG 212 Cl, a metabolite of pimobendan, under acidotic condition in canine ventricular myocardium. J Pharmacol Exp Ther 298 (3):1060-1066.

Torres J, Darley-Usmar V, Wilson MT (1995). Inhibition of cytochrome c oxidase in turnover by nitric oxide: mechanism and implications for control of respiration. Biochem J 312 (Pt 1):169-173.

Trafford AW et al., (1999). A novel, rapid and reversible method to measure Ca^{2+} buffering and time-course of total sarcoplasmic reticulum Ca^{2+} content in cardiac ventricular myocytes. Pflugers Arch. 437 (3):501-503.

Trochu JN, Bouhour JB, Kaley G, Hintze TH (2000). Role of endothelium-derived nitric oxide in the regulation of cardiac oxygen metabolism: implications in health and disease. Circ Res 87(12):1108-1117.

Wang Y, Youm JB, Jin CZ, Shin DH, Zhao ZH, Seo EY, Zhang YH (2015). Modulation of L-type Ca^{2+} channel activity by neuronal nitric oxide synthase and myofilament Ca^{2+} sensitivity in cardiac myocytes from hypertensive rat. Cell Calcium 58(3):264-274.

Welter R, Yu L, Yu CA (1996). The effects of nitric oxide on elecontrolon transport complexes. Arch Biochem Biophys 331 (1):9-14.

Young ME, Leighton B (1998). Fuel oxidation in skeletal muscle is increased by nitric oxide cGMP - evidence for involvement of cGMP-dependent protein kinase. Febs Letters 424(1-2): 79-83.

Zhang YH (2016). Cardiac inotropy, lusitropy, and Ca^{2+} handling with major metabolic substrates in rat heart. Pflugers Arch 468(11-12):1995-2006.

Zhang YH (2016). Neuronal nitric oxide synthase in hypertension - an update. Clin Hypertens 22:20.

Zhang YH, Casadei B (2012). Sub-cellular targeting of constitutive NOS in health and disease. J Mol Cell Cardiol 52 (2):341-350.

Zhang YH, Dingle L, Hall R, Casadei B (2009). The role of nitric oxide and reactive oxygen species in the positive inotropic response to mechanical stretch in the mammalian myocardium. Biochim Biophys Acta 1787 (7):811-817.

Zhang YH, Jin CZ, Jang JH, Wang Y (2014). Molecular mechanisms of neuronal nitric oxide synthase in cardiac function and pathophysiology. J Physiol 592 (15):3189-3200.

Zhang YH, Zhang MH, Sears CE, Emanuel K, Redwood C, El-Armouche A, Kranias EG, Casadei B (2008). Reduced phospholamban phosphorylation is associated with impaired relaxation in left ventricular myocytes from neuronal NO synthase-deficient mice. Circ Res 102 (2):242-249.

Zhao ZH, Jin CL, Jang JH, Wu YN, Kim SJ, Jin HH, Cui L, Zhang YH (2016). Assessment of Myofilament Ca^{2+} Sensitivity Underlying Cardiac Excitation-contraction Coupling. J Vis Exp 1: (114).

Zhao ZH, Youm JB, Wang Y, Lee JH, Sung JH, Kim JC, Woo SH, Leem CH, Kim SJ, Cui L, Zhang YH (2016). Cardiac inotropy, lusitropy, and Ca^{2+} handling with major metabolic substrates in rat heart. Pflugers Arch 468(11-12):1995-2006.

국 문 초 록

심장의 수축 기능과 이온 항상성 유지를 위한 ATP 합성 수요는 매우 높으며, 생리적으로 지방산이 주요 대사물질이다. 그러나 지금까지 심근세포 연구에서 지방산의 작용을 직접 연구한 결과는 거의 없다. 이 연구는 정상과 고혈압 쥐의 심장에서 포화지방산이 좌심실 심근세포 수축 및 미토콘드리아 기능을 조절하는 효과를 분석하였다.

정상과 고혈압 군에서 팔미트산 (PA, 100μM)은 산소소모량을 모두 증가시켰으나, 심근수축과 세포내 ATP의 변화는 정상군에서만 증가되었다. Carnitine palmitoyl transferase I (CPT-1) 억제제인 etomoxir 는 정상과 고혈압군에서 모두 PA에 의한 산소소모량과 ATP 변화를 줄였지만, 수축강화작용의 억제는 정상군에서만 관찰되었다. PA는 정상군에서 칼슘채널을 통한 칼슘유입을 변화시키지 않고 근섬유의 칼슘감수성을 감소시키면서, 결과적으로 세포 내 칼슘 최대값을 증가시켰다. 고혈압군에서 PA는 근섬유의 칼슘감수성에 영향을 주지 않으며, 칼슘채널을 통한 칼슘유입은 감소시켰다.

신경성 산화질소 합성효소 (nNOS)는 심근세포 근섬유의 칼슘민감도 및 심근수축을 조절하는 데 중요하다. 고혈압 모델에서 PA는 nNOS에 의한 NO 생성을 증가시켰고, nNOS 억제제인 SMTC는 PA이 유발한 산소소모량 증가도 억제하였다. SMTC는 심근수축을 증가시켰으며, 칼슘채널과 칼슘농도 변화를 증가시키고 칼슘감수성을 증가시켰다. 방사성동위원소 ^{18}F-FTHA 와 PET-CT 를 이용하여 심근의 지방산대사를 관찰하였을 때, 고

혈압모델에서 nNOS 억제 시 지방산대사가 증가되는 것을 관찰하였다. 내피세포형 산화질소합성효소 (eNOS)의 활성은 심장근육에서 지방산의존성 산화과정에 필수적이므로 eNOS 억제제인 L-NAME 과 eNOS 유전자 결실은 심근수축과 산소소모량에서 PA의 조절을 막음으로써, eNOS가 심근세포에서 지방산의 영향을 매개하는 역할을 드러냈다.

S-palmitoylation 은 심근세포를 포함한 다양한 세포에서 표적 단백질의 이동 및 활성에 영향을 미치는 중요한 분자수준의 수식과정이며, eNOS 또한 그런 변화가 알려져 있다. 정상군과 고혈압군에서 PA는 좌심실 심근세포에서 eNOS의 palmitoylation을 증가시켰고 억제제인 2BP (100μM)은 depalmitoylation을 증가시켰다. PA는 eNOS 인산화을 증가시키지 않았지만, 2BP는 PA가 있거나 없는 상태에서 모두 eNOS 인산화를 감소시켰다. 흥미롭게도 PA에 의한 수축 및 산소소모량 증가는 2BP의 영향을 받지 않았다. 고혈압모델에서 PA는 eNOS의 palmitoylation 과 인산화 또는 심근수축에 영향을 미치지 않았다. 그러나 2BP는 PA의 존재와 상관 없이 eNOS palmitoylation 및 인산화를 감소시켰으나 심근수축은 변화시키지 않았다. 결론적으로 정상군에서 PA는 심근세포의 칼슘과 미토콘드리아의 활성을 증가시켜서 심근수축을 높인다. 고혈압모델에서 PA에 의한 심근수축 증강은 nNOS에 의한 칼슘신호 조절을 통하여 억제성 조절을 받는다. 또한, 이 연구 결과는 eNOS의 palmitoylation 을 확인하였으나, 이는 심근수축과 미토콘드리아 활성화에는 큰 영향을 주지 못하는 것으로 보인다.

실험 결과의 일부는 Pflugers Archive European Journal of Physiology (Eur J Physiol, 2017 Apr 25; Pflugers Arch - Eur J Physiol, 2017 May 22) 학술지에 출판되었다.

주요어: 심근세포, 수축성, 세포내 칼슘, 대사, 지방산, 근섬유칼슘감수성, 신경형 산화질소 합성효소(nNOS), 내피세포형 산화질소 합성효소(eNOS), 미토콘드리아 산소소모량, S-palmitoylation

학번: 2013-30816